University College of Southeast Norway

Master Thesis

Characterization of Acoustic Material Properties Using Broadband Through-Transmission Technique

Author:
Hoa T. K. Tran

Supervisor:
Professor Lars Hoff

A thesis submitted in fulfillment of the requirements
for the degree of Master of Engineering
in the

Department of Micro and Nano Systems Technology

May 2016

UNIVERSITY COLLEGE OF SOUTHEAST NORWAY

Abstract

Faculty of Technology and Maritime
Department of Micro and Nano Systems Technology

Master of Engineering

**Characterization of Acoustic Material Properties
Using Broadband Through-Transmission Technique**

by Hoa T. K. Tran

Acoustic properties of materials such as velocity and attenuation are important properties in many ultrasonic applications, i.e. non-destructive evaluation and ultrasound tissue characterization. When designing acoustic devices, e.g. ultrasound transducers, accurate knowledge of the acoustic properties of the materials is essential. Reliable characterization of these acoustic properties is necessary to give experimental data for the design and modeling of transducers. In addition, for complex materials such as composites, the dispersions of velocity and attenuation may deform the acoustic pulse and cause inappropriate interpretation of the acoustic pulse signal. Thus, it is more important to understand the characteristics and structure of these materials. The material properties are not unique values, but may vary with frequency and temperature. Consequently, the effects of temperature and frequency variation in acoustic parameters should be taken into account when characterizing materials.

In this thesis, an experimental setup of the broadband through-transmission technique was implemented and calibrated in our laboratory. A LabVIEW program to acquire pulses was available, while MATLAB code were written to process the measured data according state of the art methods found in the literature. Using this implemented system, the acoustic properties such as the acoustic impedance, the group velocity, the phase velocity, and attenuation of compressional and shear waves in both homogeneous and composite materials can be measured over an investigated frequency range from 2.5 MHz to 10.5 MHz. In addition, temperature

effects on ultrasonic phase velocity and attenuation in both PMMA and Eccosorb MF-117 materials are studied and compared.

Acknowledgements

I wish to express my special appreciation and sincere thanks to my supervisor, Prof. Lars Hoff for his continuous encouragement, guidance, and discussion throughout my Master study. Prof. Lars Hoff's advice have been motivated me to grow as a research scientist. Without his dedicated guidance and persistent help my scientific papers and thesis would not have been possible.

I would especially like to express my gratitude to Dr. Tung Manh for his endless helps in my laboratory work, as well as his helpful comments and valuable suggestions to my papers and thesis. Appreciation is given to Svein Mindrebøe for his kind help in providing lab instruments. The support and encouragement of all the faculty and staff members of the department are also greatly appreciated and acknowledged. I also would like to sincerely thank the company Kongsberg Maritime for their providing samples and discussions.

Special thanks go to Binh Duc Truong and Uyen Phuong Do for their kind help in discussions and solving MATLAB code during my research. I also wish to especially thank to my research colleagues, juniors, and friends from other research groups for supporting me for everything.

Most of all, I am truly grateful to my parents who has been inspired me throughout my life, and encouraged me through the months of writing. Last but not least, I want to thank my boyfriend Hai Le The for all his love and support. From the bottom of my heart I would like to dedicate this thesis to them for their unconditional devotion, sacrifice, support, encouragement.

Contents

List of Figures

List of Tables

Abbreviations

FFT	Fast Fourier Transform
NDT	Non-destructive testing
PMMA	Polymethyl methacrylate
SNR	Signal-to-noise ratio

This page is intentionally left blank

Chapter 1

Introduction

1.1 Introduction

Acoustic properties of materials such as velocity and attenuation are important in many ultrasonic applications, i.e. non-destructive evaluation and ultrasound tissue characterization [1][2]. Design of ultrasound transducers for e.g. clinical applications requires reliable characterization of these properties. Therefore, characterization of the acoustic properties of materials especially transducer materials is necessary to give experimental data for the design and modeling of transducers. In addition, for complex materials such as composites, the dispersions of velocity (phase velocity as a function of frequency) and attenuation may deform the acoustic pulse and cause inappropriate interpretation of the acoustic pulse signal. Thus, it is more important to understand the characteristics and structure of these materials. Some applications require the knowledge on the frequency dependent material in wide range of frequencies and temperatures. Consequently, the effects of temperature and frequency variation in acoustic parameters should be taken into account when characterizing materials.

Various techniques have been developed for measuring velocity and attenuation of ultrasonic waves in materials, which are reported by Bolef and De Klerk for continuous wave techniques [3] and McSkimmin for pulse techniques [4]. Continuous wave techniques are useful in the determination of small changes in the attenuation or sound velocity. However, this technique is time consuming and subject to errors due to reflections or other interfering signals

[5]. With easy operation and rapid, non-invasive measurement, pulse techniques are known as the most widely used technique for measuring ultrasonic properties of materials [6]. They are categorized into two techniques, which are pulse-echo technique and through-transmission technique. For the pulse-echo technique, only one transducer is used as a transmitter-receiver; whereas for the through-transmission technique two separate transducers are used as a transmitter and a receiver.

1.1.1 Pulse-echo technique

Pulse-echo technique is carried out either in the immersion mode or contact mode. In the immersion mode, as described by Selfridge [7], a transducer and a parallel-sided sample are immersed in a small water tank. The schematic reverberation path between the transducer and sample is shown in Figure 1.1. The transducer is excited by using a tone-burst pulse containing a number of cycles of a given frequency from a signal generator. A train of echoes due to the reverberation of ultrasound in the sample, and water path between the sample and transducer are observed. An example of pulse-echo signal is shown in Figure 1.2, where A_1 and A_2 are the reflected echoes from the front face and the back face of the sample; A_3 and A_4 are the reflected echoes due to the reverberations within the sample. From the received pulse-echo signal, the velocity and attenuation of compressional waves can be determined as in [7]. By using this method, a wide range of materials has been characterized, as shown in [8]. However, the main disadvantage of this method is that shear wave properties cannot be characterized by using this configuration. In addition, to determine the attenuation versus frequency, several transducers with center frequencies covering the frequency range of interest are needed. As the "wave-shape" changes significantly after passing through a material with high attenuation, it is almost impossible to unambiguously identify the equivalent points in the signals received, with and without sample inserted. Therefore, this method is unavailable for characterizing high attenuation materials [9].

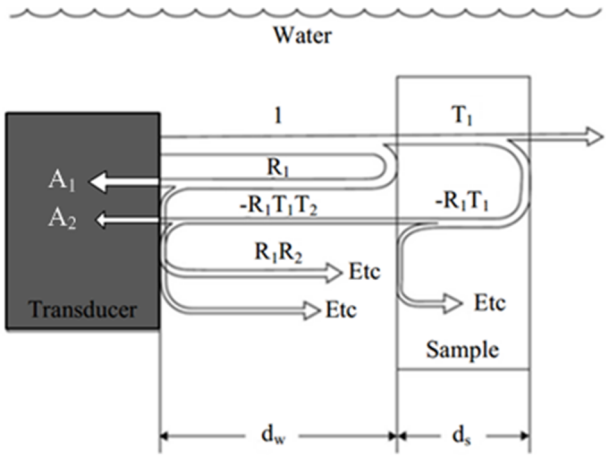

Figure 1.1. Schematic reverberation path between transducer and sample [7].

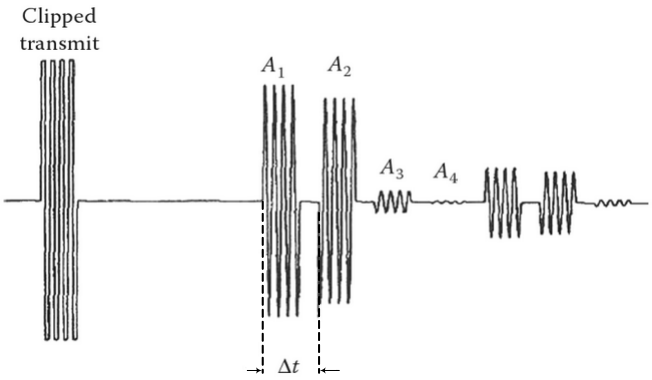

Figure 1.2. Measured pulse-echo signal for flat solid sample perpendicular to ultrasonic beam [7].

However, the immersion mode is only valid with a sample submerged in a coupling medium. The acoustic mismatch between a gas and a solid is so large that air-coupled ultrasound impossible, and a liquid is needed for coupling. Hence, most measurements are done in water, but other liquids, like oils, may be used if water is not acceptable. An alternative is done use the direct contact mode. A pulse-echo contact configuration between the transducer and sample can be used with the aid of an appropriate couplant, as shown in Figure 1.3. As can be seen in Figure 1.3, a layer of couplant is required between the transducer and sample to promote the transfer of sound energy into the sample. The transducer is excited with electrical pulses and converted them into ultrasonic pulses. The ultrasonic pulses are propagated through the sample and reflected back to the transducer. The transducer now acts as a receiver, and converts ultrasonic pulses into electrical pulses which are displayed on the oscilloscope. The

velocity and attenuation are determined by analyzing these echoes. This method can be used to generate both compressional and shear waves within the sample. However, to generate shear waves, different experimental arrangements using different transducers as shear transducers are required [10]. In addition, the pulse-echo method requires good transducer-to-sample coupling and the signal-to-noise-ratio (SNR) can be limited by inaccuracies in phase measurements, particularly in dispersive and attenuating media [11][12]. Additionally, pulse-echo method has limited use for very thick and high attenuation materials, as the pulse travels through the sample twice and experiences twice the signal loss.

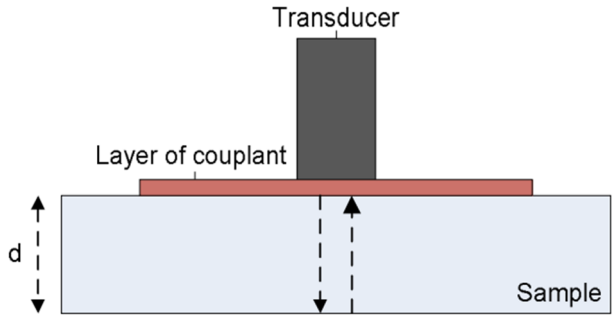

Figure 1.3. Schematic of pulse-echo contact configuration.

1.1.2 Through-transmission technique

Through-transmission technique employs two transducers which are coaxial aligned. One transducer is used as a transmitter, and another is utilized as a receiver. A sample with parallel sides is inserted between two transducers and aligned. For the through-transmission immersion technique, the sample is immersed in a coupling medium usually water, between two transducers. The experimental setup of the through-transmission immersion technique is shown in Figure 1.4. The sample can be rotated while the two transducers are fixed, or vice versa. In order to characterize materials over the wide range of frequencies, the broadband through-transmission technique is applied. The principle of this technique is shown in Figure 1.5. A short electrical pulse excitation is applied to the transmitter, and the signal received by the receiver is recorded on a digital oscilloscope. A sample is then inserted between two transducers, and the received pulse after transmitting through the sample is recorded. Phase velocity and attenuation as function of frequency are calculated from the phase and magnitude

of the received spectra over a wide bandwidth. More detailed description of this method can be found in [9][13].

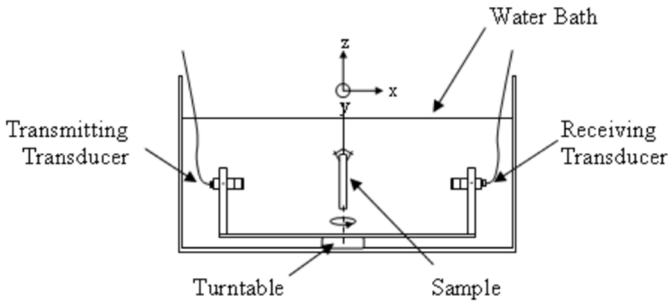

Figure 1.4. Experimental setup of through-transmission immersion technique [14].

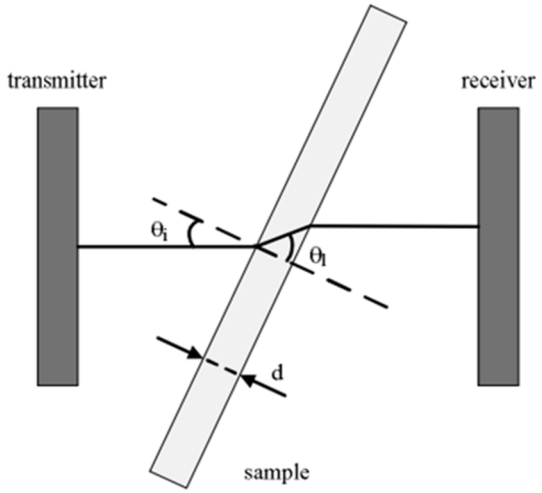

Figure 1.5. Principle of the broadband through-transmission technique.

In contrast with the contact measurements, this method allows the sample to be oriented relative to the transducers so that the incident angle between the acoustic wave and the normal of the sample can be adjusted. Using this technique with the mode conversion, allows measuring acoustic properties of both compressional waves and shear waves in solids, including porous and composite materials [13]. Moreover, in the immersion technique, the coupling medium is well behaved at all incident angles, and gives repeatable measurements as long as wetting of the sample is consistent. Thus, the requirement of a good transducer-to-sample coupling which can occur when using contact configuration such as in the pulse-echo technique is eliminated. In addition, in the broadband through-transmission technique, ultrasonic waves travel only once through the material, thus they suffer less energy loss. As a

result, this method is useful for characterizing high attenuation materials, e.g. bone. However, because the samples are immersed in a water tank, the use of samples susceptible to corrosion is limited. Furthermore, this system suffers from a lack of mobility because of the numerous devices needed for the measurements. In addition, the tank needs to be filled with water some hours before the experiments in order to reduce the air-bubbles [15].

An improved version of the traditional broadband through-transmission technique is proposed by He and Zheng [16], as shown in Figure 1.6. In this proposed method, in addition to recording two transmitted pulses, two reflected pulses are also recorded, one from the front surface and one from the back surface of the sample. The phase velocity, attenuation and the thickness of the sample can be determined from the phase spectra of the four recorded pulses. Using this method, the attenuation coefficient can be calculated very accurately even when the density of the material is unknown. However, the procedure of experiments and signal analysis in this method is quite complex, and it is required that the interface conditions on both sides of the sample should be equal.

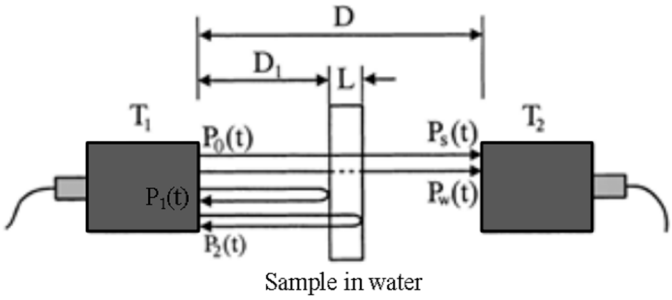

Figure 1.6. Signal paths in the immersion experiment for measuring attenuation, dispersion and thickness using the broadband-pulse technique [16].

From the review of previous techniques and the requirement for characterizing various kinds of materials over the wide range of frequency, in this thesis the broadband through-transmission technique is chosen to characterize acoustic properties of both compressional and shear waves in materials. Homogeneous materials, i.e. Polymethylmethacrylate (PMMA) and aluminum (Al), and composite materials, i.e. Eccosorb MF-117 and unknown materials from the company Kongsberg Maritime, are chosen to characterize. An experimental setup of the broadband through-transmission technique is implemented and calibrated in our laboratory.

The MATLAB code were written to process the measured data according state of the art methods found in the literature. Using this implemented system, the acoustic properties such as the acoustic impedance, the group velocity, the phase velocity and attenuation of compressional and shear waves in both homogeneous and composite materials can be measured over an investigated frequency range from 2.5 MHz to 10.5 MHz. In addition, temperature effects on ultrasonic phase velocity and attenuation in both PMMA and Eccosorb MF-117 materials are studied and compared.

1.2 Objectives of this thesis

From the advantages and disadvantages of previously proposed techniques in literature for characterizing acoustic properties of materials as well as the above motivations, the objectives of this thesis are:

- Implement and calibrate a system for acoustic material characterization, using the broadband through-transmission technique. Two pairs of transducers are used, one pair with a center frequency of 5 MHz (Olympus C309-SU, Olympus Inc., Waltham, MA), and the other pair with a center frequency of 10 MHz (Olympus V327-SU, Olympus Inc., Waltham, MA).
- Characterize materials by measuring the group velocity, phase velocity and attenuation of both compressional and shear waves in samples. Estimate the uncertainties in the measurements of velocity and attenuation, and the correction for diffraction effects in attenuation measurement.
- Characterize homogeneous materials, using known materials, e.g. aluminum and PMMA, as references to verify the accuracy of the measurement system. Thereafter, characterize Eccosorb MF-117 and unknown materials from the company Kongsberg Maritime.
- Study on how the temperature influences the phase velocity and attenuation for compressional and shear waves, measured in the PMMA and Eccosorb MF-117 materials.

1.3 Outline of this thesis

This thesis is organized as follows. Chapter 1 presents an introduction including the background and motivation, the review of previous work, and the thesis objectives. Chapter 2 presents the theory and fundamentals of ultrasound to provide the necessary knowledge of ultrasonic waves, their propagation and their attenuation. Chapter 3 presents the method developed to determine the velocity and attenuation of ultrasonic waves in the characterized samples. Chapter 4 presents the experimental setup of the broadband through-transmission technique for characterizing the acoustic properties of materials. The detailed information on how it was built in our laboratory and the method for measuring thickness and density of samples are also described in this chapter. Chapter 5 follows with the measurement results of acoustic properties introduced in Chapter 3 for different materials using the broadband through-transmission technique mentioned in Chapter 4, including homogeneous materials, aluminum and Polymethyl methacrylate (PMMA), and composite materials, Eccosorb MF-117 and samples from Kongsberg Maritime. In addition, the temperature effects on acoustic properties of PMMA and Eccosorb MF-117 materials are studied. The discussions of obtained results and source of errors in measuring velocity and attenuation are also given in Chapter 5. Finally, the conclusion of this thesis and the suggestion for future work are presented in Chapter 6. Last but not least, the developed MATLAB codes for calculating the acoustic material properties are presented in the Appendix.

Chapter 2

Theory and Fundamentals of Ultrasound

2.1 Introduction of ultrasound

Ultrasounds are sound waves with frequencies greater than 20 kHz. Ultrasonic waves can propagate through solids, liquids, gases and vapors. Ultrasonic waves propagate in a material due to the vibrations or oscillatory motions of particles within the material. The velocity of ultrasound remains constant in a particular medium if the temperature is fixed. The velocity (c) can be calculated from the frequency (f) and the wavelength (λ).

$$c = \lambda f \tag{2.1}$$

There are many types of waves that can propagate in materials. They can be divided depending on the direction of vibration in relation to their travelling direction, e.g. compressional waves, shear waves, Rayleigh waves, Lamb waves. A good illustration of the different modes is found in the PhD-thesis of Sukomski [18] (Figure 2.1).

Compressional waves, also known as longitudinal waves or p-waves, propagate so that particle vibrations are parallel to the direction of wave travel, as shown in Figure 2.1(a). Compressional waves can propagate in solids, liquids and gases, and are the most commonly used mode in ultrasonics.

Shear waves, also known as transverse waves or s-waves, propagate so that particle vibrations are perpendicular to the direction of wave propagation, as shown in Figure 2.1(b).

Shear waves can propagate in solid objects. Sound waves in liquids and tissues are generally considered to be all compressional as shear waves are not supported, except in bone which is the only biological tissue that can support propagation of shear waves easily [17]. Shear wave are relatively weak compared with compressional waves. In fact, shear waves are usually generated in materials using some of the energy from compressional waves.

Rayleigh waves are also known as surface waves because they propagate on the surface of materials. Rayleigh waves propagate so that particle motion follows an elliptical path, having both compressional and shear motions, as shown in Figure 2.1(c). Rayleigh waves can be used to inspect areas that other waves may have difficulty reaching because they are sensitive to surface defects and they follow the surface around curves [18].

Lamb waves, also known as plate waves or guided waves, are the combination of compressional wave and shear wave that only occur in thin sheets or thin plates. Lamb waves are dispersive and exist in several modes, such as symmetrical waves (Figure 2.1d) or asymmetrical waves (Figure 2.1e). Lamb waves are particularly useful for detecting longitudinal separations in metals or composite laminates.

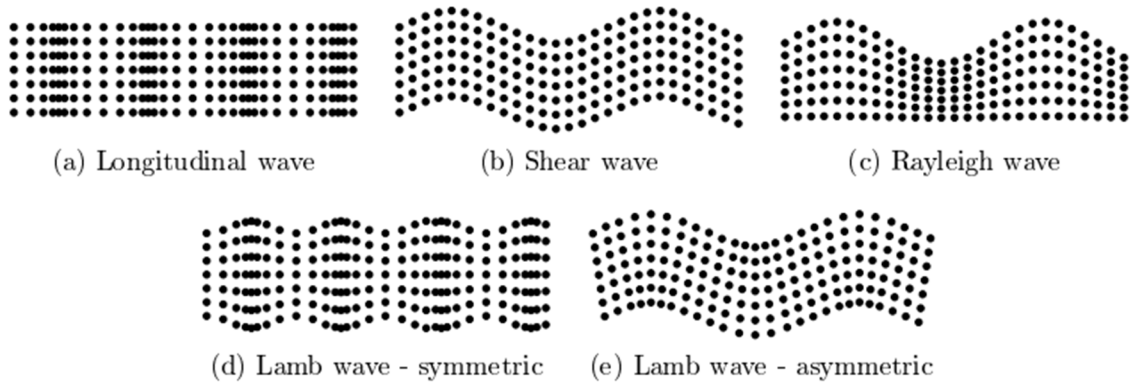

Figure 2.1. Different types of ultrasonic waves [18].

2.2 Characteristic acoustic impedance, reflection and transmission

Impedance is frequently used in electrical and mechanical applications to describe energy transfer characteristics at various boundaries. The *acoustic impedance* Z_a is defined as the ratio

between the pressure and velocity in an acoustic wave. For a plane propagating wave, this is a material property called the *characteristic acoustic impedance*, and is equal to:

$$Z = \rho c, \tag{2.2}$$

where ρ is the material density and c is the wave velocity.

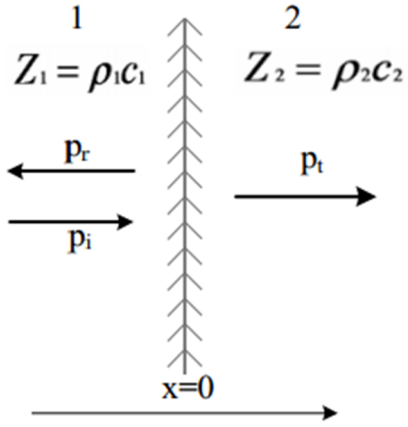

Figure 2.2. Normal incident wave at the boundary between two media [19].

When an acoustic wave strikes a plane boundary between two media with different characteristic acoustic impedance as shown in Figure 2.2, part of the wave will be reflected and the rest will be transmitted. The greater the difference, the larger the amount of energy will be reflected. When the characteristic acoustic impedances are known at both sides, it is possible to calculate the pressure transmission and reflection coefficients [19]:

$$T_p = \frac{2Z_2}{Z_1 + Z_2} \tag{2.3}$$

$$R_p = \frac{Z_2 - Z_1}{Z_1 + Z_2} \tag{2.4}$$

where Z_1 and Z_2 are the characteristic acoustic impedances of material 1 and 2 given by (2.2).

2.3 Phase velocity and group velocity

Phase velocity is the speed at which the phase of any one frequency component of the wave propagates in space. In other words, it is the velocity of a single frequency. The phase velocity (c_p) is given by [20]:

$$c_p = \omega / k, \tag{2.5}$$

where $k = 2\pi/\lambda$ is the wave number, and $\omega = 2\pi f$ is the angular frequency.

In a dispersive medium, phase velocity is a function of frequency, causing the shape of a pulse to change with the propagation distance. Therefore, it may be necessary to take into account the fact that the propagation speed is frequency-dependent.

Group velocity of a wave is the velocity with which the variations in the shape of the wave's amplitude, known as the envelope of the wave, propagate through space. Group velocity corresponds physically to the velocity at which energy or information is conveyed along the direction of propagation. An example of the phase velocity and group velocity is shown in Figure 2.3.

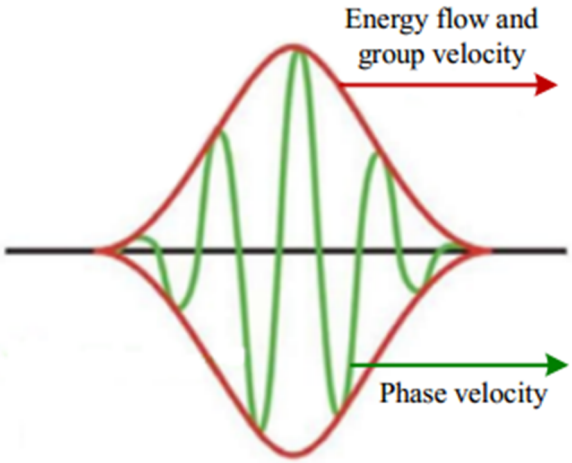

Figure 2.3. Group velocity and phase velocity.

The group velocity (c_g) is given by [20]:

$$c_g = \frac{d\omega}{dk} \tag{2.6}$$

The group velocity can be expressed in terms of the phase velocity by the following equation [20]:

$$c_g = c_c - \lambda \frac{dc_p}{d\lambda} \tag{2.7}$$

where c_c is the phase velocity at the center frequency.

2.4 Wave propagation

2.4.1 Wave propagation in homogeneous elastic media

It was mentioned previously that sound waves propagate due to the vibrations or oscillatory motions of particles within a materials. In the solids, both compressional and shear waves can propagate and the propagation of acoustic waves is given by [20]:

$$\begin{aligned} \frac{\partial^2 V_L}{\partial t^2} &= c_l^2 \nabla^2 V_L \\ \frac{\partial^2 V_S}{\partial t^2} &= c_s^2 \nabla^2 V_S, \end{aligned} \tag{2.8}$$

where V_L and V_S are the particular velocity vectors; c_l and c_s are the compressional and shear wave velocities, respectively.

The compressional and shear wave velocities in a solid material is given by [20]:

$$\begin{aligned} c_l &= \sqrt{\frac{E(1-\nu)}{\rho(1+\nu)(1-2\nu)}} \\ c_s &= \sqrt{\frac{E}{2\rho(1+\nu)}} = \sqrt{\frac{G}{\rho}}, \end{aligned} \tag{2.9}$$

where E is Young's modulus, G is the shear modulus, ν is Poisson's ratio of material, and ρ is the density of material.

Solving these equations for E and ν gives:

$$\begin{aligned} \nu &= \frac{1-2\left(\frac{c_s}{c_l}\right)^2}{2-2\left(\frac{c_s}{c_l}\right)^2} \\ E &= 2\rho c_s^2(1+\nu) \end{aligned} \tag{2.10}$$

Therefore, it is possible to determine E and ν if the values of ρ, c_l, and c_s are known.

2.4.2 Wave propagation in anisotropic elastic media

In anisotropic elastic media, the elastic properties depend on the direction of propagation of the acoustic waves. For an arbitrary direction in a crystal, three wave types can generally propagate, i.e. one quasi-longitudinal wave and two quasi-transverse waves. However, there are

special directions called symmetry axes along which pure compressional or shear waves propagate. The relationship between sound velocity and elastic properties for infinite anisotropic elastic solids is described in detail in [21].

In the case of composite materials, if the scattering particles in the materials are assumed to be spherical and much smaller than the wavelength, the elastic properties can be modeled to show how the amount of scatters (volume fraction of filler) affects velocity. Many models have been formulated to describe the bulk properties of random heterogeneous composite materials. Two common models are Reuss and Voigt [22]. These two models are the simplest models applied to two phase composites, and lead to extreme upper and lower limits. Hashin and Shtrikman proposed a better approach in [23]. Devaney and Levine have proposed another model based on a self-consistent formulation of multiple-scattering theory. From these models, it is possible to predict the compressional and shear wave velocities of composite materials. It was noted that Devaney model has agreed best with experimental data reported in literature [24]. In this thesis, without having the properties of components inside the composite material, the acoustic properties of the composite materials cannot be modeled and predicted.

2.5 Attenuation of ultrasonic waves

When sound travels through the medium, its intensity decreases with travelling distance. Ultrasonic attenuation is specifically defined as the decay rate of acoustic waves as it propagates through the material. It is responsible for the loss of acoustic energy due to scattering and absorption [25].

Scattering is the reflection of sound in directions other than its original direction of propagation. It results from the fact that the material is not strictly homogeneous but contains acoustic interfaces in which densities or sound velocities are different [25]. Therefore, when an ultrasonic wave is incident on a discontinuity, e.g. dispersed particle, small cracks, it is scattered in directions different from that of the incident wave. By that way, the ultrasonic intensity is decreased. Scattering by particles with the diameters much smaller than the

wavelength is called Rayleigh scattering. Rayleigh scattering has strong frequency dependence, thus useful for tissue characterization.

Absorption is the process where ultrasonic energy is transformed into other forms of energy and ultimately into heat. It is influenced by the ultrasound frequency, the viscosity and relaxation time of the medium [26]. The relaxation time describes the rate at which molecules return to their original position after being displayed by a force. If the medium has a long relaxation time, the molecules are still moving when the compression phase of the next wave arrives. Therefore, more energy is required to stop and reverse the direction of the molecules, thereby producing more heat. A highly viscous fluid has more absorption than a low viscosity fluid. In term of frequency, the molecules move more often when increasing the frequency, thereby generating more heat from the drag caused by friction. As the frequency is increased, less time is available for molecules to recover during relaxation process, so the molecules remain in motion and more energy is necessary to stop and redirect them, thus producing more absorption [26].

The attenuation increases so consequently the intensity of ultrasound decreases with increasing distance, which is why the depth of penetration in medical imaging is reduced as the operating frequency increases. Attenuation is generally expressed in terms of the amplitude of an acoustic wave in the form of the exponential function [25]:

$$A = A_0 e^{-\alpha d}, \tag{2.11}$$

where A_0 is the amplitude of the propagating wave at some locations, A is the reduced amplitude after the wave has traveled a distance d from the initial location, and α is the attenuation coefficient expressed in Nepers per unit length.

The attenuation coefficient can be expressed in units of decibels (dB) per unit length as follows [25]:

$$\alpha_{dB} = \frac{20}{d} \log_{10} \frac{A_0}{A} \tag{2.12}$$

Chapter 3

Determination of Velocity and Attenuation of Ultrasonic Waves

3.1 Speed of sound in water

The speed of sound in water was measured by using two different approaches, and compared to each other. Figure 3.1 shows the schematic diagram of the experiment setup for measuring the speed of sound in water with two different approaches.

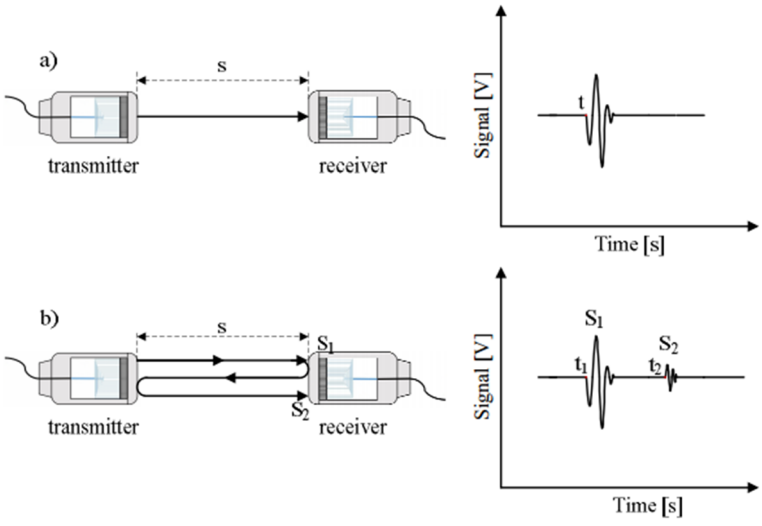

Figure 3.1. Schematic diagram of the experiment setup for measuring the speed of sound in water: (a) the first approach, and (b) the second approach.

In the first approach (Figure 3.1a), the speed of sound in water is the ratio of travelling distance (s) to transmission time (t) of the acoustic wave between two transducers, as given by:

$$c_w = \frac{s}{t} = \overline{c_w} + \Delta c_w \tag{3.1}$$

where $\overline{c_w}$ and Δc_w are the mean value and the uncertainty of the speed of sound in water, respectively. The distance between two transducers was measured with a caliper.

The measurement accuracy of the speed of sound in water is calculated as a geometrical sum of the uncertainties of the measurements of the travelling distance and the transmission time of the acoustic wave [27]:

$$\Delta c_w = \sqrt{\left(\frac{\partial c_w}{\partial s}\Delta s\right)^2 + \left(\frac{\partial c_w}{\partial t}\Delta t\right)^2} = \sqrt{\left(\frac{1}{t}\Delta s\right)^2 + \left(\frac{s}{t^2}\Delta t\right)^2} \tag{3.2}$$

where $\frac{\partial c_w}{\partial i}$ is the partial derivative of c_w with respect to the i^{th} measured variable, Δs and Δt are the uncertainties of the measurements of the travelling distance and the transmission time of the acoustic wave, respectively.

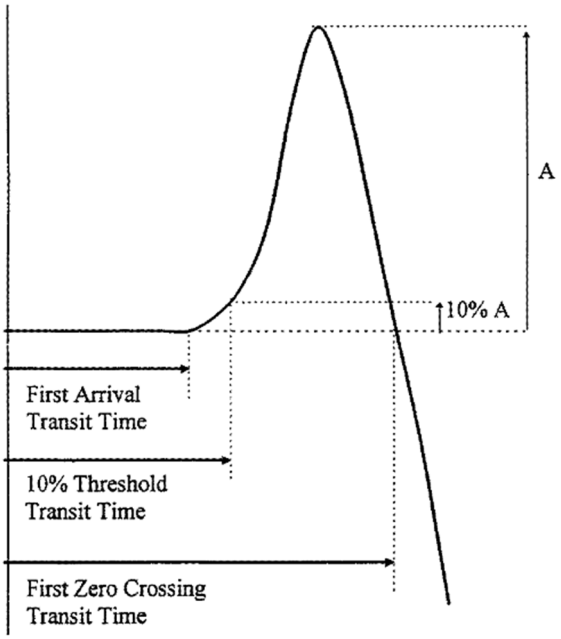

Figure 3.2. Different criteria for measuring transmission time of ultrasonic waves [5].

In order to determine the transmission time (t), i.e. transit time, three different criteria have been presented in [5], as shown in Figure 3.2. These different criteria are as follows: (i) *First arrival:* the time marker is placed at the point of first apparent deviation from the horizontal

(time) axis; (ii) *Thresholding:* the amplitude of the first half cycle of the received wave is measured, and the time marker is positioned at a point on the rising edge of the signal corresponding to 10% of that amplitude; (iii) *First zero crossing:* the time marker is placed at the point where the received waveform first crosses the time axis. These different criteria for transit time measurement result in significant differences in the calculated velocities. In this first approach, the first arrival criterion was used for assessing the transit time. However, this criterion still involves subjective assessments, thus resulting in errors in the measurement.

To obtain a better result, the second approach was implemented as shown in Figure 3.2(b). S_1 is the first received pulse without reflection backs to the transmitter, and S_2 is the second received pulse after consecutively reflecting at the front face of the receiver, the transmitter, and coming back to the receiver. The speed of sound in water is then calculated as follows:

$$c_w = \frac{2s}{t_2 - t_1} = \overline{c_w} \pm \Delta c_w \tag{3.3}$$

where $t_2 - t_1$ is the time difference of the transmission time between the first pulse and the second pulse received at the receiver. The measurement uncertainty is calculated by:

$$\Delta c_w = \sqrt{\left(\frac{\partial c_w}{\partial s}\Delta s\right)^2 + \left(\frac{\partial c_w}{\partial t}\Delta t\right)^2} = \sqrt{\left(\frac{2}{t_2 - t_1}\Delta s\right)^2 + \left(\frac{-2s}{(t_2 - t_1)^2}\Delta t\right)^2} \tag{3.4}$$

The time difference ($t_2 - t_1$) is determined by two ways: using the first arrival criterion as mentioned above to determine t_1 and t_2, or taking the auto-correlation of the signal and finding its maximum. This can be done in software, e.g. MATLAB (The MathWorks, Natick, MA), which has this as a built-in. This approach is preferred to other criteria such as threshold detection, which has been shown to be more accurate and performs better in low signal to noise ratio environments, especially in highly attenuated materials [28].

3.2 Cross-correlation algorithm for estimating the transit time difference between two signals

Cross-correlation is a mathematical operation that is used to measure the similarity of two waveforms. It is widely used to estimate the relative time between two signals [29]. Without a sample inserted, an ultrasonic waveform transmitted through water between two transducers is recorded at the receiver as a reference signal $x(t)$. After inserting a sample, another ultrasonic waveform $y(t)$ is recorded, and compared with the reference signal. The cross-correlation between two signals is defined by [30]:

$$R_{xy}(\tau) = \lim_{T\to\infty}(\frac{1}{T})\int_0^T \mathrm{x(t)}\,\mathrm{y}(t+\tau)dt \tag{3.5}$$

where T is the recording period. Cross-correlation measures the similarity between x and shifted (lagged) copies of y as a function of the lag. The time difference (τ) is determined by locating the time at which the cross-correlation R_{xy} reaches a maximum. This point is equal to the time shift that the received signal has been shifted to overlap with the reference signal. At this time-shift, the two signals are most similar.

An example of the cross-correlation function is shown in Figure 3.3. With an aluminum sample inserted, the received signal arrives before the reference signal and the amplitude of the signal is reduced (Figure 3.3a). The correlated signal is defined when the received signal with the Al sample inserted (red line) has been shifted along the time axis while keeping the received signal without the Al sample (blue line). The peak of the correlation function occurs when the peak of the received signal with the Al sample inserted coincides with the received signal without the Al sample. The time difference is the time lag of the maximum peak of the correlation function (Figure 3.3b). As can be seen in Figure 3.3, the reference pulse from propagation in water is shown in blue. The red curve is the trace received after propagation when a sample is inserted into the water. The graph below shows the cross-correlation between the two traces. A positive lag corresponds to a pulse arriving before the reference pulse. The

cross-correlation curve has several peaks, corresponding to the time-shifts where the pulse traversed though the sample, and its reverberations, overlap with the reference pulse.

If the signal $y(t)$ is replaced by signal $x(t)$,we have the auto-correlation function [30]:

$$R_{xx}(\tau) = \lim_{T\to\infty}(\frac{1}{T})\int_0^T \mathrm{x(t)\,x}(t+\tau)dt \tag{3.6}$$

The auto-correlation function is used to determine the time delay between the first received pulse (S_1) and the second received pulse (S_2) shown in Figure 3.1(b).

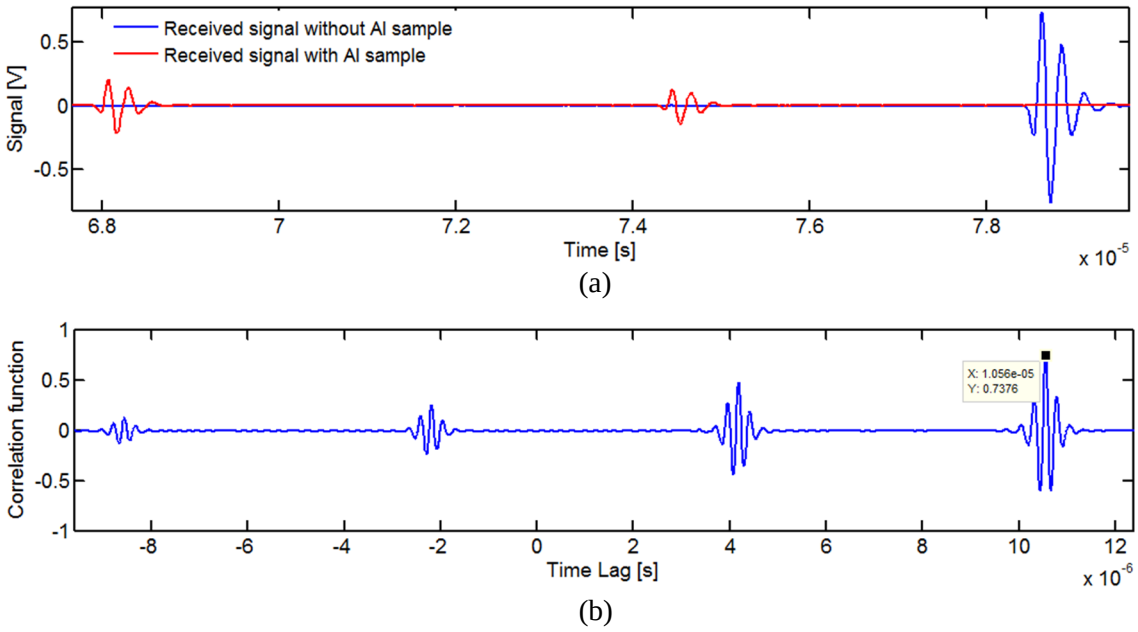

Figure 3.3. (a) Received signals with and without an aluminum (Al) sample inserted, and (b) the cross-correlation function of two signals.

3.3 Mode conversion at oblique incidence angle

In non-viscous liquid, the propagation of shear waves is not possible because the energy is totally dissipated; thus only compressional waves exist. In viscous liquids, the shear waves are strongly attenuated, and can only travel a very small distance in order of micrometers. Therefore, only compressional waves can be propagated in liquids [31][32]. However, the wave propagation in solids is more complex than in liquids because both compressional and shear waves can simultaneously propagate in solids.

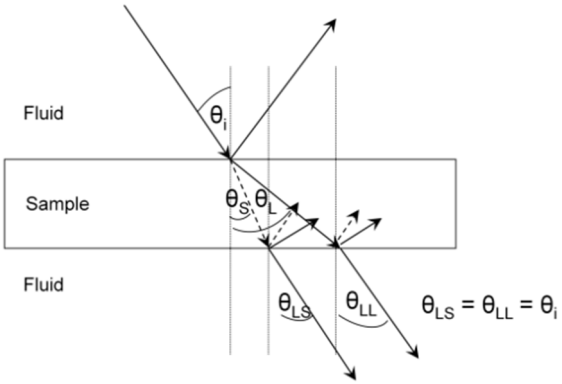

Figure 3.4. Mode conversion of an acoustic wave in a fluid-immersed sample at an oblique incidence angle [10]. The solid-lines represent the compressional waves and the dashed-lines represent the shear waves.

The incident angle is defined as the angle between the acoustic axis and the normal vector of the reflecting surface of the sample. When an acoustic wave impinges upon a sample from water with a normal incidence angle, only compressional waves are transmitted. However, when an acoustic wave impinges with an oblique incidence angle $\theta_i > 0$, another type of waves are generated. This phenomenon is called mode conversion. Mode conversion occurs when a wave encounters an interface between materials of different acoustic impedances at an oblique incidence angle. A part of the acoustic wave is reflected back into water, whereas the remaining acoustic wave is transformed into compressional waves and shear waves inside the sample. Since fluids cannot support shear wave propagation, only the compressional wave is reflected back into the fluid at the fluid-solid interface, as shown in Figure 3.4. The angles θ_l and θ_s are the transmission angles of the compressional and shear waves in the solid sample, respectively. These angles will be the incident angles for the coming acoustic wave at the next solid-fluid interface. The transmitted waves emerge with the angles of θ_{LL} and θ_{LS} to the normal vector of the solid-fluid interface. If same fluid is used on both sides, which is most common, the wave will leave the sample at the same angle as the incident wave, i.e. $\theta_{LL} = \theta_{LS} = \theta_i$. These two transmitted waves are the compressional waves in the fluid, one generated from the transmission of the compressional wave and the other converted from the transmitted shear wave. The angles θ_s and θ_l are also the incident angles of the acoustic waves reflected at the solid-fluid interface into both compressional and shear wave components.

According to the Snell's law, the relationship between these above-mentioned angles and the wave velocities is as follows:

$$\frac{c_w}{\sin\theta_i} = \frac{c_l}{\sin\theta_l} = \frac{c_s}{\sin\theta_s}, \tag{3.7}$$

where c_l and c_s are the velocity of compressional and shear waves in materials, respectively.

At the normal incidence angle ($\theta_i = 0$), only the compressional waves are propagated in the sample. Increasing the incident angle results in the propagation of both compressional and shear waves. If the speed of sound in the sample is larger than in the liquid, there will exist a critical angle. When the sample is rotated beyond this first critical angle at which the refracted angle for compressional waves reaches 90 degrees, the compressional waves no longer exist in the material. Therefore, only the shear waves are propagated in the sample. The calculation of the first critical angle θ_{cr1} is as follows:

$$\theta_{cr1} = \sin^{-1}(\frac{c_w}{c_l}) \tag{3.8}$$

The incident angle at which the refracted angle for the shear waves reaches 90° is called the second critical angle. Increasing θ_i greater or equal to the second critical angle θ_{cr2}, shear waves are no longer generated in the sample. Instead, surface waves are propagated along the surface of the sample. All the ultrasonic energy is reflected and transformed into the interface wave propagation [10]. The second critical angle θ_{cr2} is defined by:

$$\theta_{cr2} = \sin^{-1}(\frac{c_w}{c_s}) \tag{3.9}$$

Based on these principles, it is possible to excite the compressional and shear modes separately in the sample, and determine the velocity of compressional and shear waves. For materials, with c_w is greater than c_s, the second critical angle does not exist. Also, for the somewhat less common situation where c_w is greater than c_l, even the first critical angle will not exist.

3.4 Group velocity of ultrasonic waves

3.4.1 Group velocity of compressional waves

The group velocity of compressional wave in the sample can be determined by two different methods: time-of-flight method and reverberation method. These two methods only consider ultrasonic pulses at a normal incidence angle, i.e. the acoustic wave is normally incident to the sample.

In the time-of-flight method, the transit time of the ultrasonic waves from the transmitter to the receiver in the presence of the sample (t_s) and without the sample (t_w) is measured. The time-of-flight difference, i.e. time difference ($\Delta t = t_s - t_w$), between these two received signal is then calculated. The time difference (Δt) can be determined by determining t_s, and t_w using the first arrival criterion (see Section 3.1), or by using the cross-correlation. The velocity of compressional wave in the sample (c_l) can be calculated as [9][33]:

$$c_l = \frac{c_w}{1 + \frac{(t_s - t_w)\, c_w}{d}} = \overline{c_l} \pm \Delta c_l \tag{3.10}$$

where c_w is the speed of sound in water obtained in the Section 3.1, and d is the sample thickness; $\overline{c_l}$ and Δc_l are the mean value and the uncertainty of the velocity of compressional wave in the sample, respectively. The uncertainty of the velocity of compressional wave is calculated as follows:

$$\Delta c_l = \sqrt{\left(\frac{\partial c_l}{\partial c_w}\Delta c_w\right)^2 + \left(\frac{\partial c_l}{\partial (t_s - t_w)}\Delta t\right)^2 + \left(\frac{\partial c_l}{\partial d}\Delta d\right)^2} \tag{3.11}$$

The time difference between two signals (Δt) is negative when the velocity of compressional wave in the sample is larger than the speed of sound in water. For most solids, this will be the case, and the time difference is negative. However, for some materials like soft polymers, the compressional velocity within the sample is lower than the speed of sound in water, thus the time difference is positive.

By using the time-of-flight method, the determination of the compressional velocity can be done without knowing the distance between two transducers, thus reducing the uncertainty in the measurement of velocity. Only the propagation of the signal through the sample with thickness (*d*) immersed in water is compared to the propagation of the reference signal through the same water distance. However, this method requires the knowledge of the speed of sound in water.

In the reverberation method (Figure 3.5), the first received pulse (S_1) is the transmitted pulse in a straight line through the sample without reflection, and the second received pulse (S_2) is the pulse reflected consecutively at the back side and the font side of the sample before going to the receiver. The velocity of compressional wave in this case is calculated as:

$$c_l = \frac{2d}{t_2 - t_1} = \overline{c_l} \pm \Delta c_l \tag{3.12}$$

The uncertainty of the velocity of compressional wave in this case is given by:

$$\Delta c_l = \sqrt{\left(\frac{\partial c_l}{\partial d}\Delta d\right)^2 + \left(\frac{\partial c_l}{\partial (t_2 - t_1)}\Delta t\right)^2} = \sqrt{\left(\frac{2}{t_2 - t_1}\Delta d\right)^2 + \left(\frac{-2d}{(t_2 - t_1)^2}\Delta t\right)^2} \tag{3.13}$$

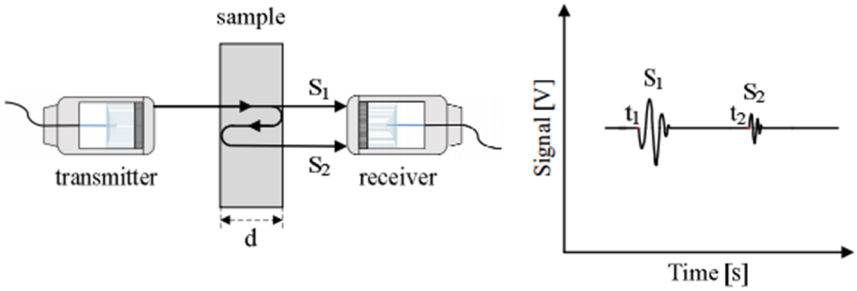

Figure 3.5. Signal paths in measuring the velocity of compressional wave in a sample.

3.4.2 Group velocity of shear waves

The measurement of the shear wave velocity is implemented similar to that of the compressional wave. However, the measurement of the time-of-flight difference ($\Delta t = t_s - t_w$) is more complex due to the difference in the travelling distances between the reference signal transmitted through only water and the signal transmitted through both water and sample. Figure 3.6 shows the geometry diagram for determining the shear wave velocity. The shear

wave is propagated through a sample of thickness (d) has an incident angle (θ_i,), and a refracted angle (θ_s). The travelling distance of the shear wave in the sample is d_1, and the travelling distance of reference signal without the sample inserted is d_2.

$$\begin{aligned} d_1 &= \frac{d}{\cos\theta_s}, \\ d_2 &= \frac{d\cos(\theta_s - \theta_i)}{\cos\theta_s} \end{aligned} \tag{3.14}$$

The time for the shear wave to travel the distance d_1, and the time for the reference signal to travel a distance d_2 are as follows:

$$\begin{aligned} t_s &= \frac{d}{\mathrm{c}_s\cos\theta_s}, \\ t_w &= \frac{d\cos(\theta_s - \theta_i)}{\mathrm{c}_w\cos\theta_s} \end{aligned} \tag{3.15}$$

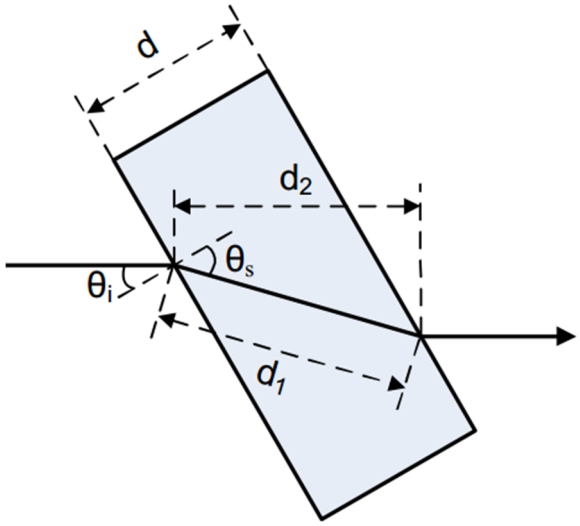

Figure 3.6. Geometry diagram for determining shear wave velocity.

The time difference between the reference signal and the transmitted shear wave is given by:

$$\Delta t = t_s - t_w = \frac{d}{\cos\theta_s}\left(\frac{1}{c_s} - \frac{\cos(\theta_s - \theta_i)}{c_w}\right) \tag{3.16}$$

From the Snell's law:

$$\sin\theta_s = \frac{\mathrm{c}_s\sin\theta_i}{c_w} \tag{3.17}$$

Furthermore, from trigonometry we have:

$$\cos(\theta_s - \theta_i) = \cos\theta_s \cos\theta_i + \sin\theta_s \sin\theta_i$$
$$\cos(\theta_s - \theta_i) = \cos\theta_i \sqrt{1 - \frac{c_s^2 \sin^2\theta_i}{c_w^2}} + \frac{c_s \sin^2\theta_i}{c_w} \tag{3.18}$$

Substituting (3.17) and (3.18) into (3.16), the time difference is given by:

$$\Delta t = \frac{d}{\sqrt{1 - \frac{c_s^2 \sin^2\theta_i}{c_w^2}}} \left(\frac{\cos\theta_i \sqrt{1 - \frac{c_s^2 \sin^2\theta_i}{c_w^2}} + \frac{c_s \sin^2\theta_i}{c_w}}{c_w} - \frac{1}{c_s} \right) \tag{3.19}$$

The shear wave velocity can be derived from (3.19) [33]:

$$c_s = \frac{c_w}{\sqrt{\sin^2\theta_i + \left[\frac{(t_s - t_w)c_w}{d} + \cos\theta_i \right]^2}} \tag{3.20}$$

The uncertainty of the shear wave velocity is calculated as follows:

$$\Delta c_s = \sqrt{\left(\frac{\partial c_s}{\partial c_w} \Delta c_w \right)^2 + \left(\frac{\partial c_s}{\partial (t_s - t_w)} \Delta t \right)^2 + \left(\frac{\partial c_s}{\partial d} \Delta d \right)^2 + \left(\frac{\partial c_s}{\partial \theta_i} \Delta \theta_i \right)^2} \tag{3.21}$$

where $\frac{\partial c_s}{\partial i}$ is the partial derivative of c_s with respect to the i^{th} measured variable, $\Delta\theta_i$ is the uncertainty of the rotation angle measurement.

3.5 Phase velocity and attenuation of ultrasonic waves

3.5.1 Phase velocity and attenuation coefficient of compressional waves

The phase velocity and the attenuation as function of frequency were calculated from transmission of short broadband pulses, using FFT to find their spectra. The measurement was performed in two steps. In the first step, without inserting sample between transducers, the output signal was acquired. The FFT algorithm was used to calculate the amplitude (A_w) and the phase spectra (ϕ_w) of the acquired signal. In the second step, the sample was inserted between the transducers and the output signal was obtained. Its amplitude (A_s) and phase spectra (ϕ_s)

were also computed. The phase velocity and attenuation coefficient were determined by comparing the spectra of Fourier transforms of the signals received, with and without sample inserted [9][31]. To eliminate the rapid–changing component in the phase spectrum and avoid the $\pm 2m\pi$ phase ambiguity in calculating the phase spectrum from the arctangent function, the pulse center was first shifted (circularly rotating) to the beginning of the sampling window [16][34]. The phase spectrum of the shifted pulse was then calculated.

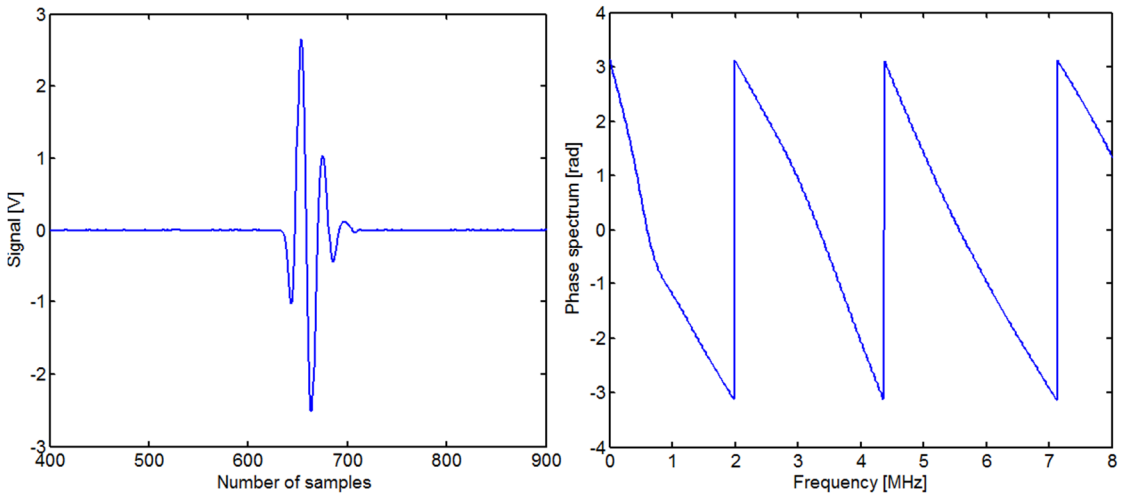

(a) (b)

Figure 3.7. (a) Original received pulse without sample inserted, and (b) its phase spectrum.

The original received pulse without sample inserted, and its phase spectrum are shown in Figure 3.7. In the measurement, the sampling window was used to extract significant parts of the received pulse; therefore the received pulse was sampled after a certain time delay (Figure 3.8a). The origin of time in calculating the phase spectrum of the received pulse using the FFT algorithm is the beginning of the sampling window. In order to reduce the phase uncertainty of the phase spectrum, after using the sampling window, the pulse was padded with zeros to fix the length (Figure 3.8b). A procedure of circularly rotating the pulse to the left was applied, and the phase spectrum was then calculated using the FFT algorithm, as shown in Figure 3.9 [16].

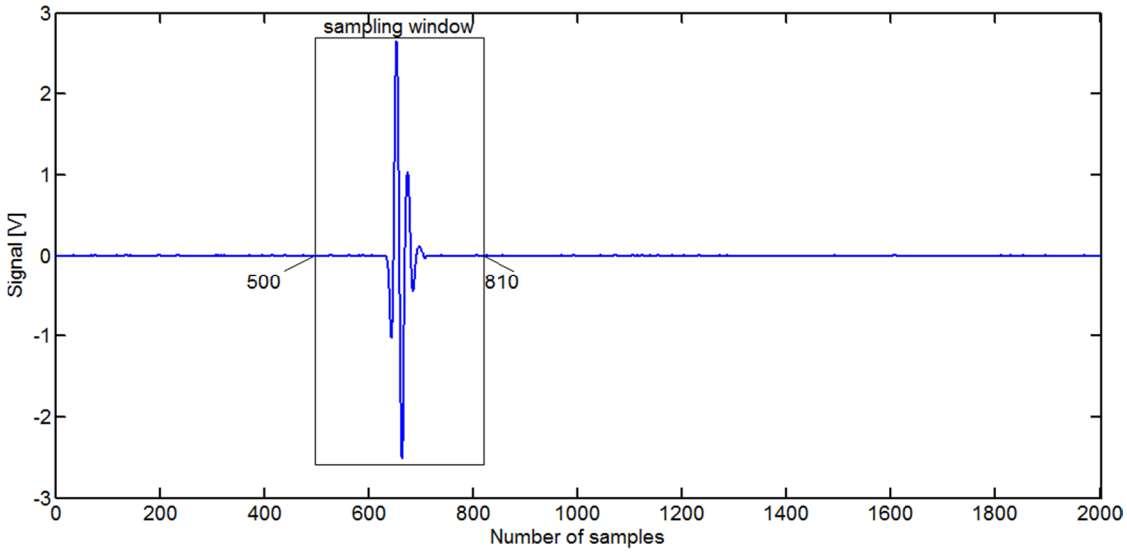

(a)

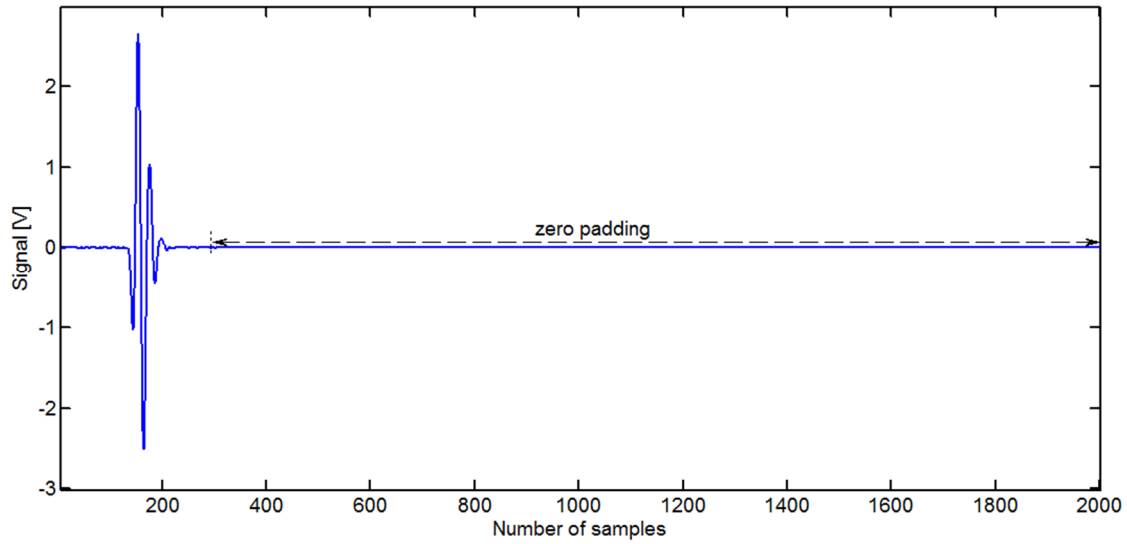

(b)

Figure 3.8. (a) Original pulse with sampling window, and (b) the pulse after using sampling window and adding with zero.

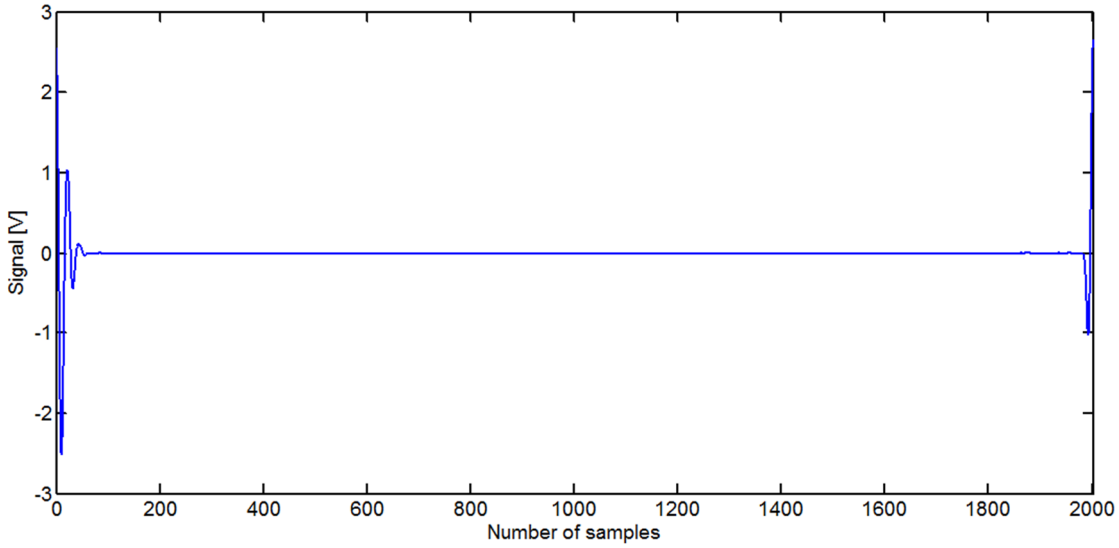

(a)

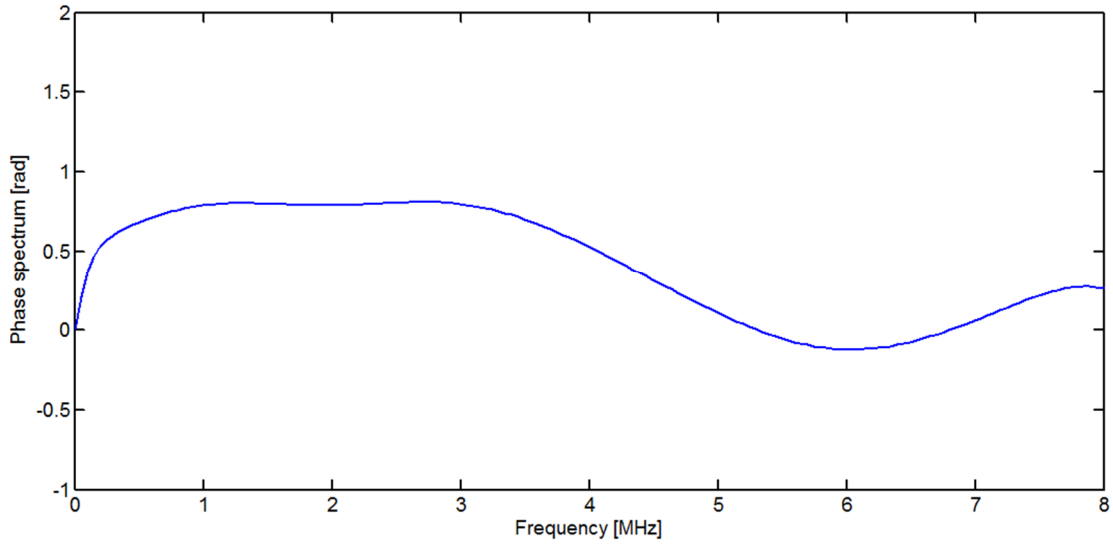

(b)

Figure 3.9. (a) The circularly shifted pulse, and (b) phase spectrum of the circularly shifted pulse.

Using this procedure, the phase velocity (c_l) and the attenuation coefficient (α_l) of the compressional wave are calculated as follows similar to the group velocity (3.20) [31][35]:

$$c_l = \frac{c_w}{1 + \frac{(\phi_s - \phi_w + 2\pi f \tau)c_w}{2\pi fd}}, \qquad \alpha_l = \alpha_w + \ln\left(\frac{T_{TP} A_w}{A_s}\right) / \mathrm{d}, \tag{3.22}$$

where α_w is the attenuation of water which is must smaller than α_l and therefore can be ignored [16], c_w is the speed of sound in water (see Section 3.1), τ is the trigger delay of the two time

windows used to acquire the signal, T_{TP} is the total transmission coefficient for the longitudinal wave. The determination of T_{TP} will be discussed in the next section.

The uncertainty of the phase velocity and attenuation of compressional wave is calculated by:

$$\Delta c_l = \sqrt{\left(\frac{\partial c_l}{\partial c_w}\Delta c_w\right)^2 + \left(\frac{\partial c_l}{\partial \tau}\Delta \tau\right)^2 + \left(\frac{\partial c_l}{\partial d}\Delta d\right)^2} \tag{3.23}$$

$$\Delta \alpha_l = \sqrt{\left(\frac{\partial \alpha_l}{\partial T_{TP}}\Delta T_{TP}\right)^2 + \left(\frac{\partial \alpha_l}{\partial d}\Delta d\right)^2} \tag{3.24}$$

where ΔT_{TP} denotes the uncertainties of the measurement of the total transmission coefficient for the compressional wave.

3.5.2 Phase velocity and attenuation coefficient of shear waves

With an incident angle greater than the first critical angle, only shear waves can propagate through the sample. The phase velocity (c_s) and the attenuation coefficient (α_s) of the shear wave can be calculated similar to the group velocity (3.20) [9][35]:

$$\begin{aligned} c_s &= \frac{c_w}{\sqrt{\sin^2\theta_i + \left[\frac{(\phi_s - \phi_w + 2\pi f\tau)c_w}{2\pi fd} + \cos\theta_i\right]^2}}, \\ \alpha_s &= \alpha_w \cos(\theta_l - \theta_i) + \ln\left(\frac{T_{TS}A_w}{A_s}\right)\frac{\cos\theta_l}{d}, \end{aligned} \tag{3.25}$$

where θ_i is the angle of incidence, θ_l is the refractive angle of the shear wave calculated from Snell's law, T_{TS} is the total transmission of the shear wave, α_w is the attenuation of water and can be ignored.

The uncertainty of the phase velocity of the shear wave is calculated as follow:

$$\Delta c_s = \sqrt{\left(\frac{\partial c_s}{\partial c_w}\Delta c_w\right)^2 + \left(\frac{\partial c_s}{\partial \tau}\Delta \tau\right)^2 + \left(\frac{\partial c_s}{\partial d}\Delta d\right)^2 + \left(\frac{\partial c_s}{\partial \theta_i}\Delta \theta_i\right)^2} \tag{3.26}$$

3.6 Transmission coefficient of compressional and shear waves at oblique incidence angle

3.6.1 Transmission coefficients at fluid-solid interface

As shown in Figure 3.4, a compressional wave propagating in a fluid toward a solid plane boundary can result in both transmitted compressional wave and shear wave into the solid and a part of the acoustic wave is reflected back into fluid. The proportions of the energy of the original sound wave that are reflected or transmitted as compressional or shear waves are associated with reflection and transmission coefficients. The transmission coefficients of the refracted compressional wave (T_{L1}) and shear wave (T_{S1}) can be computed by the following equations [36]:

$$\begin{aligned} T_{L1} &= \frac{\rho_w}{\rho_s} \frac{2Z_L \cos 2\theta_s}{Z_L \cos^2 2\theta_s + Z_s \sin^2 2\theta_s + Z_w}, \\ T_{S1} &= -\frac{\rho_w}{\rho_s} \frac{2Z_S \sin 2\theta_s}{Z_L \cos^2 2\theta_s + Z_s \sin^2 2\theta_s + Z_w}, \end{aligned} \tag{3.27}$$

where Z_w is the acoustic impedance of the fluid, Z_L and Z_S are the acoustic impedances of the compressional and shear waves in the solid, respectively, ρ_w and ρ_s are the density of water and the sample, respectively. From (3.27), it should be noted that no shear wave is transmitted into the solid at normal incident angle, i.e. $\theta_i = 0$.

The specific acoustic impedances are given by:

$$\begin{aligned} Z_w &= \frac{\rho_w c_w}{\cos\theta_i}, \\ Z_L &= \frac{\rho_s c_l}{\cos\theta_l}, \\ Z_S &= \frac{\rho_s c_s}{\cos\theta_s} \end{aligned} \tag{3.28}$$

where θ_i is the angle of incidence, θ_l and θ_s are the refractive angle of the compressional wave and shear wave calculated from Snell's law, respectively.

3.6.2 Transmission coefficients at solid-fluid interface

Figure 3.10 shows the reflection and refraction of the ultrasonic waves at a solid-fluid interface. The compressional wave (I_L) impinges on the solid-fluid interface, resulting in three types of waves: reflected compressional wave (R_{L1}), shear wave (R_{S1}), and refracted compressional wave (T_{LL}), as shown in Figure 3.10(a). The refracted angle of the refracted compressional wave transmitted into the fluid is equal to the incident angle of the original wave impinges onto the liquid-solid interface (see Figure 3.4). Figure 3.10(b) shows that when the shear wave (I_S) impinges on a solid-fluid interface, reflected compressional wave (R_{L2}), shear wave (R_{S2}), and refracted compressional wave (T_{LS}) are obtained.

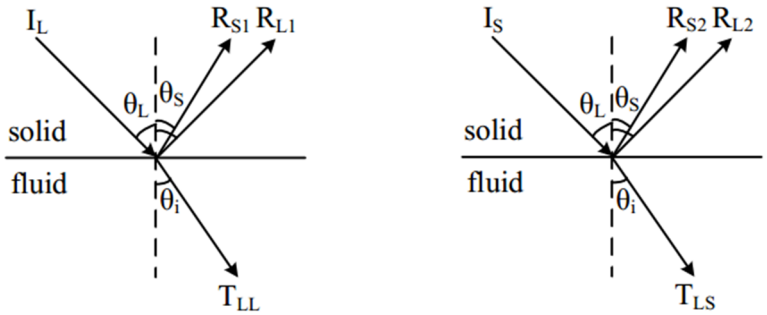

(a) (b)

Figure 3.10. Reflection and refraction of (a) a compressional wave, and (b) a shear wave at a solid-fluid interface.

The transmission coefficients of the shear wave (T_{S2}) and the compressional wave (T_{L2}) at the solid-fluid interface are calculated as follows [36]:

$$T_{L2} = \frac{c_w \cos\theta_l}{c_l \cos\theta_i \cos 2\theta_s}\left(1 - \frac{Z_w + Z_S \sin^2 2\theta_s - Z_L \cos^2 2\theta_s}{Z_w + Z_S \sin^2 2\theta_s + Z_L \cos^2 2\theta_s}\right) \tag{3.29}$$

$$T_{S2} = \frac{\tan\theta_i}{2\sin^2\theta_s}\left(1 - \frac{Z_w + Z_L \cos^2 2\theta_s - Z_S \sin^2 2\theta_s}{Z_w + Z_L \cos^2 2\theta_s + Z_S \sin^2 2\theta_s}\right)$$

3.6.3 Total transmission coefficients

The transmission through the plate is found as the product of the two transmission coefficients above. Note that since this considers pulse transmission through a plate, reverberations are not included, as they are removed by time-gating. This should not be confused with the more

common formulation of transmission through a plate, including all internal reflections and giving thickness-dependent resonances. The total transmission coefficients for each wave mode is the product of the two transmission coefficients of the wave from water to the sample and from the sample to water [9][34]. The total transmission coefficients of the compressional wave (T_L) and shear wave (T_S) can be calculated as follows:

$$\begin{aligned} T_L &= T_{L1}T_{L2} \\ T_S &= \left|T_{S1}T_{S2}\right| \end{aligned} \tag{3.30}$$

From (3.27), (3.29) and (3.30), the transmission coefficients for the compressional wave and shear wave can be plotted as the function of the incident angle to illustrate the critical angles and transmission of the waves through the sample.

Substitute (3.27) and (3.29) into (3.30), the total transmission coefficient for the compressional wave at normal incident angle (θ_i =0), (3.30) reduces to:

$$T_{TP} = \frac{4Z_w Z_L}{(Z_w + Z_L)^2} \tag{3.31}$$

The uncertainty of the total transmission coefficient for the compressional wave at normal incidence angle is given by:

$$\Delta T_{TP} = \sqrt{\left(\frac{\partial T_{TP}}{\partial Z_w}\Delta Z_w\right)^2 + \left(\frac{\partial T_{TP}}{\partial Z_l}\Delta Z_l\right)^2} \tag{3.32}$$

where $\frac{\partial T_{TP}}{\partial i}$ is the partial derivative of T_{TP} with respect to the i^{th} measured variable, ΔZ_w, and ΔZ_l are the uncertainty of the acoustic characteristic impedance of water and the sample, respectively.

3.7 Diffraction loss in attenuation measurements

The acoustic waves emitted by a transducer into a sample are not confined to a region defined by the area of the transducer and the normal to its emitting surface as assumed in the simplest case [37]. Because of the finite size of the transducer, the acoustic beam spreads out into a

diffraction field. This geometrical phenomenon, called diffraction, causes an apparent amplitude loss and phase shift in the received echo signal. When the diameter of the transducer is much larger than the acoustic wavelength, the effects of diffraction on the phase of the received signal have been found very small [2]. A number of authors have studied the effects of diffraction for the diffraction correction [37][38][39]. The expression of the diffraction correction is given by [39]:

$$D_L = 1 - e^{-j(2\pi/s)}\left[J_0(2\pi/s) + jJ_1(2\pi/s)\right] \tag{3.33}$$

According to (3.32), the effects of diffraction are solely determined by the parameters $s = zc/(fa^2)$ where a is the radius of the transducer, z is the travelling distance, c is the ultrasonic velocity, and f is the ultrasonic frequency [16].

The diffraction corrections with the sample (D_{Ls}) and without the sample (D_{Lw}) are calculated as follows [9].

$$\begin{aligned} D_{Ls} &= 1 - e^{-j(2\pi/s_s)}\left[J_0(2\pi/s_s) + jJ_1(2\pi/s_s)\right] \\ D_{Lw} &= 1 - e^{-j(2\pi/s_w)}\left[J_0(2\pi/s_w) + jJ_1(2\pi/s_w)\right] \end{aligned} \tag{3.34}$$

where s_w, and s_s are the Fresnel parameters [16]:

$$\begin{aligned} s_w &= \frac{Dc_w}{fa^2}, \\ s_s &= \frac{(D-d)c_w}{fa^2} + \frac{dc_l(f)}{fa^2} \end{aligned} \tag{3.35}$$

where D is the distance between two transducers, d is the sample thickness, c_w and c_l are frequency dependent phase velocities of water and the sample, respectively.

The attenuation coefficients in (3.22) and (3.25) are then modified as follows:

$$\begin{aligned} \alpha_l &= \alpha_w + \ln\left[\left(\frac{T_{TP}A_w}{A_s}\right)\left|\frac{D_{Ls}}{D_{Lw}}\right|\right]/\mathrm{d} \\ \alpha_s &= \alpha_w \cos(\theta_l - \theta_i) + \ln\left[\left(\frac{T_{TS}A_w}{A_s}\right)\left|\frac{D_{Ls}}{D_{Lw}}\right|\right]\frac{\cos\theta_l}{d} \end{aligned} \tag{3.36}$$

If the transducer is focused, both the distance z and radius a need to be normalized by a factor $\gamma = F/|F - z|$ where F is the focal distance.

Chapter 4

Setup for Acoustic Material Characterization

4.1 Broadband through-transmission technique

Figure 4.1 shows the experimental setup for the broadband through-transmission technique for measuring acoustic velocity and attenuation of materials. Two pairs of transducers were used, one with center frequency 5 MHz (Olympus C309-SU, Olympus Inc., Waltham, MA), and another with center frequency 10 MHz (Olympus V327-SU, Olympus Inc., Waltham, MA). Each pair of transducers was coaxial aligned and immersed in a cylindrical water tank ($\emptyset_{inner}$ = 128 mm, $\emptyset_{outer}$ = 160 mm, h = 320.5 mm). A sample with thickness *d* was mounted vertically in a manual 360° rotation stage, where the rotation axis goes through the center of the sample. Three different sample holders were tested; these are shown in Figure 4.2. The sample was placed halfway between the two transducers, and could be rotated to vary the incident angle of the acoustic wave relative to the sample. The transmitting transducer was excited by a pulser-receiver (Panametrics 5800, Olympus Inc., Waltham, MA), set to transmit short electrical pulses with a repetition rate of 100Hz. The output waveforms were recorded by a digital oscilloscope (LeCroy 9310AM, Teledyne LeCroy, Chestnut Ridge, NY). The signals were sampled at sampling rate 100 MS/s at 8 bit vertical resolution. Each of the digitized waveforms was averaged over 64 times to improve signal to noise ratio (SNR). The receiving transducer was connected to the “CH1” port of the oscilloscope. The “CH2” port of the oscilloscope was

connected to “SYNC Out” of the pulser-receiver. The oscilloscope was set to start acquisition when a sync-pulse was received from the pulser-receiver. The pulses received by the oscilloscope were transferred to a computer using the GPIB interface, using software written in LabVIEW (National Instruments Inc., Austin, TX) and stored to disk. Processing was done offline using MATLAB software (The MathWorks, Natick, MA).

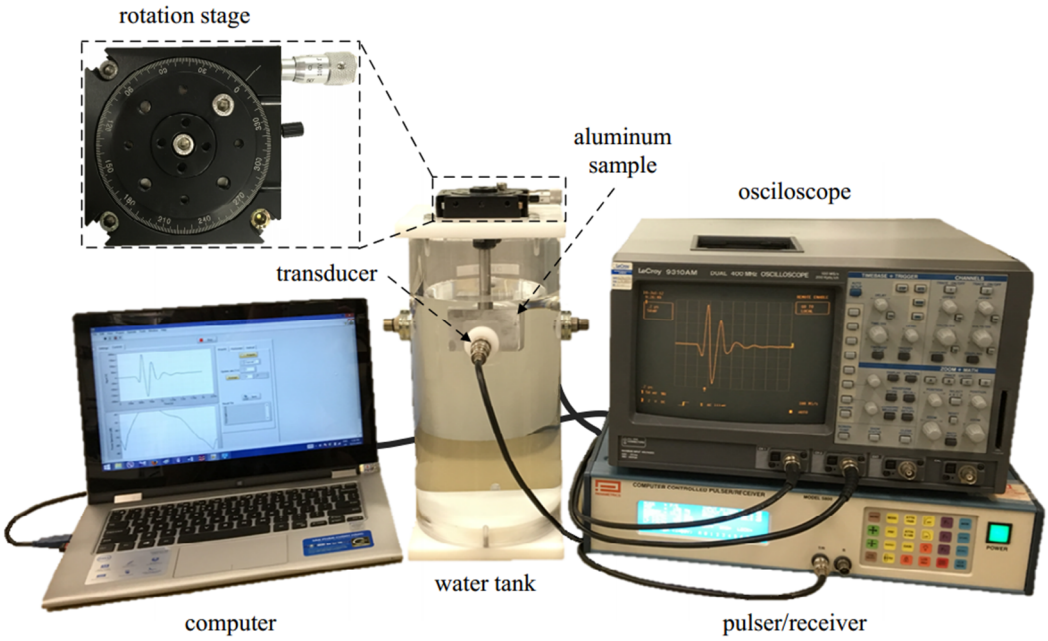

Figure 4.1. Experimental setup for the broadband through-transmission technique for characterizing acoustic properties of materials.

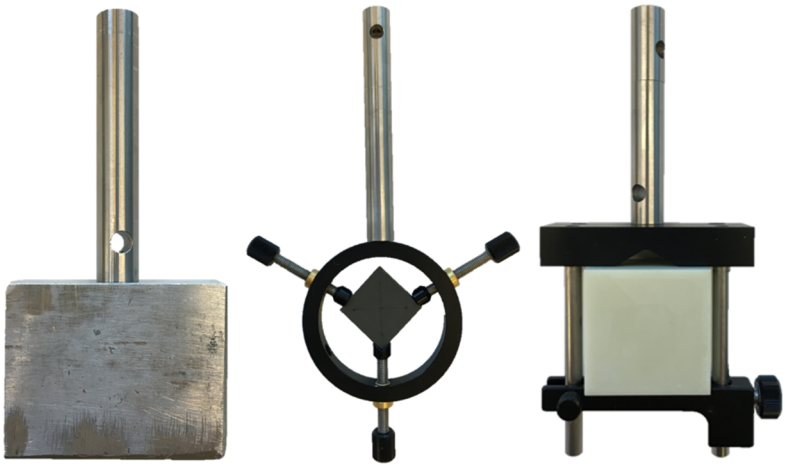

Figure 4.2. Three different types of sample mounts. The holder to the left is obtained by making threads in the sample, and screwed the post into the sample. The holders to the right are based on optical mounts from Standa ltd. (Vilnius. Lithuania).

Before measuring the speed of sound in samples, the speed of sound in water was measured. The travelling time between the two transducers was registered using the sync-signal from the pulser-receiver as the start reference, and registering the received pulse on the oscilloscope using delayed trigger and zoom. This allowed reading the received pulse at the full 100 MS/s sample rate, i.e. at 10 ns precision. In addition, the position where the sample surface is perpendicular to the acoustic axis could be found by using the pulse-echo mode of the pulser-receiver. At normal incidence, the amplitude of echoes from front and back faces of the sample, and all the reverberations, reaches their maximum level. The speed of sound in the samples was measured using the through-transmission mode. The measurement procedure was as follows. Without inserting the sample, the output signal received at the receiving transducer was obtained. A sample was then immersed in the water tank, and placed between the two transducers. The trigger delay was adjusted so that the shifting of the waveform caused by putting the sample into the water tank was approximately compensated, keeping the received pulse inside the oscilloscope window. The sample was rotated to find the angle giving normal incidence, $\theta_i = 0$. This was obtained by looking at the signal in the oscilloscope, and rotated to maximum amplitude of the main signal and the reverberations. At this angle, the second signal was acquired.

In most samples, the compressional wave velocity is larger than the speed of sound in water. In this case, there exists a critical angle of incidence, above which no sound is transmitted into the sample. The critical angle was measured in both directions by rotating the sample clockwise and counterclockwise while observing the oscilloscope and registering at which angles the first signal vanished. These angles were interpreted as the critical angles, hence, the critical angle was found as half of the difference between these two angles. When the sample was rotated above the critical angle, the signal from the compressional wave disappeared, while a new signal with smaller amplitude appeared. This signal is somewhat delayed compared to the signal from the compressional wave, and is interpreted as coming from shear wave propagation in the sample. In order to achieve better accuracy, the sample was

rotated until the compressional wave signal disappears completely. Figure 4.3 shows the received signal measured with the 5 MHz transducer pair in the case with Eccosorb MF-117 sample inserted at the normal incidence angle ($\theta_i=0^0$) and at an oblique incidence angle greater than critical angle ($\theta_i=45^0$). It was noted that at the normal incidence angle, there are some pulses in the received signal because of reverberations from the front face and back face of the sample. When the sample was rotated to $\theta_i=45^0$ above the critical angle, the new received signal (red line) showed a smaller amplitude and more delayed compared to the received signal at the normal incidence angle (blue line). In addition, it can be seen that the compressional component totally disappears when rotating the sample over the critical angle.

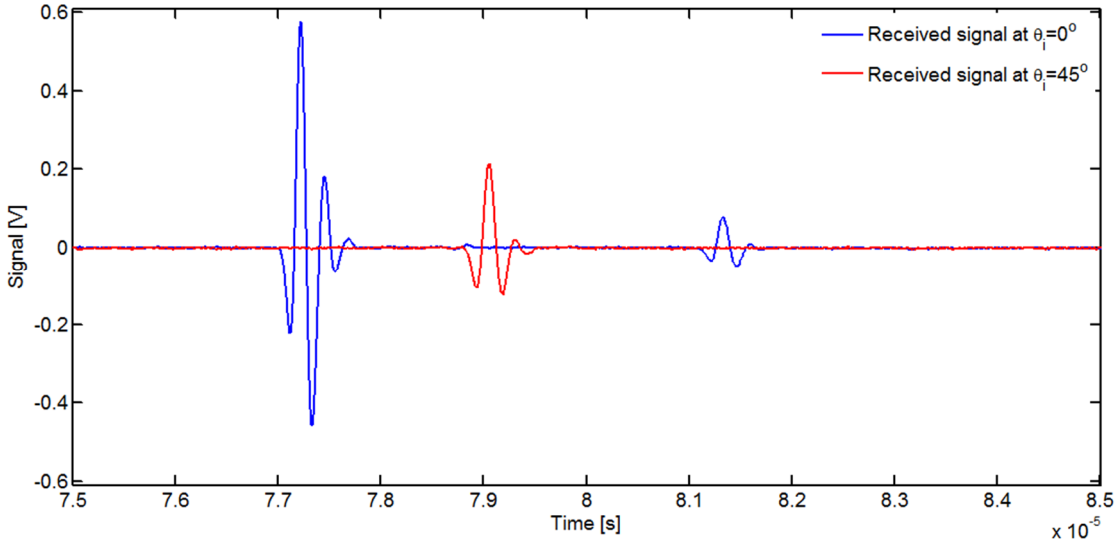

Figure 4.3. Received signal measured with the 5 MHz transducer pair in with Eccosorb MF-117 inserted at a normal incidence angle (blue line), and at an oblique incidence angle (red line).

The speed of sound in the sample was determined as the group velocity, as described in Section 3.4. The compressional wave properties were measured at normal incidence, as this allows reading out the reverberations, obtaining the best accuracy. The shear wave properties were measured at oblique incidence, as no shear wave conversion exists at normal incidence. The amplitude and phase spectra of the received signal were calculated by Fast Fourier Transform, FFT. By comparing the spectra of the signals received with and without sample inserted, the phase velocity and attenuation of the ultrasonic waves as function of frequency were calculated.

Most measurements were done at room temperature, but the temperature was monitored by a thermometer. In addition, one study was made to investigate how the temperature influenced the phase velocity and attenuation in samples of the materials PMMA and Eccosorb MF-117. The temperature was controlled by first heating the water in the tank containing the sample. Then, the acoustic properties of the sample were measured as the water and the sample passively cooled down, while monitoring the temperature. The procedure of first heating and then passively cooling was chosen to avoid creation of air-bubbles due to the heating.

This thesis describes measurements on a selection of materials, both homogenous, i.e. aluminum (one sample) and PMMA (one sample), and composites, i.e. Eccosorb MF-117 (two samples with different thicknesses). In addition, six samples of two different materials were provided from Kongsberg Maritime. The composition of these materials is unknown to us. For each sample, the measurement procedure was repeated at least 5 times in order to improve the measurement accuracy.

4.2 Measuring sample dimensions and densities

The main reason for investigating the aluminum block, was to test the performance of the system on a known reference material. Note however that aluminum comes in different alloys, and the exact composition of this block was not known. The aluminum block was rectangular block with a surface area of 58.34 × 45.96 mm^2. A Heidenhain-Metro length gauges (MT 60M Dr. Johannes Heidenhain GmbH, Traunreut, Germany) was used to measure the sample thickness. The thickness was measured at ten different points, as illustrated in Figure 4.3, five points (brown dots) on the front side, and five points on the back side at the same positions. The results are given in Table 4.1.

The standard deviation of the Al sample thickness was calculated as follows:

$$\sigma = \sqrt{\frac{\sum_{i=1}^{n}(d_i - \bar{d})^2}{n-1}}, \tag{4.1}$$

where σ is the standard deviation, $\bar{d}$ and d_i are the mean value and the i^{th} measured thickness, n is the total number of measurements. The MT 60M length gauge has accuracy ± 0.5 μm [40], which is much smaller than the variations found in the measurements, hence, the uncertainty in this measurement depends mainly on the standard deviation.

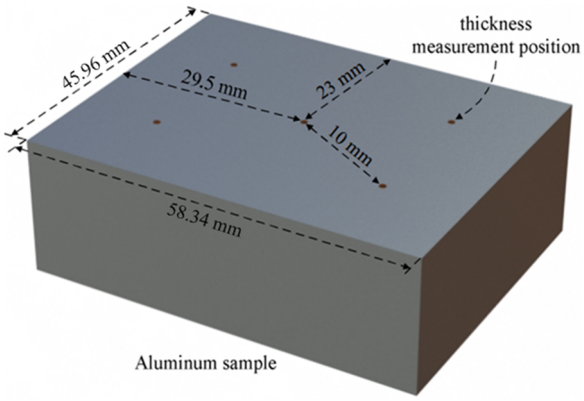

Figure 4.4. Geometry of the measured Al sample and thickness measurement procedure.

Table 4.1. Thickness measurement of the Al sample.

Measurement No.	Measured thickness (mm)
1	20.383
2	20.385
3	20.357
4	20.370
5	20.389
6	20.393
7	20.397
8	20.372
9	20.364
10	20.375
Mean value	20.379

The density of the Al sample can be calculated as the ratio of its mass to volume, $\rho_{Al} = m_{Al}/V_{Al}$. The mass of the Al sample was measured by using a SI-234 weighting scale (Denver Instruments, Bohenmia, NY, USA) [41]. The volume of the Al sample was calculated by multiplying its width, length, and thickness.

A polymethyl methacrylate (PMMA) rectangular block with a surface area of 49.05× 44.96 mm^2 and the two Eccosorb MF-117 samples with different thicknesses are shown in Figure 4.4 and Figure 4.5, respectively. Six samples of two different materials were provided from Kongsberg Maritime is shown in Figure 4.6. Because two Eccosorb MF-117 samples are small,

therefore the volume of these samples is measured by using the Graduated Cylinder 100 ml. The thickness and density of other samples were calculated in the same way as for Al sample.

Figure 4.5. Geometry of PMMA sample.

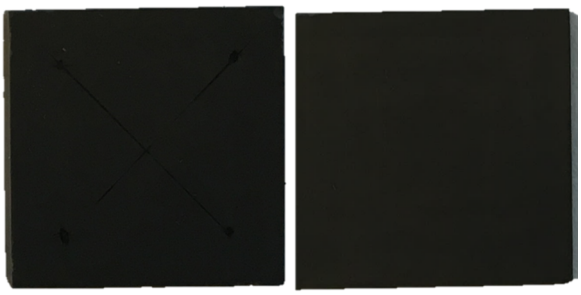

(a) (b)

Figure 4.6. Geometry of two Eccosorb MF-117 samples: (a) sample 1, and (b) sample 2.

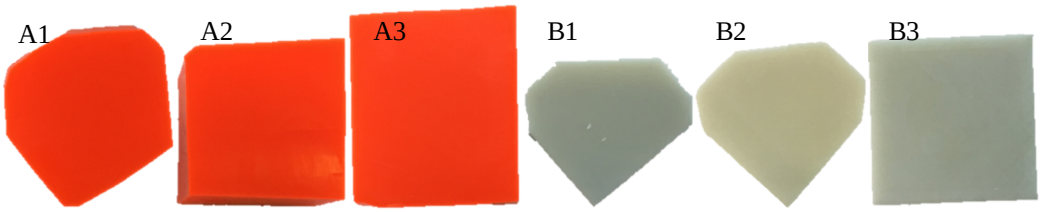

Figure 4.7. Geometry of six unknown material samples from Kongsberg Maritime.

Chapter 5

Results and Discussions

5.1 Thickness and density of samples

Prior to measuring the acoustic properties of the samples, their thicknesses and densities were measured. The measurement results of the thickness and density of samples are shown in Tables 5.1 and 5.2.

Table 5.1. Thickness and density of Al, PMMA, and Eccosorb MF-117 samples.

Sample No.	Density (g/cm^3)	Thickness (mm)
Al	2.69 ± 0.09	20.38 ± 0.01
PMMA	1.18 ± 0.06	29.78 ± 0.02
Eccosorb sample 1	4.18 ± 0.20	5.16 ± 0.01
Eccosorb sample 2		1.94 ± 0.03

Table 5.2. Thickness and density of six unknown material samples from Kongsberg Maritime.

Sample No.	Density (g/cm^3)	Thickness (mm)
A1	1.15 ± 0.06	34.67 ± 0.05
A2		24.90 ± 0.01
A3		20.12 ± 0.01
B1	1.42 ± 0.07	29.45 ± 0.01
B2		19.06 ± 0.01
B3		9.34 ± 0.01

5.2 Speed of sound in water

The speed of sound in water was measured at 19.5°C ± 0.5°C by using the setup shown in Figure 4.1, without a sample inserted between two transducers. Using the first approach in Section 3.1 (Figure 3.1a) and the 5 MHz transducer pair, the signal and its power spectrum

were obtained, as shown in Figure 5.1. The distance between two transducers was measured by using a stainless hardened digital caliper with a precision of ±0.03 mm [42]. Table 5.3 presents the measured distance and the transmit time of signal from transmitter to receiver. Using (3.1) and (3.2), the speed of sound in water (c_w) was 1480.3 ± 0.5 m/s.

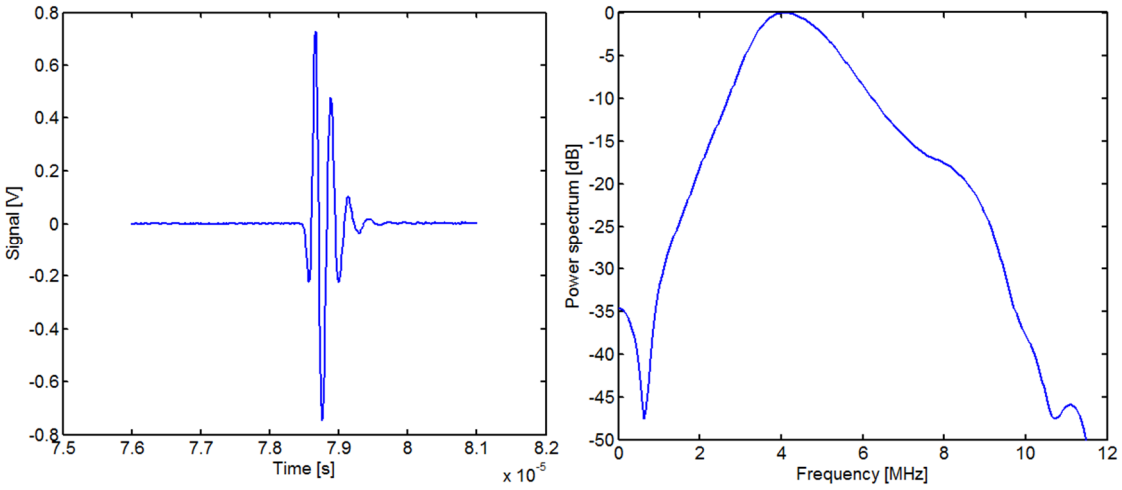

(a) (b)

Figure 5.1. (a) Received signal measured with the 5 MHz transducer pair without a sample inserted, and (b) its power spectrum.

Table 5.3. Travelling distance and transmit time of the signal between two transducers.

Testing No.	Travelling distance (mm)	Transit time (μs)
1	116.15	78.48
2	116.18	78.47
3	116.14	78.46
Mean value ± Δ	116.16 ± 0.03	78.47 ± 0.02

Using the second approach in Section 3.1 (Figure 3.1b), the speed of sound in water was also calculated. The time differences obtained by using the first arrival criterion and the auto-correlation function in MATLAB (Figure 5.2) were 156.88 ± 0.02 μs, and 156.90 ± 0.01 μs, respectively. Using (3.3) and (3.4), the speed of sound in water was 1480.9 ± 0.4 m/s and 1480.7 ± 0.4 m/s, corresponding to the time differences calculated by using the first arrival criterion or the auto-correlation function, respectively.

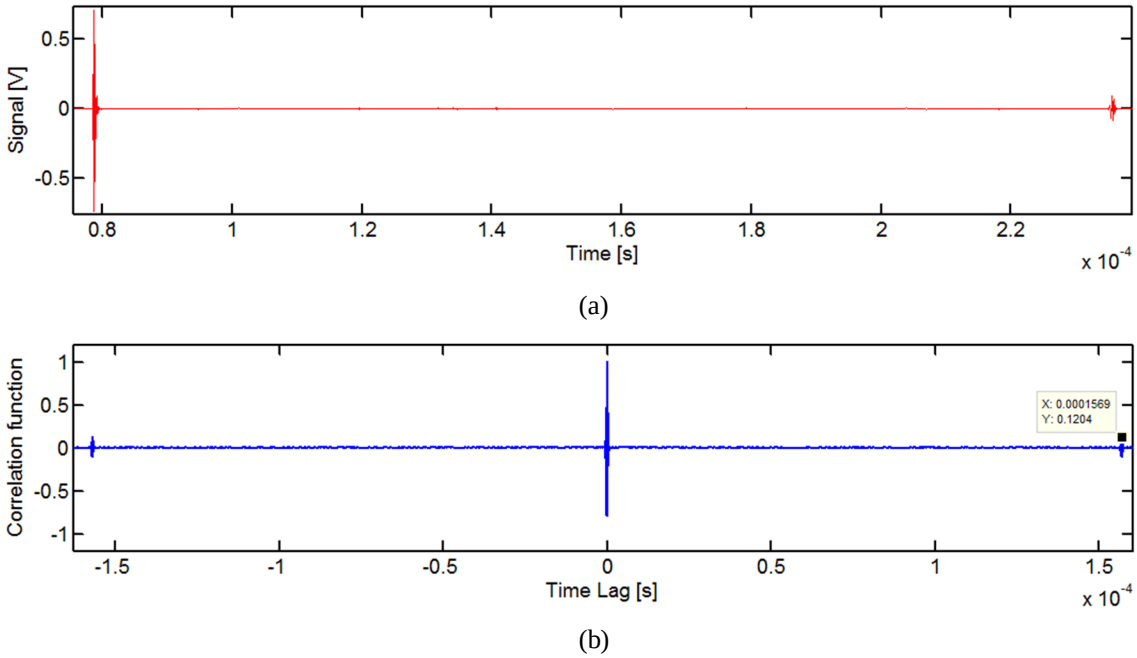

Figure 5.2. (a) Received signal measured with the 5 MHz transducer pair without a sample inserted, and (b) its auto-correlation function.

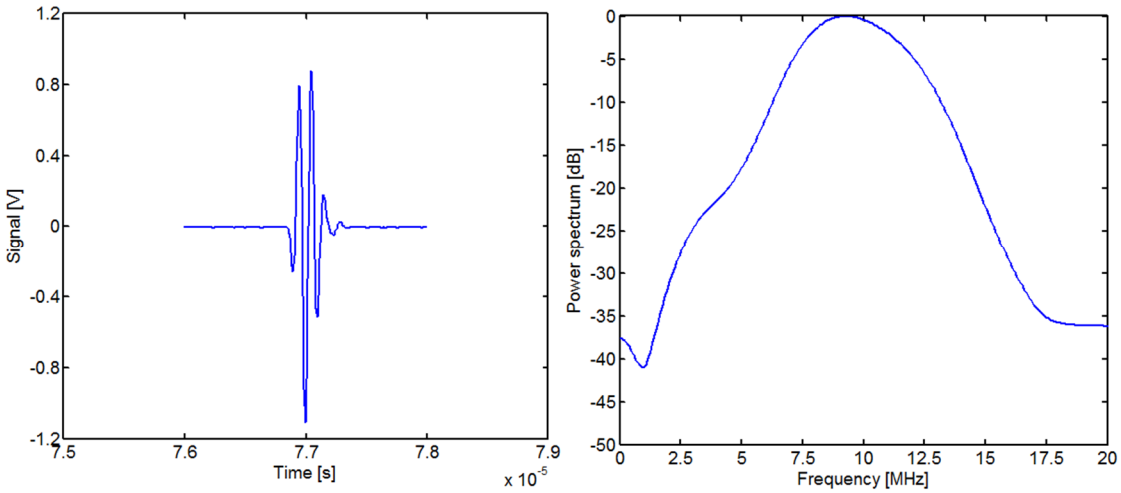

Figure 5.3. (a) Received signal measured with the 10 MHz transducer pair without a sample inserted, and (b) its power spectrum.

Using the 10 MHz transducer pair, the signal and its power spectrum were obtained, as shown in Figure 5.3. In this case, the measured distance between two transducers was 113.74 ± 0.03 mm. Table 5.4 presents the comparison of the speed of sound in water between two measurement approaches and literature. The speed of sound in water obtained by using these two approaches was relevant with the published values in literature, except slightly higher in

the speed of sound measured with the 10 MHz transducer pair. A small difference of 0.1% in the speed of sound in water was found when measuring with two transducer types. The difference could come from the uncertainty in the measurement of the travelling distance. Using the auto-correlation function could give better results with higher accuracy [28]. Therefore, these values were chosen for further calculations in this thesis, i.e. 1480.7 ± 0.4m/s (at 5 MHz) and 1481.0 ± 0.4 m/s (at 10 MHz).

Table 5.4. Comparison of the speed of sound in water measured with two different approaches and literature.

Speed of sound in water (m/s)	Measured values (at 5 MHz)	Measured values (at 10 MHz)	Published values
First approach	1480.3 ± 0.5	1480.4 ± 0.6	1480.80 [43]
Second approach (using the first arrival criterion)	1480.9 ± 0.4	1481.2 ± 0.4	1480.81 [44]
Second approach (using auto-correlation function)	1480.7 ± 0.4	1481.0 ± 0.4	

5.3 Acoustic properties of the aluminum sample

5.3.1 Group velocity of ultrasonic waves

Figure 5.4 shows the received signals with and without Al sample inserted, and their cross-correlation function. Using the time-of-flight method, the time difference between the received signals, with and without sample inserted, was 10.56 ± 0.01 μs, determined by using the cross-correlation function in MATLAB. The measurements were done at 19.5°C ± 0.5°C. From (3.10) and (3.11), the group velocity of compressional wave in the Al sample (c_l) was 6362 ± 18 m/s, using the speed of sound in water of 1480.7 ± 0.4 m/s (at 5 MHz).

Using the reverberation method (see Figure 5.5), the time difference between the received signals was 6.37 ± 0.01 μs, determined by using the auto-correlation function in MATLAB (Figure 5.5). From (3.12) and (3.13), the group velocity of compressional wave in the Al sample was 6398 ± 7 m/s. Table 5.5 shows the group velocity of compressional wave in Al sample measured with the 5 MHz and 10 MHz transducer pairs.

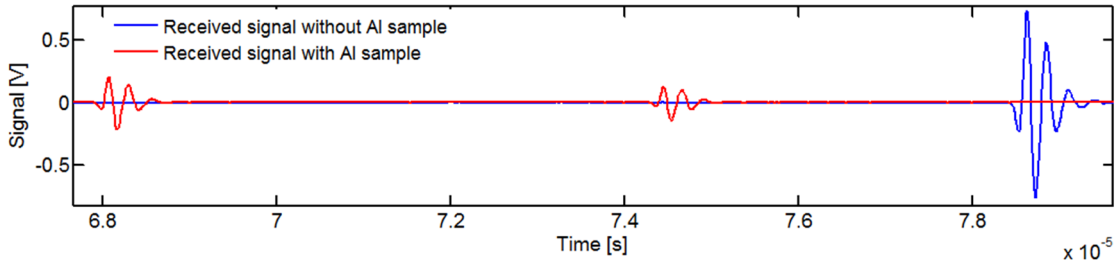

(a)

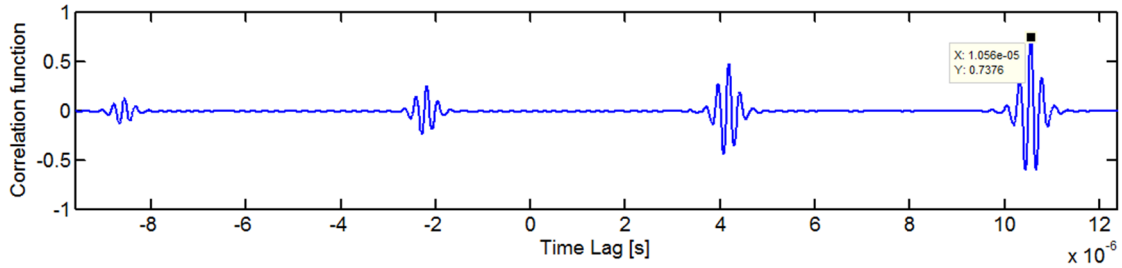

(b)

Figure 5.4. (a) Received signals measured with the 5 MHz transducer pair with and without the Al sample inserted, and (b) their cross-correlation function.

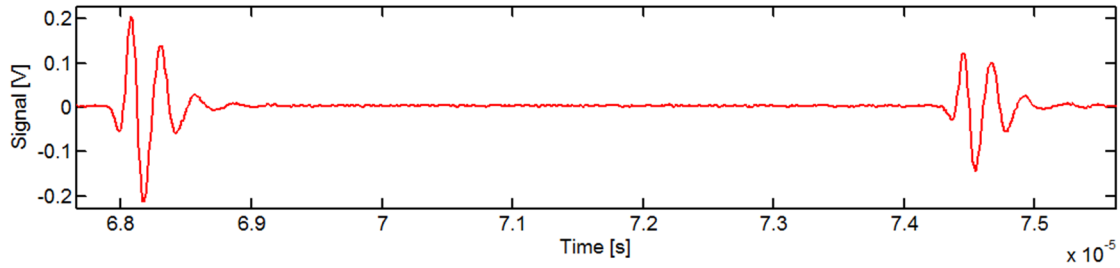

(a)

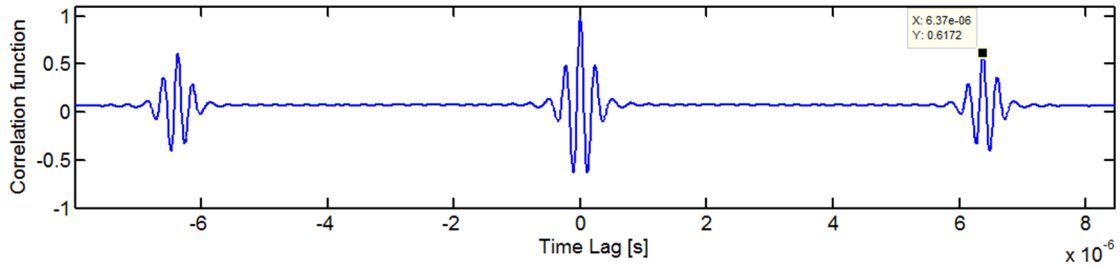

(b)

Figure 5.5. (a) Received signal measured with the 5 MHz transducer pair with Al sample inserted, and (b) its auto-correlation function.

Table 5.5. Group velocity of compressional wave in the Al sample.

Transducer pair	Method	Time-of-light	Reverberation
5 MHz	Group velocity of compressional wave (m/s)	6362 ± 18	6398 ± 7
10 MHz		6338 ± 18	6388 ± 7
References		6374 [45][46][47], 6420 [7], 6330 [48]	

From Table 5.5, the biggest difference in the compressional wave velocity in Al sample between different methods is less than 0.9%. The obtained values are close to the published values given in the literature. It was noted that aluminum comes in different alloys, and the exact composition of this Al sample is not known. The values in the references are the velocity of compressional wave in different kinds of aluminum. For the time-of-flight method, the uncertainty of the group velocity of compressional wave is approximately 0.3 % in both cases, and mainly affected by the measurement of sample thickness. However, for the reverberation method, the uncertainty is approximately 0.1%, more dependent on the measurement of transit time. Using the reverberation method, the requirement of the speed of sound in water is eliminated. The uncertainty is just only affected by the measurement of time and thickness as seen in (3.13), thus resulting in a lower uncertainty.

At an oblique incidence angle, both compressional wave and shear wave are propagated in the samples. Because the first critical angle for the water-aluminum interface is approximately 13.4°, an incidence angle of 15° was chose to determine the group velocity of shear wave. Table 5.6 presents the group velocity of shear wave in the Al sample, calculated by using (3.23) and the uncertainty of the shear wave velocity was calculated by using (3.24). The group velocity of shear wave in the Al sample measured with both transducer types was identical and relevant to published values. The uncertainty in the measurement of the group velocity of shear wave in Al sample was 0.6%. The main error probably resulted from the uncertainty in measuring the incident angle.

Table 5.6. Group velocity of shear wave in the Al sample.

Transducer pair	**Group velocity of shear wave (m/s)**
5 MHz	3121 ± 18
10 MHz	3121 ± 18
References	3111 [45][46][47], 3120 [48]

The acoustic impedance of the Al sample was calculated from the obtained group velocity of compressional wave. The acoustic impedances of Al sample at 5 MHz and 10 MHz were

17.21 MRayl and 17.18 MRayl, respectively, which are relevant to the value of 17.21 MRayl reported in [48]. Figure 5.6 shows the total transmission coefficients of compressional and shear waves as a function of incident angle, using (3.30) with the material parameters measured from experiments: ρ_{Al} = 2.69 g/cm^3, c_l = 6398.4 m/s, c_s = 3121.3 m/s (at 5 MHz), and c_l = 6388.4 m/s, c_s = 3121.5 m/s (at 10 MHz). Using (3.31), the total transmission coefficient of compressional wave measured at 5 MHz and 10 MHz with the normal incidence angle is T_L = 0.2913 and T_L = 0.2918, respectively (Figure 5.6). It should be noted that at the normal incidence angle only compressional wave is transmitted. Increasing the incident angle (θ_i), both compressional and shear waves are excited in the Al sample. When the incident angle is larger than the first critical angle of ~14°, the compressional wave is extinguished. The conversion efficiency to the shear waves then becomes greater than that for compressional waves prior to the first critical angle. As can be seen in Figure 5.6, the transmission coefficients of compressional and shear waves were equal to zero at the first critical angle (~14°), and the second critical angle (~28°), respectively. Similar diagrams are shown in [49].

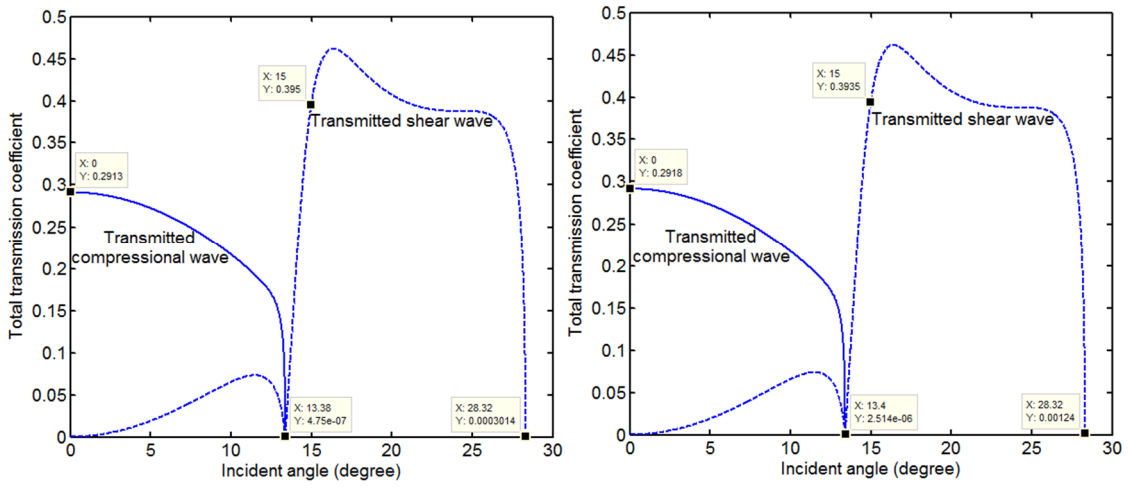

(a) (b)

Figure 5.6. Calculated total transmission coefficients of the compressional and shear waves in the Al sample based on velocity measured with (a) the 5 MHz transducer pair, and (b) the 10 MHz transducer pair at 19.5°C ± 0.5°C.

5.3.2 Phase velocity and attenuation of ultrasonic waves

Figure 5.7 shows two received signals measured with the 5 MHz transducer pair at the normal incidence angle and their power spectra. The power spectrum of the received signal with the Al

sample inserted was normalized by dividing with that without the Al sample. It was observed that with the Al sample inserted, the amplitude of the received signal decreases compared with that without the Al sample. This is natural as a portion of ultrasonic energy was reflected back into water, and the signal was attenuated when propagating in the Al sample. Based on the -6 dB bandwidth of the received pulse without Al sample inserted, the useful frequency ranges were chosen from 2.5 MHz to 6.0 MHz for the 5 MHz transducer pair, and from 5.5 MHz to 10.5 MHz for the 10 MHz transducer pair.

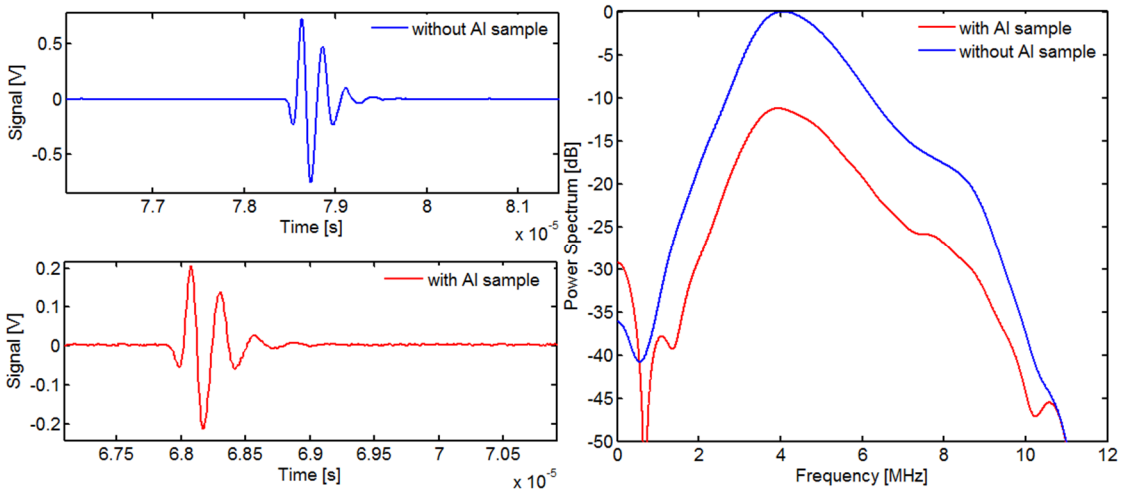

(a) (b)

Figure 5.7. (a) Received signals measured with the 5 MHz transducer pair at the normal incidence angle, with and without the Al sample inserted, and (b) their power spectra.

Figure 5.8 shows the phase velocity of compressional wave and shear wave, calculated by using (3.22) and (3.25). A small dispersion of the phase velocity was observed in the investigated frequency range from 2.5 MHz to 10.5 MHz, showing a good agreement with the published values in [50]. We found an increase of approximately 0.5% in the phase velocity of compressional wave (from 6345 m/s to 6374 m/s), and a decrease of 0.5% in the phase velocity of shear wave (from 3136 m/s to 3121 m/s) over the frequency range from 2.5 MHz to 10.5 MHz. The dispersion of the phase velocity of compressional and shear waves were 3.6 m/s/MHz and 1.9 m/s/MHz, respectively. In addition, the phase velocity values of compressional and shear waves were similar when measuring with both transducer types. The phase velocity of ultrasonic waves in the Al sample at 5 MHz and 10 MHz are close to the

group velocity shown in Table 5.5 and Table 5.6. The summary of acoustic properties of the Al sample is presented in Table 5.7, in which the uncertainty of the phase velocity of compressional and shear waves were calculated by using (3.23) and (3.26), respectively.

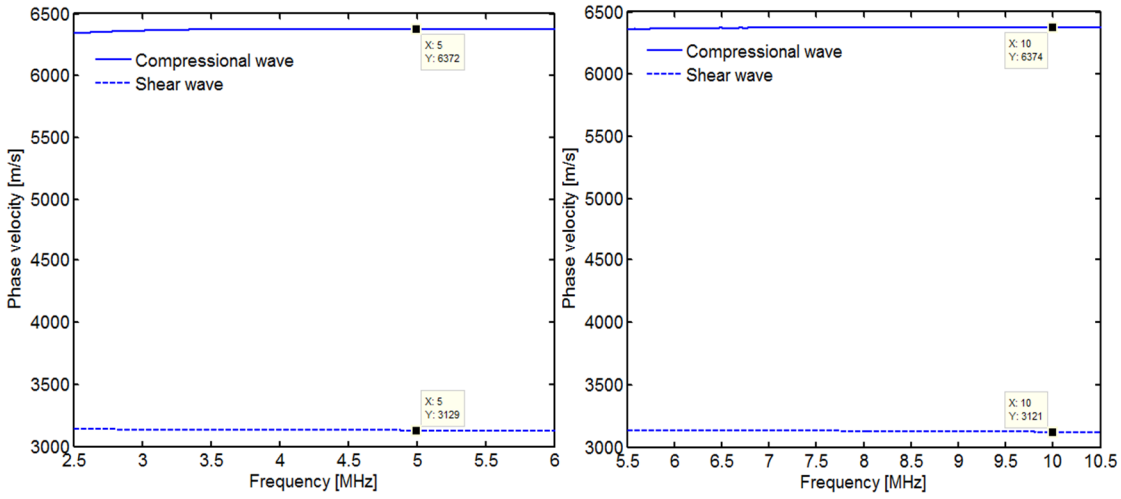

(a) (b)

Figure 5.8. Phase velocity of compressional and shear waves in the Al sample versus frequency measured with (a) the 5 MHz transducer pair, and (b) the 10 MHz transducer pair at 19.5°C ± 0.5°C.

Table 5.7. Acoustic properties of the Al sample.

Frequency	Acoustic impedance (MRayl))	Phase velocity (m/s)	
		Compressional wave	Shear wave
5 MHz	17.21	6372 ± 15	3129 ± 18
10 MHz	17.18	6374 ± 15	3121 ± 18

Similar to the measurement of group velocity, the measuring thickness of the Al sample and resolution of incident angle are the two main sources that lead to errors in measuring phase velocity of compressional and shear waves, respectively.

Using (3.22) and (3.25), the attenuation of ultrasonic waves in the Al sample, measured with the 5 MHz transducer pair, was calculated (Figure 5.9). The attenuation of compressional and shear waves in the Al sample were 0.32 ± 0.11 dB/cm and 4.18 ± 0.07 dB/cm, respectively. As can be seen in Figure 5.9, the plot diagram of the attenuation is significantly fluctuated, especially for the compressional wave attenuation. The attenuation of compressional wave is slightly higher than the published value in [51], i.e. 0.2 dB/cm.

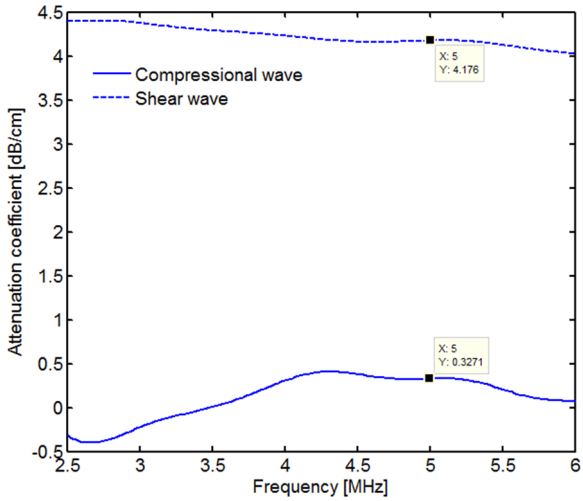

Figure 5.9. Attenuation coefficients of compressional and shear waves in the Al sample measured with the 5 MHz transducer pair at 19.5°C ± 0.5°C.

From Table 5.7, when measuring with the 5 MHz transducer pair, the acoustic impedance of Al was (Z_{Al} = 17.21 MRayl), which is quite different from the acoustic impedance of water (Z_{water} = 1.5 MRayl [7]). Thus, a part of ultrasonic energy could be reflected to water. Approximately 70% ultrasonic energy was reflected from Al because the transmission coefficient of compressional wave in Al is ~0.29. Aluminum is a low absorbing material and the fluctuated curve as shown in Figure 5.9 could be result from the influence of noises on the received signal. The attenuation of ultrasonic waves in the Al sample at 10 MHz had also measured, but the obtained results are unreliable thus they were not reported in this thesis.

Since aluminum gives strong reflections at the interfaces, while the attenuation is very low, small uncertainties in the transmission coefficients will have strong influence on the attenuation calculations, and precise attenuation measurements are difficult.

5.4 Acoustic properties of the PMMA sample

5.4.1 Group velocity of ultrasonic waves

The speed of sound in water was first measured by using the second approach (see Section 3.1), i.e. c_w = 1482.3 ± 0.4 m/s. The measurements were done at 20°C ± 0.5°C. Figure 5.10 shows the received signals measured using the 5 MHz transducer pair at the normal incidence angle,

with and without PMMA sample inserted, and their power spectra calculated using the FFT. As shown in Figure 5.10(a), the received signal with the PMMA sample inserted arrived before compared with that received without the PMMA sample inserted. The amplitude of the received signal in the presence of PMMA sample was lower than that without PMMA sample. Based on the -6dB bandwidth of the power spectrum of the received signal without sample inserted, the useful frequency ranges were chosen from 2.5 MHz to 6 MHz with the 5 MHz transducer pair. The group velocity of compressional wave was calculated by using (3.10) and (3.11).

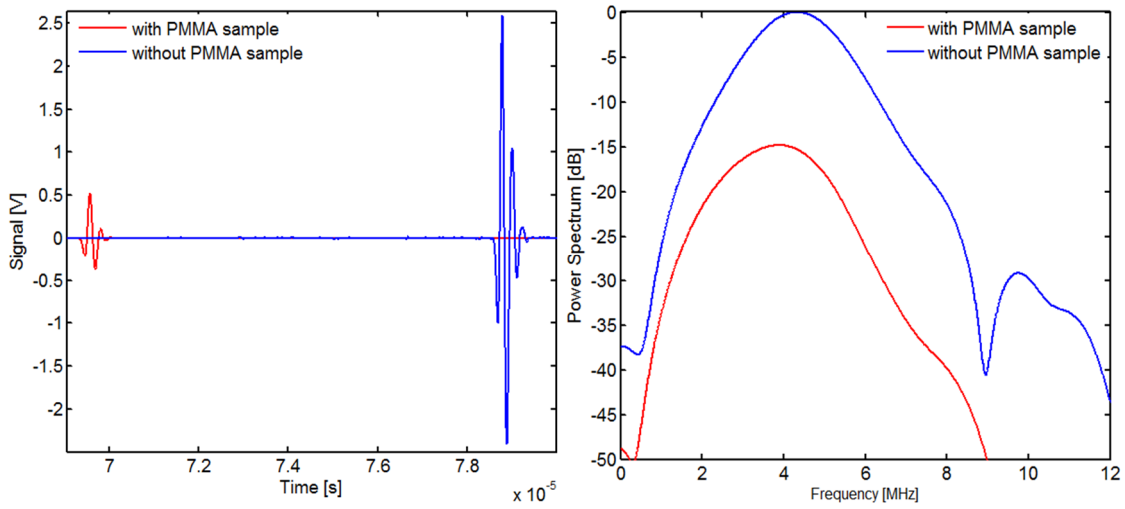

(a) (b)

Figure 5.10. (a) Received signals measured with the 5 MHz transducer pair without and with PMMA sample at the normal incidence angle, and (b) their power spectra.

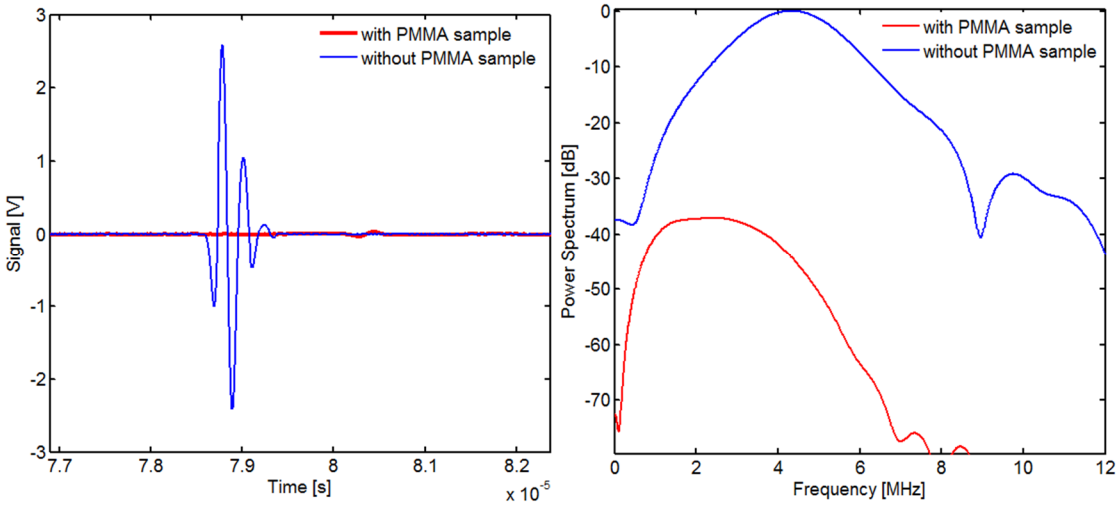

(a) (b)

Figure 5.11. (a) Received signals measured with the 5 MHz transducer pair without and with PMMA sample at an oblique angle of 38°, and (b) their power spectra.

An incident angle of 38° was chosen for the measurement of shear waves in PMMA, which is larger than the first critical angle of 32.79° for water-PMMA interface, calculated by using (3.8). In this case, the received signals and their power spectra are shown in Figure 5.11. A small-amplitude of the received signal in the case with PMMA sample inserted was observed. This could be because a large amount of ultrasound energy was absorbed while propagating through the PMMA sample at the oblique angle of 38°.

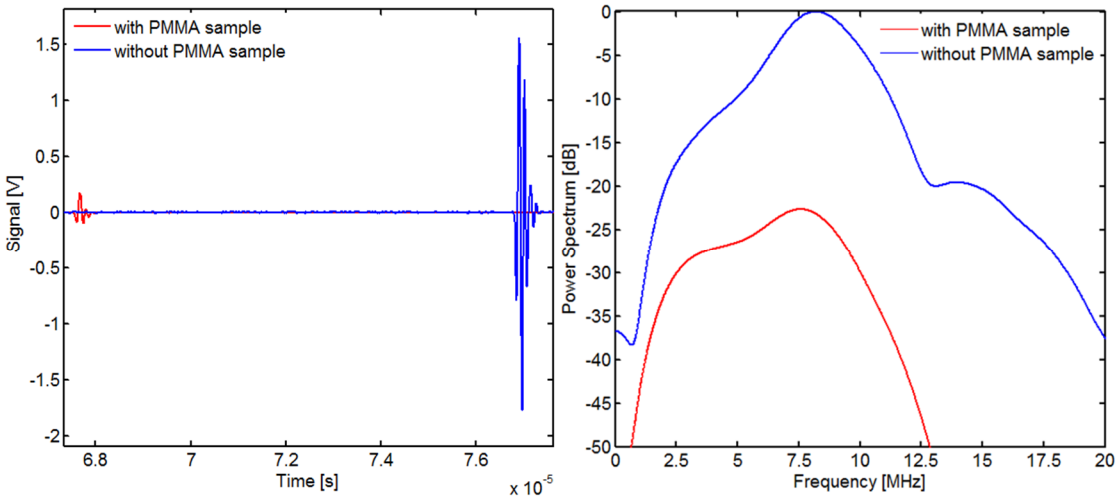

(a) (b)

Figure 5.12. (a) Received signals measured with the 10 MHz transducer pair without and with PMMA sample at the normal incidence angle, and (b) their power spectra.

For the 10 MHz transducer pair, the investigated frequency was chosen from 5.5 MHz to 10.5 MHz based on the -6 dB bandwidth of the power spectrum of the signal received without PMMA sample inserted. The received signals measured at the normal incidence angle, with and without PMMA sample inserted, and their power spectra are shown in Figure 5.12. From the observation, a higher ultrasonic energy was absorbed when ultrasonic waves propagate through the PMMA sample, compared with the previous results obtained with the 5 MHz transducer pair (Figure 5.10b).

Table 5.8 presents the comparison of the acoustic properties of PMMA between the measurement results and published values in literature, which shows a good agreement. In addition, the group velocity of compressional wave in the PMMA sample measured with both transducer types was similar.

Table 5.8. Comparison of the acoustic properties of PMMA between measurement results and published values in literature.

Transducer pair	Acoustic impedance (MRayl)	Group velocity (m/s)	
		Compressional wave	Shear wave
5 MHz	3.22	2737.1 ± 2.3	1390.1 ± 0.7
10 MHz	3.22	2739.6 ± 2.3	1400.9 ± 0.6
References	3.26 [52]	2746 ± 3 [53], 2740 [15]	1392 ± 2 [53], 1390[54]

5.4.2 Phase velocity and attenuation of ultrasonic waves

The phase velocity and attenuation of compressional and shear waves in the PMMA sample measured with the 5 MHz and 10 MHz transducer pairs are shown in Figures 5.13 and 5.14, respectively. The phase velocity of compressional and shear waves was determined by using (3.22) and (3.25), respectively. In both cases, the phase velocity of both compressional and shear waves had small negative dispersion within the investigated frequency range. For the 5 MHz transducer pair, the changes in the phase velocities of compressional and shear waves were 0.2% (from 2746.8 m/s to 2740 m/s) and 0.4% (from 1394 m/s to 1388 m/s), respectively (Figure 5.13). Their average dispersion values were ~2 m/s/MHz for both compressional and shear wave velocity. The phase velocity found for the compressional wave at 5 MHz was 2741 ± 2 m/s, which is close to the reported value in [55], i.e. 2750 m/s. As can be seen in Figure 5.13, the attenuation coefficients increased linearly with frequency, which is the characteristic of viscoelastic materials [9]. Alternatively, the attenuation increased 0.8 dB/cm/MHz for the compressional wave and 2 dB/cm/MHz for the shear wave. It was noted that the attenuation of shear wave was much larger than that of the compressional wave. The attenuation of the compressional wave at 5 MHz was 5.17 dB/cm (~59.5 Np/m), which corresponds well with published values in literature, i.e. 60.84 Np/m [55] and 61 Np/m [56].

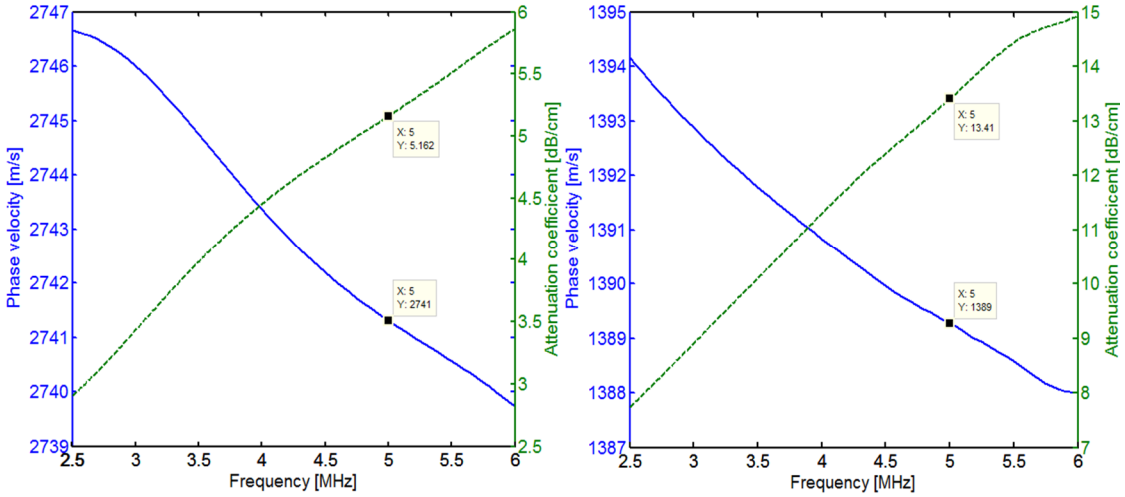

(a) (b)

Figure 5.13. Phase velocity and attenuation of (a) compressional and (b) shear waves in the PMMA sample measured at 20°C ± 0.5°C using the 5 MHz transducer pair.

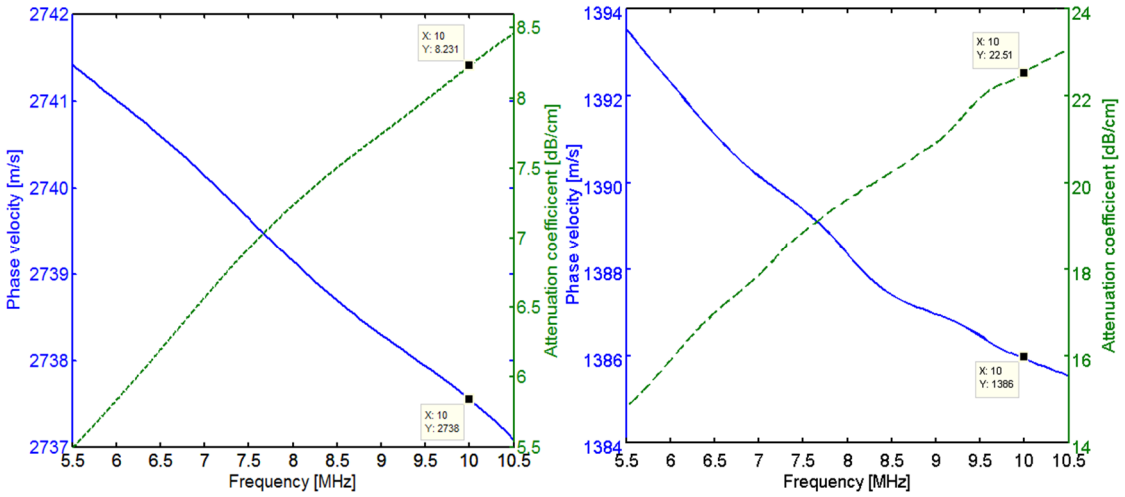

(a) (b)

Figure 5.14. Phase velocity and attenuation of (a) compressional and (b) shear waves in the PMMA sample measured at 20°C ± 0.5°C using the 10 MHz transducer pair.

For the 10 MHz transducer pair, the trend was similar (Figure 5.14). The percentage negative dispersion of the phase velocity of the compressional wave and shear wave were 0.16% (from 2741.4 m/s to 2737 m/s), and 0.6% (from 1393.5 m/s to 1385.5 m/s), respectively. Their dispersion values were ~0.9 m/s/MHz and 1.7 m/s/MHz for compressional wave and shear wave, respectively. In addition, the phase velocity of compressional wave in the PMMA sample almost doubled that of the shear wave. Moreover, the phase velocity of compressional wave was about twice that of the shear wave. The difference in the phase velocities measured at

5 MHz and 10 MHz were less than 0.3%. At 10 MHz, the phase velocity of compressional wave and shear wave was 2738 ± 2 m/ and 1386 ± 0.5 m/s, respectively. In addition, these values are close to the group velocity shown in Table 5.6. In the frequency range from 1 MHz to 10 MHz, materials have very small dispersion; thus the phase velocity is approximately equal to the group velocity [9].

According to the power-law relation, the attenuation also significantly increases when using the 10 MHz transducer pair [19]. However, the percentage increase in attenuation of the compressional wave and shear wave over the investigated range was lower, i.e. 54% (0.6 dB/cm/MHz) and 55% (1.8 dB/cm/MHz) respectively. The attenuation coefficient of compressional wave was 8.23 dB/cm (~94.76 Np/m), which is lower than the value of 105.90 Np/m reported in [55]. This difference could be because the published data was obtained at higher temperature (21.24°C). A summary of acoustic properties of the PMMA sample are presented in Table 5.9 in which the uncertainty of the attenuation measurement of compressional wave was calculated from (3.24), whereas the uncertainty of the attenuation measurement of shear wave was the standard deviation of the measurements.

Table 5.9. Acoustic properties of the PMMA sample.

Frequency	Compressional wave		Shear wave	
	Phase velocity (m/s)	**Attenuation (dB/cm)**	**Phase velocity (m/s)**	**Attenuation (dB/cm)**
5 MHz	2741 ± 2	5.17 ± 0.06	1389 ± 0.6	13.4 ± 0.4
10 MHz	2738 ± 2	8.23 ± 0.06	1386 ± 0.5	22.5 ± 0.4

Figure 5.15 shows the total transmission coefficients of compressional wave and shear wave as a function of the incident angle, calculated by using (3.30). The first critical angle for the water-PMMA interface, calculated from (3.8), was approximately 32.8° when using both transducer types. At the normal incidence angle, only compressional wave was excited in the PMMA, the compressional transmission coefficient was approximately 0.86 for both cases, and the shear transmission coefficient was zero. When increasing the incident angle prior to the first critical angle, both compressional and shear waves were excited in PMMA. At this angle, several interesting phenomena occurred. First, the transmission coefficient was zero, this means

all of the incident energy was reflected and no energy was being carried away from the surface. Second, the shear transmission coefficient was zero at the first critical angle, beyond which the shear wave reappeared. Because the velocity of shear wave in PMMA is slower than the speed of sound in water, thus no second critical angle or shear wave critical angle phenomena occurred.

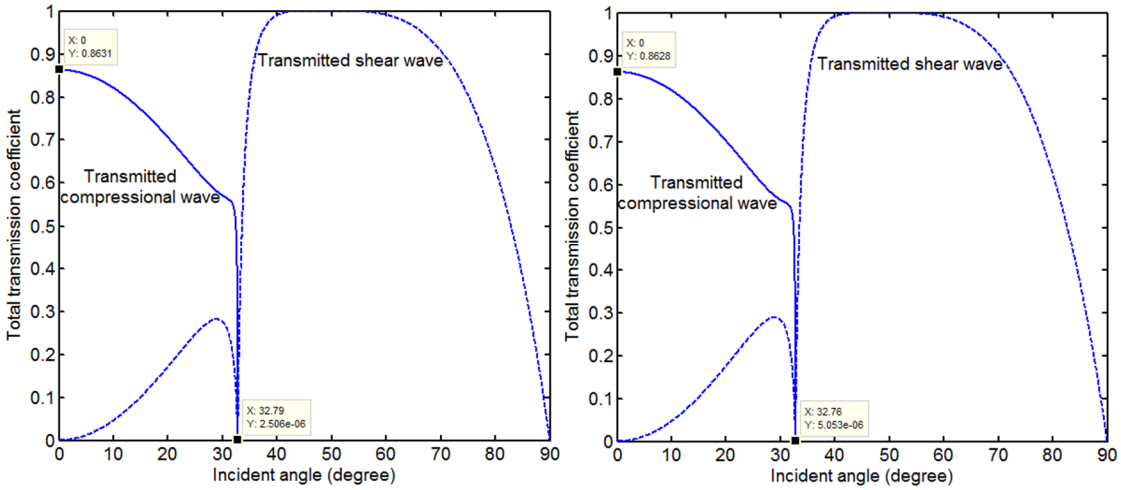

(a) (b)

Figure 5.15. Total transmission coefficients of compressional and shear waves in the PMMA sample measured with (a) the 5 MHz transducer pair, and (b) the 10 MHz transducer pair at 20°C ± 0.5°C.

5.5 Acoustic properties of the Eccosorb MF-117 samples

5.5.1 Group velocity of ultrasonic waves

The speed of sound in water was first measured by using the second approach (see Section 3.1), i.e. c_w = 1482.3 ± 0.4 m/s. Two samples of Eccosorb MF-117 with different thicknesses were characterized at 19°C ± 0.5°C. Figures 5.16 and 5.17 show the received signal measured with the 5 MHz transducer pair at the normal incidence angle, with and without the Eccosorb samples 1 and 2 inserted, and their power spectra. As can be seen from Figure 5.17(a), because of having a thin thickness of 1.94 mm, there was an interference between the first and second pulse in the received signal with the Eccosorb sample 2 inserted (red line). With a larger thickness of 5.16 mm, more ultrasonic energy was absorbed when ultrasonic waves propagate

through the Eccosorb sample 1. As a result, the amplitude of the received signal with the Eccosorb sample 1 inserted was lower than that of the Eccosorb sample 2 inserted. The group velocity of compressional and shear waves were calculated by using (3.10), (3.11), (3.23) and (3.24). The obtained results are presented in Table 5.10. In each sample, the difference in the group velocity between using the 5 MHz transducer pair and the 10 MHz transducer pair was less than 0.6%. The uncertainty in the measurement of group velocity in both samples were less than 0.3% and the uncertainty in the measurement of group velocity in the Eccosorb sample 2 was higher than that of the Eccosorb sample 1 because the thickness measurement of sample 1 is more exactly.

Table 5.10. Acoustic impedance and group velocity of ultrasonic waves in Eccosorb MF-117 samples.

Transducer pair	Sample	Acoustic impedance (MRayl)	Group velocity (m/s)	
			Compressional wave	Shear wave
5 MHz	1 (d = 5.16 mm)	10.43	2495.0 ± 7	1359.6 ± 2
	2 (d = 1.94 mm)	10.36	2480.2 ± 22	1386.9 ± 4
10 MHz	1 (d = 5.16 mm)	10.48	2507.1 ± 7	1367.2 ± 2
	2 (d = 1.94 mm)	10.38	2484.5 ± 22	1380.5 ± 4

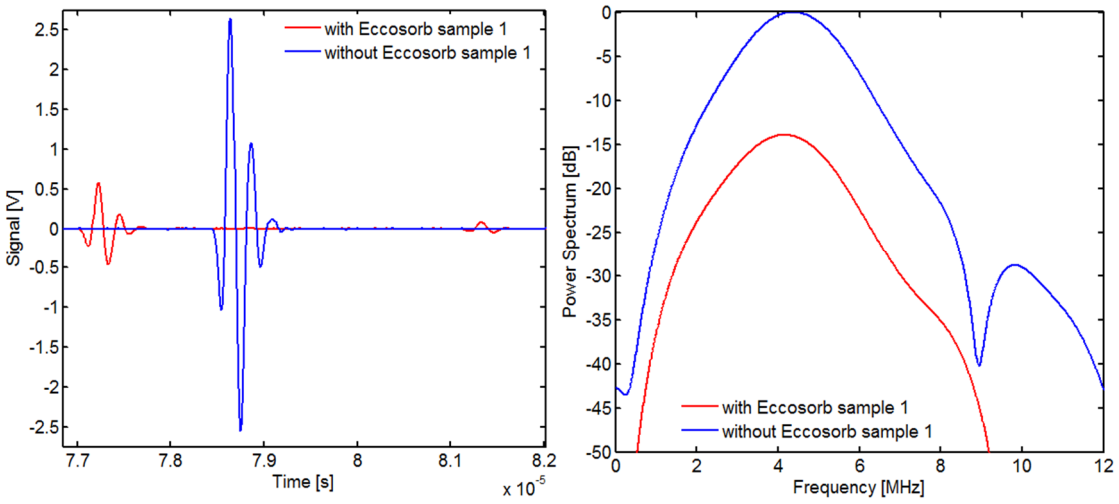

(a) (b)

Figure 5.16. (a) Received signals measured with the 5 MHz transducer pair at the normal incidence angle with and without the Eccosorb sample 1 inserted (d = 5.16 mm), and (b) their power spectra.

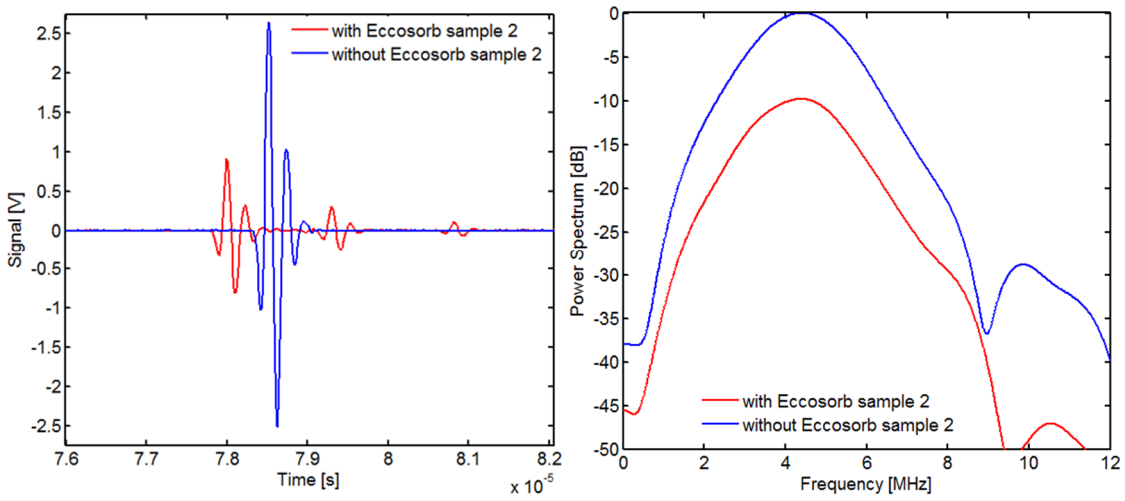

(a) (b)

Figure 5.17. (a) Received signals measured with the 5 MHz transducer pair at the normal incidence angle with and without the Eccosorb sample 2 inserted (d = 1.94 mm), and (b) their power spectra.

5.5.2 Phase velocity and attenuation of ultrasonic waves

The interference in the received signals due to the thin thickness of the Eccosorb sample 2 leads to the difficulty in accurately determining the phase velocity and attenuation of the compressional wave. Therefore, at the normal incidence angle only the phase velocity and attenuation of compressional wave in the Eccosorb sample 1 were obtained. Figures 5.18 and 5.19 show the phase velocity and attenuation of compressional and shear waves in the Eccosorb sample 1 as a function of frequency measured with the 5 MHz and 10 MHz transducer pairs, respectively. The phase velocity of compressional and shear waves in the Eccosorb sample 1 showed a small negative dispersion as in the PMMA sample, though it was slightly higher.

For the 5 MHz transducer pair, the percentage dispersion of phase velocity of compressional wave and shear wave were 0.7% (from 2511 m/s to 2493 m/s) and 1% (1372 m/s to 1358 m/s) over the investigated frequency range, respectively (Figure 5.18).Their average dispersion values were 5 m/s/MHz and 4 m/s/MHz for the phase velocity of compressional and shear waves, respectively. On the contrary, the attenuation of compressional and shear waves increased linearly with the increasing frequency. An increase of 91% (from 8.3 dB/cm to 15.9 dB/cm) for the attenuation of compressional wave and an increase of 101% (from 19.9 dB/cm to 40 dB/cm) for the attenuation of shear wave were observed over the studied frequency range.

The attenuation showed a strong dependence on frequency with the increasing of 2.2 dB/cm/MHz and 5.8 dB/cm/MHz for compressional and shear wave attenuation, respectively. It was noted that the attenuation of shear wave was higher than that of compressional wave.

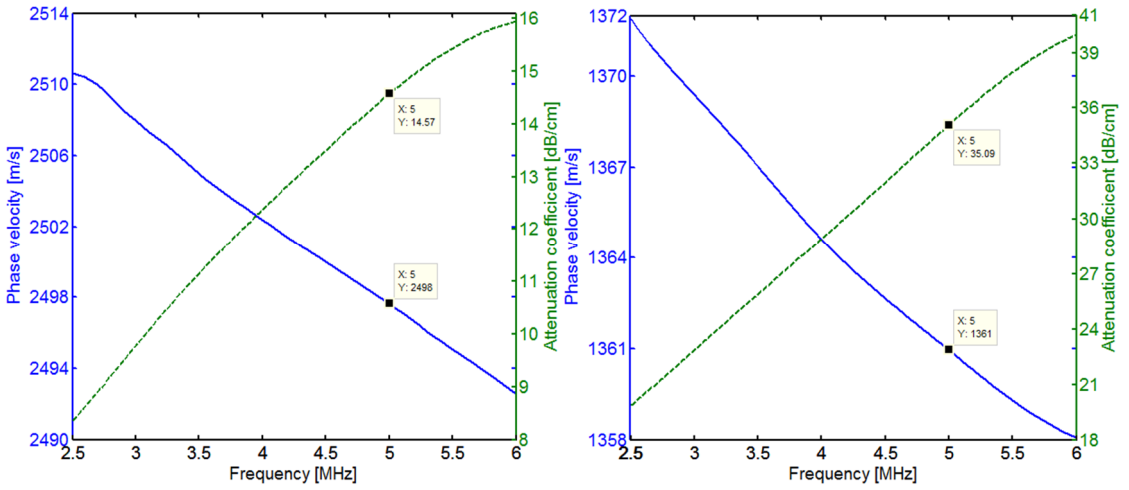

(a) (b)

Figure 5.18. Phase velocity and attenuation of (a) compressional wave and (b) shear wave in the Eccosorb sample 1 (d = 5.16 mm) measured with the 5 MHz transducer pair.

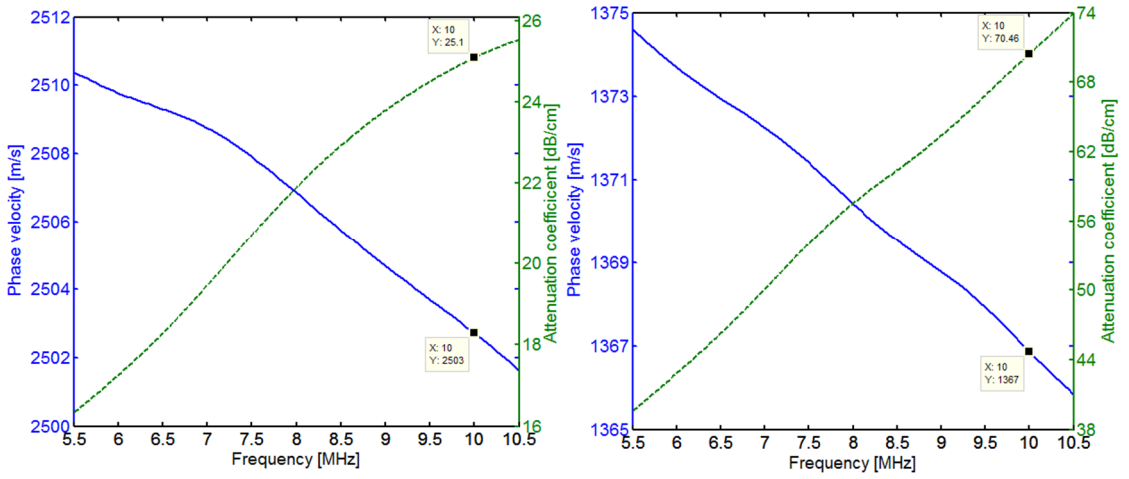

(a) (b)

Figure 5.19. Phase velocity and attenuation of (a) compressional wave and (b) shear wave in the Eccosorb sample 1 (d = 5.16 mm) measured with the 10 MHz transducer pair.

For the 10 MHz transducer pair, the phase velocity of compressional and shear waves decreased by 0.3% (from 2510 m/s to 2502 m/s) and 0.7% (from 1375 m/s to 1366 m/s) over the investigated frequency range, respectively. The negative dispersion of the phase velocity of compressional and shear waves were 1.8 m/s/MHz and 2 m/s/MHz, respectively. It was found that the differences in phase velocities at 5 MHz (2498 m/s) and 10 MHz (2503 m/s) were less

than 0.2 %. In addition, the attenuation also increased linearly with frequency, i.e. a 36% increase (2 dB/cm/MHz) in compressional wave attenuation and an 87% increase (6.8 dB/cm/MHz) in shear wave attenuation. The attenuation of shear wave was around 2.5 times higher than that of the compressional wave. At 10 MHz, a high attenuation of shear wave in the Eccosorb MF-117 sample 1 was obtained, which is 70.46 dB/cm.

Figure 5.20(a) shows a cross-section SEM image of the Eccosorb MF-117 sample. As can be seen in Figure 5.20(a), the Eccosorb MF-117 sample contains particles with diameters ranging from approximately 1 μm to 5 μm, which is much smaller than the wavelengths studied here, being larger than 250 μm (at 10 MHz) and 491 μm (at 5 MHz). This could explain to the reason why the frequency had minor effects on the phase velocity. The element analysis of one particle was also done, which showed a large percentage of iron in the particle (Figure 5.20b).

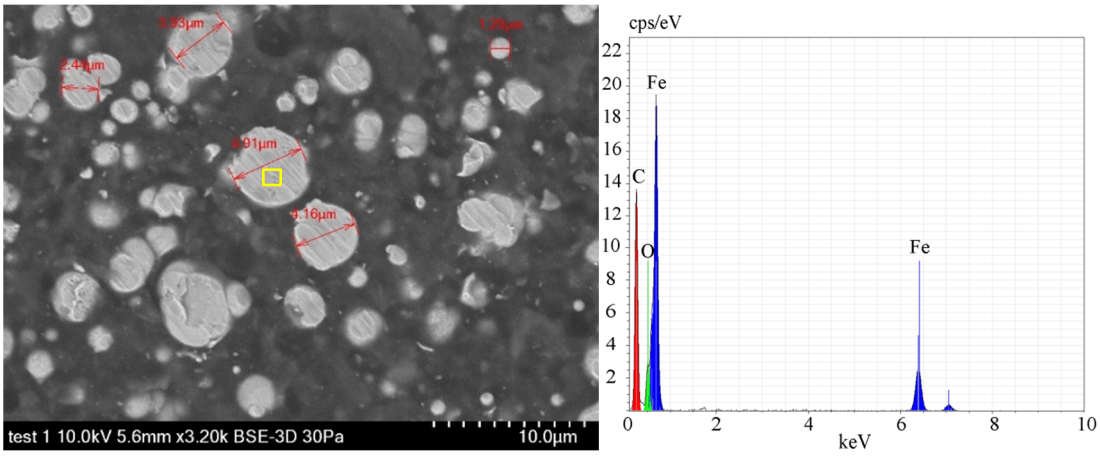

(a) (b)

Figure 5.20. (a) Cross-section SEM image of the Eccosorb MF-117 sample, and (b) the element analysis of one particle.

Figure 5.21 shows the calculated total transmission coefficients of the compressional and shear waves in the Eccosorb sample 1. Similar results were obtained when measuring with both transducer types. The first critical angle, calculated from (3.8), was around 36°. The shear wave velocity in the Eccosorb MF-117 was approximately 1361 m/s, less than the speed of sound in water at the same temperature, therefore the second critical angle at the water-Eccosorb interface could not observed.

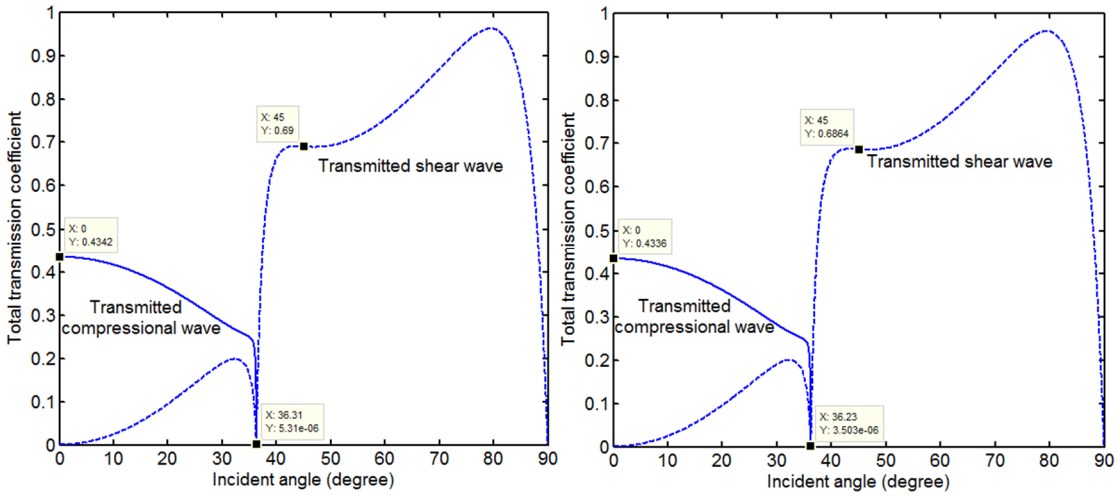

(a) (b)

Figure 5.21. Total transmission coefficients of compressional and shear waves in the Eccosorb sample 1 measured with (a) the 5 MHz transducer pair and (b) the 10 MHz transducer pair.

The phase velocity and attenuation of the shear wave in the Eccosorb sample 1 were also characterized at different incident angles (Figure 5.22). A small variation in the phase velocity and attenuation of the shear wave was observed in the incident angle range from 38° to 50°. The difference in phase velocities at different incident angles in the studied angle range was less than 0.4%.

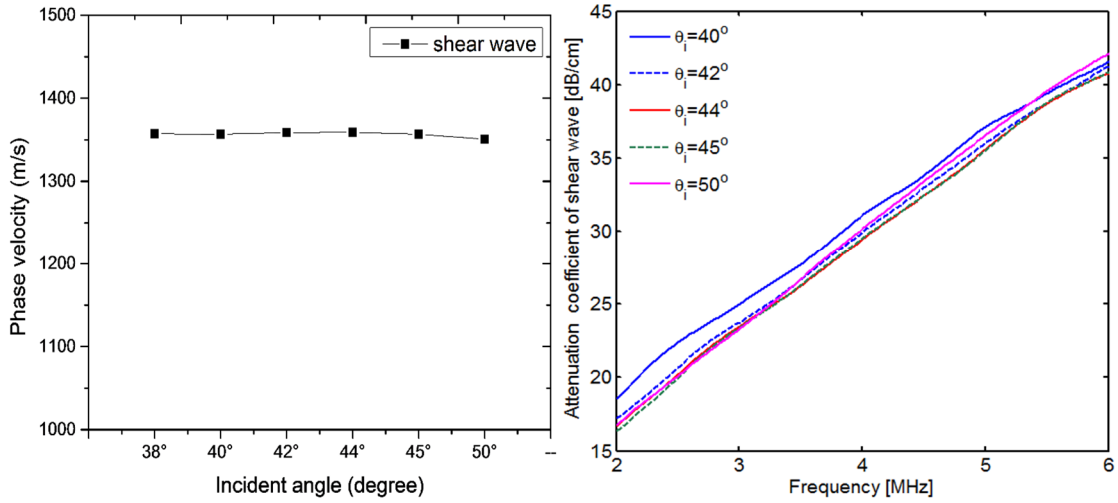

(a) (b)

Figure 5.22. (a) Phase velocity and (b) attenuation of shear wave in the Eccosorb sample 1 at different incident angles.

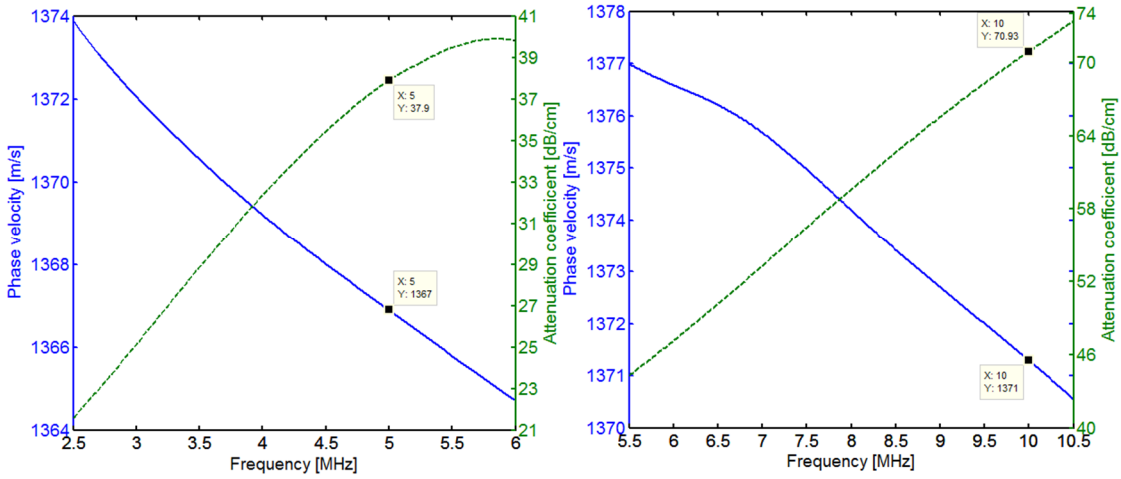

(a) (b)

Figure 5.23. Phase velocity and attenuation of shear wave in the Eccosorb sample 2 (d = 1.94 mm) measured with (a) the 5 MHz transducer pair and (b) the 10 MHz transducer pair.

Table 5.11. Acoustic properties of the Eccosorb MF-117 samples.

Transducer pair	Sample	Compressional wave		Shear wave	
		Phase velocity (m/s)	Attenuation (dB/cm)	Phase velocity (m/s)	Attenuation (dB/cm)
5 MHz	1 (d = 5.16 mm)	2498 ± 2	14.6 ± 0.6	1361 ± 1	35.1 ± 0.8
	2 (d = 1.94 mm)	X	X	1367 ± 2	37.9 ± 0.8
10 MHz	1 (d = 5.16 mm)	2503 ± 2	25.1 ± 0.6	1367 ± 1	70.5 ± 1.1
	2 (d = 1.94 mm)	X	X	1371 ± 2	70.9 ± 1.2

Figure 5.23 shows the phase velocity and attenuation of shear wave in the Eccosorb sample 2 measured with the 5 MHz transducer pair and the 10 MHz transducer pair. For the 5 MHz transducer pair, we found a decrease of 0.7% (2.6 m/s/MHz) in phase velocity and an increase of 85% (5.3 dB/cm/MHz) in attenuation of the shear wave over the frequency range from 2.5 MHz to 6 MHz. For the 10 MHz transducer pair, a decrease of 0.4% (1.2 m/s/MHz) and an increase of 66% (5.8 dB/cm/MHz) in the phase velocity and attenuation of shear wave were obtained, respectively.

The mean average values of the shear wave velocity and attenuation of the Eccosorb sample 2 over the frequency range investigated when using the 5 MHz transducer pair were 1369.5 m/s and 31 dB/cm, respectively. For the 10 MHz transducer pair, these values were 1373.3 m/s and 62 dB/cm. These values are similar to those of the Eccosorb sample 1. The acoustic properties of Eccosorb MF-117 at 5 MHz and 10 MHz measured at 19°C ± 0.5°C are

summarized in Table 5.11. It was noted that the phase velocity and attenuation of the shear wave in the Eccosorb samples 1 and 2 were almost the same, thus showing small variation in this kind of material.

5.6 Acoustic properties of the unknown material samples from Kongsberg Maritime

5.6.1 Group velocity of ultrasonic waves

Figure 5.24 shows the received signal measured with the 5 MHz transducer pair at the normal incidence angle, with and without the sample A3 inserted, and their power spectra at 20°C ± 0.5°C. For the sample B1, the received signals at the normal incidence angle, with and without sample inserted, and their power spectra are shown in Figure 5.25. As can be seen in Figures 5.24 and 5.25, the attenuation of compressional wave in the samples A, and B was quite large because the signal amplitude received with the sample inserted are much lower than that received without the sample. Table 5.10 presents the group velocity of the compressional wave in the samples A, and B with different thicknesses, calculated by using (3.10) and (3.11). Table 5.10 shows that for each material the group velocity of compressional wave was similar.

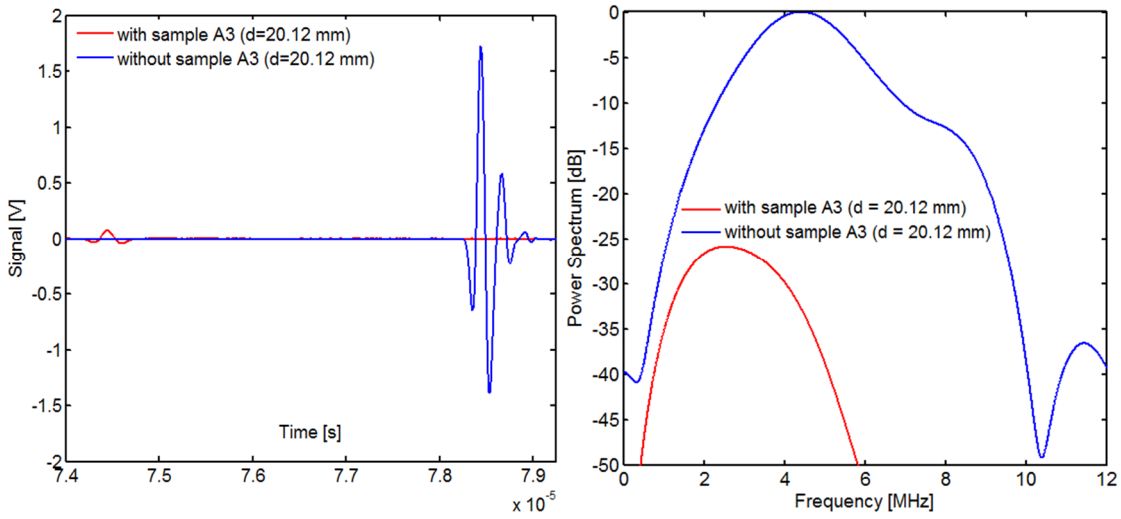

(a) (b)

Figure 5.24. (a) Received signals measured with the 5 MHz transducer pair at the normal incidence angle, with and without sample A3 inserted, and (b) their power spectra.

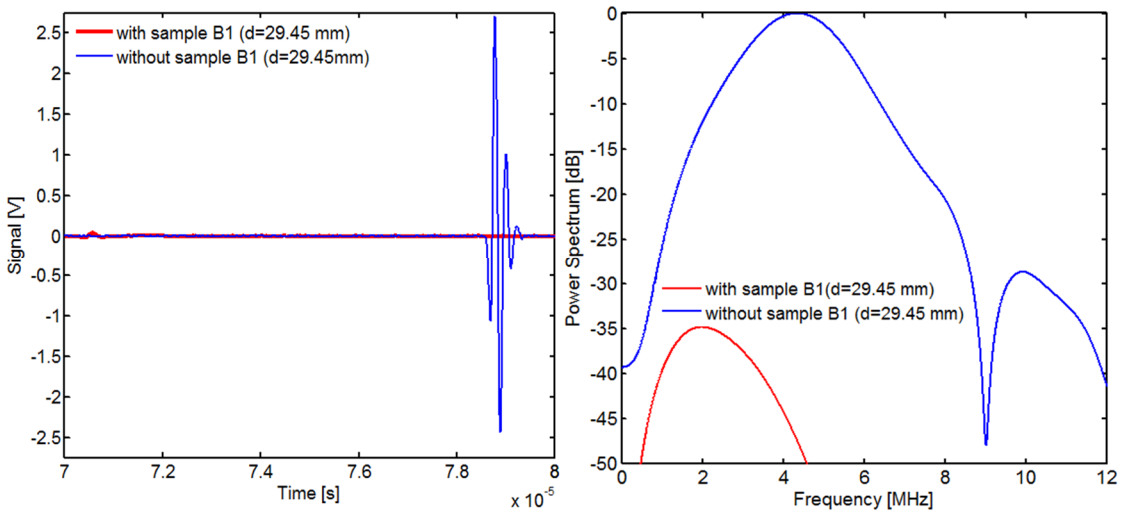

(a) (b)

Figure 5.25. (a) Received signals measured with the 5 MHz transducer pair at the normal incidence angle, with and without sample B1 inserted, and (b) their power spectra.

Table 5.12. Acoustic impedance and group velocity of compressional wave in the samples A, and B.

Sample	Acoustic impedance (MRayl)	Group velocity of compressional wave (m/s)
A1 (d = 34.67 mm)	2.43	2110.5 ± 2.0
A2 (d = 24.90 mm)	2.43	2113.2 ± 1.9
A3 (d = 20.12 mm)	2.41	2097.1 ± 2.1
B1 (d = 29.45 mm)	2.87	2519.3 ± 2.1
B2 (d = 19.06 mm)	2.87	2522.4 ± 2.0
B3 (d = 9.34 mm)	2.87	2527.2 ± 2.3

5.6.2 Phase velocity and attenuation of ultrasonic waves

Figure 5.26 shows the phase velocity and attenuation of the compressional wave in the samples A with different thicknesses as a function of frequency range from 2.5 MHz to 6 MHz. The phase velocity of the compressional wave in all samples A had a negative velocity dispersion of approximately 0.7% within the investigated frequency range (Figure 5.26a). The difference in phase velocity between the samples A was less than 0.4%. The phase velocity of compressional wave in the samples A1, A2, and A3 at 5 MHz were 2102 m/s, 2106 m/s, and 2098 m/s, respectively. The dispersion values in the sample A1, A2, and A3 were 4.6 m/s/MHz, 4.3 m/s/MHz, and 4.0 m/s/MHz, respectively. In addition, the attenuation was found to increase linearly with increasing frequency, approximately 145% for the sample A1 and 170% for the samples A2, and A3. The attenuation of compressional wave in the sample A1, A2 increased by

3.5 dB/cm/MHz and 4.2 dB/cm/MHz for sample A3. There was a small fluctuation in the phase velocity and attenuation of the compressional wave in the samples A1 and A2 in the frequency range from 5.2 MHz to 6 MHz. This could be because the effects of noises on the measurement of the velocity and attenuation. As shown in Figure 5.26(b), the attenuation of compressional wave in the samples A is quite high, thus leading to the significant decrease in the signal amplitude received with the samples A inserted (see Figure 5.24). The attenuation of compressional wave in the samples A with different thicknesses were close to each other.

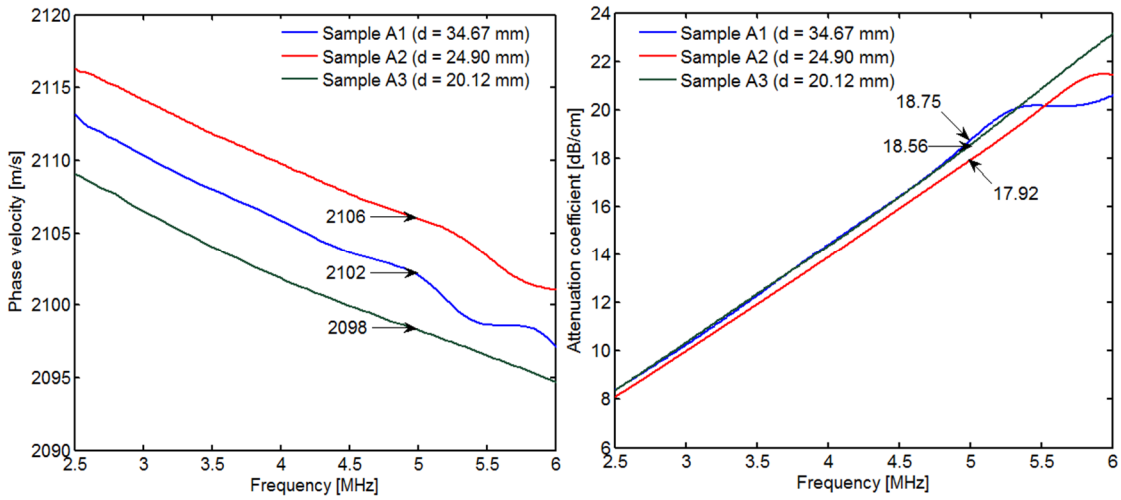

(a) (b)

Figure 5.26. (a) Phase velocity and (b) attenuation of compressional wave in the samples A with different thicknesses measured with the 5 MHz transducer pair.

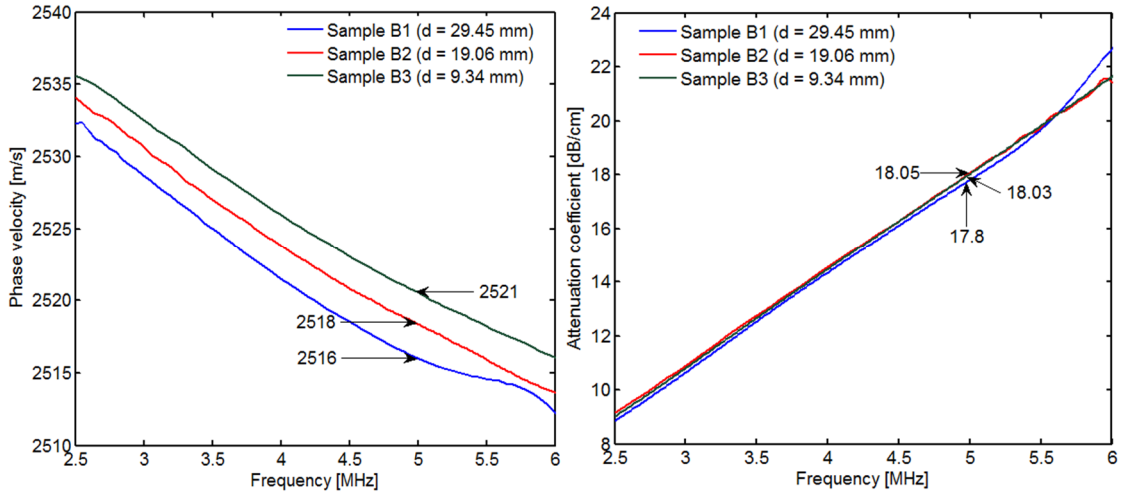

(a) (b)

Figure 5.27. (a) Phase velocity and (b) attenuation of compressional wave in the samples B with different thicknesses measured with the 5 MHz transducer pair.

The first critical angle, which was calculated from (3.8) is approximately 45° (for all samples A1, A2 and A3). The received signal at the incident angle of 50° was acquired to calculate the phase velocity and attenuation of the shear wave in the samples A1, A2, A3. Because of high attenuation, the amplitude of the received signal at the incident angle ($\theta_i=50^0$) greater was very small. This causes the interference between the received pulses and noises. Although the settings about energy, gain and attenuation parameters for the pulser-receiver (Panametrics 5800, Olympus Inc., Waltham, MA) had changed to increase the amplitude of received signals and reduce noises, but the shear wave velocity and corresponding attenuation coefficient could not be able to measure in the samples A1, A2, A3 exactly. In addition, another sample with larger surface dimension 92×58 mm^2 and smaller thickness (d = 18mm) was also used to characterize the acoustic properties of the shear wave, but still could not measure the shear wave velocity and attenuation exactly.

The phase velocity and attenuation of the compressional wave in the samples B1, B2, B3 are shown in Figure 5.27. In all the samples, the phase velocity of the compressional wave showed a similar trend to that on samples A1, A2, A3 but slightly higher. The dispersive percentage of the compressional wave phase velocity in the different samples B1, B2, B3 was approximately 0.95% within the frequency range of interest. Their average dispersion values were approximately 6.1 m/s/MHz for samples B1, B2 and 5.8 m/s/MHz for the sample B3. On the contrary, the attenuation of compressional wave showed a strong dependence on frequency with the increasing of 215% (3.9 dB/cm/MHz) for the sample B1 and 190% (3.5 dB/cm/MHz) for the samples B2, B3 within the studied frequency range. The phase velocity and attenuation of the compressional wave in different samples are summarized in Table 5.13.

As can be seen from Table 5.13, there are small differences in phase velocity and attenuation of the compressional wave in the different samples with various thicknesses. This could be because the differences in the material distribution among the samples. Comparing to the values of group velocity in Table 5.12, the difference between the values of group velocity and phase velocity was less than 0.4%. The phase velocity of the compressional wave in the

sample A3 and B1 at 5 MHz were 2098 ± 1 m/s and 2516 ± 1.3 m/s, respectively; these values are approximately 0.5% higher than given values from the company, i.e. 2090 m/s and 2500 m/s for the sample material A and B, respectively.

Using (3.8), the first critical angle of the water-sample B interface was approximately 36.1°. The received signal when the angle of incidence 40° was acquired to calculate the shear wave velocity and attenuation. However, the phase velocity of the shear wave and corresponding attenuation could not measure because of the high attenuation.

Table 5.13. Phase velocity and attenuation of compressional wave in samples A, and B at 5 MHz.

Samples	Compressional wave	
	Phase velocity (m/s)	**Attenuation (dB/cm)**
A1 (d = 34.67 mm)	2102 ± 1.5	18.75 ± 0.04
A2 (d = 24.90 mm)	2106 ± 0.9	17.72 ± 0.05
A3 (d = 20.12 mm)	2098 ± 1.0	18.56 ± 0.04
B1 (d = 29.45 mm)	2516 ± 1.3	17.80 ± 0.08
B2 (d = 19.06mm)	2518 ± 1.5	18.05 ± 0.09
B3 (d = 9.34 mm)	2521 ± 1.5	18.03 ± 0.09

5.7 Temperature effects on acoustic properties of PMMA and Eccosorb MF-117 samples

The temperature dependence of the speed of sound in water was first investigated. It has been known that the speed of sound in water depends on the temperature, and can be described as a function of the temperature by the following polynomial [43].

$$c_w = \sum_{n=0}^{5} k_n T^n \tag{5.1}$$

where T is the temperature, and k_n is the polynomial coefficients presented in Table 5.14.

Table 5.14. Polynomial coefficients [43].

n	k_n
0	$0.140238754 \times 10^{4}$
1	$0.503711129 \times 10^{1}$
2	$-0.580852166 \times 10^{-1}$
3	$0.334198834 \times 10^{-3}$
4	$-0.147800417 \times 10^{-5}$
5	$0.314643091 \times 10^{-8}$

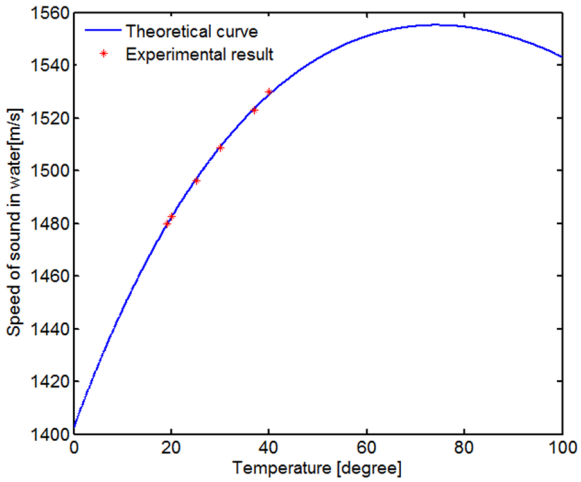

Figure 5.28. Speed of sound in water as a function of temperature.

Figure 5.28 shows the experiment results of the measurement of the speed of sound in water at different temperatures 19°C, 20°C, 25°C, 30°C, 37°C, and 40°C (red points) compared to the theoretical curve plotted from (5.1). It was observed that the speed of sound in water is relevant with theoretical results. The difference between obtained results and theoretical results was less than 0.1%. The speed of sound in water increased with temperature, reaching the maximum value of 1557 m/s at 74 °C. Above this temperature, the speed of sound in water decreased with the increasing temperature.

The temperature effects on phase velocity and attenuation of compressional and shear waves in the PMMA and Eccosorb MF-117 samples were investigated in a temperature range from 19 °C to 37°C. Figure 5.29 shows the phase velocity and attenuation of compressional and shear waves in the Eccosorb MF-117 samples versus temperature. For Eccosorb MF-117, at both 5 MHz (5 MHz transducer pair) and 10 MHz (10 MHz transducer pair), the phase velocity decreased 4.7% and the attenuation increased 30% with increasing the temperature from 19 °C to 37°C, for both compressional wave and shear wave. At 5 MHz, the phase velocity decreased from 2498 m/s to 2381 m/s for compressional wave, and from 1361 m/s to 1296 m/s for shear wave. There was only a small difference in phase velocity between 5 MHz and 10 MHz. As mentioned in section 5.4.2, Eccosorb MF-117 contains particles with diameters ranging from 1 μm to 5 μm, which are much smaller than the wavelength of the acoustic waves studied here,

(491 μm at 5 MHz, and 246 μm at 10 MHz), thus may not have significant effects on the phase velocity.

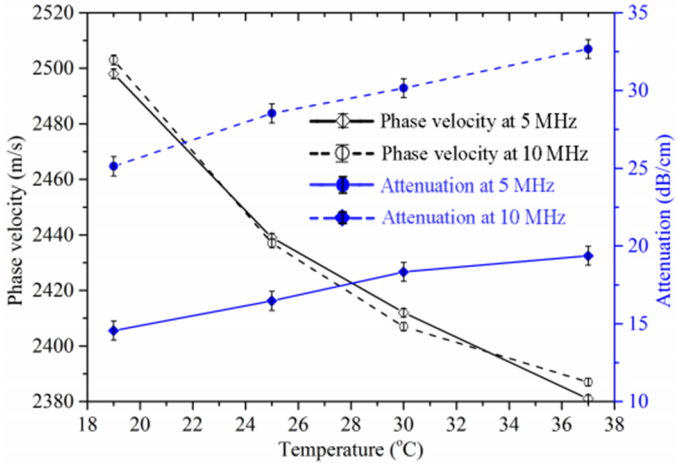

(a)

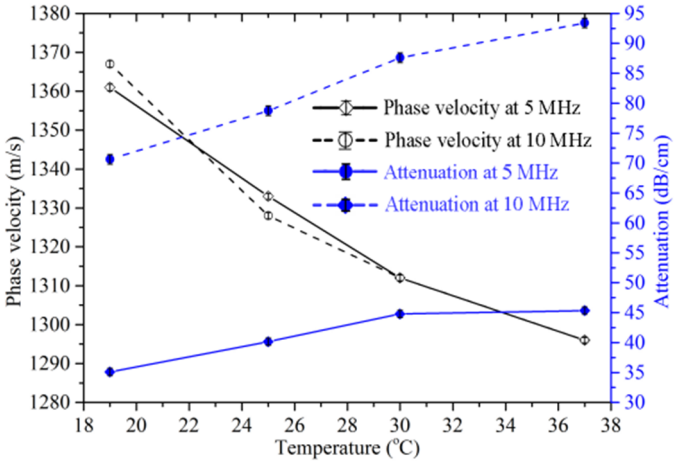

(b)

Figure 5.29. Phase velocity and attenuation of (a) compressional wave and (b) shear wave in the Eccosorb MF-117 samples versus temperature.

In addition, the attenuation was found to increase almost linearly with both frequency and temperature over the studied temperature range. According to the power-law relation, the attenuation also significantly increased when using the 10 MHz transducer pair [34]. At 5 MHz, the attenuation of compressional and shear waves increased from 14.6 dB/cm to 19.4 dB/cm and 35.1 dB/cm to 45.3 dB/cm, respectively when increasing the temperature from 19 °C to 37°C. The attenuation of the shear wave was about 2.5 times higher than that of the

compressional wave. The attenuation of shear wave in the Eccosorb MF-117 at 10 MHz was quite high, i.e. 70.6 dB/cm at 19 °C and 93.4 dB/cm at 37°C.

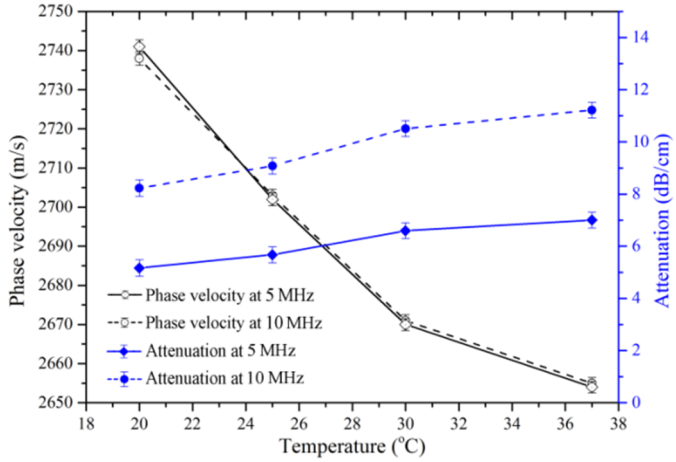

(a)

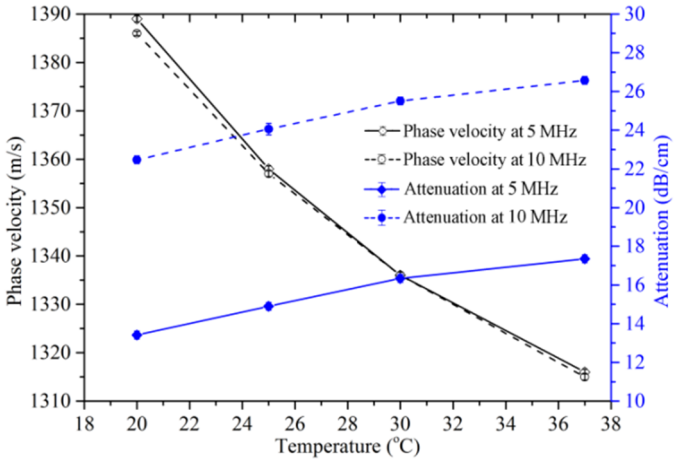

(b)

Figure 5.30. Phase velocity and attenuation of (a) compressional wave and (b) shear wave in the PMMA sample versus temperature.

The phase velocity and attenuation of the compressional and shear waves in the PMMA sample are shown in Figure 5.30. The PMMA sample showed a similar trend with the Eccosorb samples. A 3% decrease in phase velocity and a 35% increase in attenuation of the compressional wave were observed when increasing the temperature from 20℃ to 37℃, at both 5 MHz and 10 MHz. The difference in the phase velocity between 5 MHz and 10 MHz was less than 0.3%. Furthermore, the attenuation was also found to increase almost linearly with temperature over the range studied but the attenuation of ultrasonic waves in PMMA samples

were lower than that of Eccosorb MF-117. PMMA is well investigated in the literature, and our measured values were found to agree well with published values for 20℃ and 37℃. At 20℃, the phase velocity of the compressional wave in the PMMA sample measured at 5 MHz were 2741 m/s, compared with 2750 m/s in [55]; whereas 2655 m/s, compared with 2699 m/s in [55] at 37℃. The difference could come from the uncertainty in measurement temperature.

5.8 Correction for diffraction effects in attenuation measurements

Diffraction loss is may be a source of error, especially in attenuation measurement. In this section, the calculation results of the correction for diffraction effects in the attenuation measurement are presented. The diameters of the 5 MHz transducer pair (C309-SU) and the 10 MHz transducer pair (V327-SU) are 13 nm and 10 nm, respectively. Based on the phase velocity of compressional wave in the sample, the speed of sound in water, and the sample thickness, the ratio of diffraction corrections $\left|D_{Ls} / D_{Lw}\right|$ obtained with and without the sample inserted was calculated by using (3.33) and (3.34). Using (3.35), the attenuation of compressional and shear waves with the diffraction correction was calculated. The correction for diffraction effects in the attenuation measurements using the 5 MHz transducer pair and the 10 MHz transducer pair is shown in Tables 5.15 and 5.16. For most samples except Al, the ratio $\left|D_{Ls} / D_{Lw}\right|$ was very close to unity; therefore the effects of diffraction in the attenuation measurements were insignificant. The attenuation of ultrasonic waves in the Al sample with and without diffraction correction had a significant difference, especially the attenuation of compressional wave. This could be because the attenuation of ultrasonic waves in Al is very small, thus difficult to calculate exactly, as mentioned in Section 5.3.3. The attenuation of shear wave in the sample A3, and B1 is not shown due to the difficulty in measuring the attenuation of shear wave in these samples.

Table 5.15. Correction for diffraction effects in attenuation measurements using the 5 MHz transducer pair.

Sample	Attenuation of compressional wave (dB/cm)		Attenuation of shear wave (dB/cm)	
	Without diffraction correction	**With diffraction correction**	**Without diffraction correction**	**With diffraction correction**
Al	0.32	0.18	4.18	4.02
PMMA	5.17	5.15	13.40	13.40
Eccosorb sample 1	14.60	14.50	35.10	35.01
A3	18.56	18.52	X	X
B1	17.80	17.78	X	X

Table 5.16. Correction for diffraction effects in attenuation measurements using the 10 MHz transducer pair.

Sample	Attenuation of compressional wave (dB/cm)		Attenuation of shear wave (dB/cm)	
	Without diffraction correction	**With diffraction correction**	**Without diffraction correction**	**With diffraction correction**
PMMA	8.23	8.14	22.50	21.84
Eccosorb sample 1	25.10	25.09	70.50	70.47
A3	35.06	35.02	X	X
B1	34.82	34.76	X	X

5.9 Errors in measuring velocity and attenuation

There are many factors that cause errors in determination of velocity and attenuation of ultrasonic waves in sample.

5.9.1 Path length estimations

When measuring the velocity and attenuation, the precision of final results are influenced by the path length estimations such as the distance between two transducers and the sample thickness. As for the measurement of speed of sound in water, the uncertainty in determining the distance between two transducers is the main factor that leads to errors. This error is calculated by extracting the first part $\frac{\partial c_w}{\partial s}\Delta s$ in (3.2) and it results in speed error of less than 0.04%.

In measuring the uncertainty of the group velocity of compressional wave in samples using the time-of-flight method (3.11), an error in sample thickness measurement of about 0.07%

would result in a speed error of 0.3% (in the case of Al). However, in the case of Eccosorb sample 2 (d = 1.94 mm), the uncertainty in thickness measurement leads to an error of 0.9% in compressional wave velocity. As mentioned in the previous section, errors in sample thickness measurement are the main source of error when calculating the group velocity as well as phase velocity of compressional wave in sample. However, because the thickness of sample is measured by using a MT 60M length gauges with a high accuracy of ±0.5 μm [40], thus this can reduce the error of measurement speed of sound in samples.

5.9.2 Determination of arrival time

In order to measure the velocity of ultrasonic waves in samples using the time-of-flight method, the time difference between two signals can be measured by finding the difference in arrival times of the received pulses. Different criteria used to assess the arrival time of ultrasound pulses [5] will result in significant differences in calculated velocities. By using the cross-correlation algorithm, the measurement of time difference between two signals is more accurate, thus reducing errors in the measurement of velocity. Time measurement is the main source of error, e.g. 0.08% when calculating the group velocity of compressional wave using reverberation method (3.13).

5.9.3 Speed of sound in water

The uncertainty of speed of sound in water is also the source of error in determining the velocity of compressional wave and shear wave in samples. When using the published values of speed of sound in literature [43][44], the big error may be occur because the difference in temperature and purity of used water. In this thesis, the speed of sound in water is always measured before measuring the acoustic properties of sample materials. Therefore the errors from that source is reduced, it is approximately 0.05 % for the measurement of the phase velocity of compressional wave (in the case of Eccosorb MF-117). However, the speed of sound in water is also affected by the changing temperature and this could be a source of error

when measuring the velocity. It was noted that the temperature of water will increase after period time of measurement and it leads to the change in velocity. For example, the speed of sound in water at 19.5℃ is 1480.7 ± 0.4m/s while it increases to 1482.3 ± 0.4m/s at 20℃. Therefore, at 19.5℃ the temperature sensitivity is 3.2 m/s/℃. This change results in the change in speed of sound in samples.

5.9.4 Measurement of the incident angle

In practice, the uncertainty in the rotation angle measurement is ±0.5°, and it is the main source of error in measuring the shear wave velocity calculated from (3.23). However, the proportion of influence is dependent on the type of material and the oblique incidence angle used to determine the shear wave velocity. For the Al sample, because the first critical angle is small, approximately 14°, thus the shear wave velocities become sensitive with the change in incident angle. The error results from the uncertainty in the rotation angle measurement are 0.6%. On the contrary, for Eccosorb MF-117, the first critical angle is quite larger, approximately 36.3°, hence the shear wave velocities are less sensitive with the change in incident angle, as shown in Figure 5.22(a). The error from that source in the case of Eccosorb MF-117 is 0.06%.

5.9.5 Determination of the transmission coefficient

From the experimental results, the uncertainty in the determination of the transmission coefficient is the main source of errors in measuring the attenuation (3.24). For the PMMA sample, this error source leads to an error of 1% in the attenuation of compressional wave. For the attenuation of compressional wave in the Eccosorb MF-117, this error is quite high around 4%. The errors in determining the transmission coefficient is strongly influenced by the density measurement of samples. In fact, it is quite difficult to determine exactly the volume of non-flat surface samples or small volume samples. This can result in a large error in defining the density of samples, thus leading to a large error in the attenuation measurement.

5.9.6 Temperature effects

As mentioned in the section 5.7, the speed of sound in water, the phase velocity, and the attenuation of ultrasonic waves in samples are dependent on the temperature, especially for the attenuation. For PMMA samples, a 3% decrease in phase velocity and a 35% increase in attenuation were observed when increasing the temperature from 20°C to 37°C. Therefore, the temperature should be controlled when doing measurements.

Chapter 6

Conclusion

6.1 The contributions in this thesis

In this thesis, a literature review of techniques for characterizing acoustic properties of materials has been discussed. An experimental setup of the broadband through-transmission technique was implemented and calibrated in our laboratory. The LabVIEW interface for data acquisition was already available, while the MATLAB code was written from scratch to process the measured data. Using this implemented system, the acoustic properties such as the acoustic impedance, the group velocity, the phase velocity and attenuation of compressional and shear waves in both homogeneous and composite materials were measured over an investigated frequency range from 2.5 MHz to 10.5 MHz. The measurement of these properties was conducted by using two pairs of transducers with different center frequencies, one with 5 MHz and the other with 10 MHz. For samples of known materials, i.e. Al and PMMA, the measurement results showed a good agreement with published values in literature, hence, verifying the accuracy of our measurements. The differences between the obtained values of phase velocity of compressional wave in the Al, and PMMA samples are less than 0.4%, and 2.1% for the attenuation of compressional wave in the PMMA sample. For samples of unknown materials, i.e. Eccosorb MF-117 and samples from Kongsberg Maritime, their ultrasonic properties have been characterized successfully. It gives reliable data for the design and modeling of transducers.

In addition, an experimental study on how the temperature influences the phase velocity and attenuation of compressional and shear waves, measured in the PMMA and Eccosorb MF-117 materials, were also discussed in this thesis. Prior to measure the phase velocity and attenuation of acoustic waves in the samples versus the temperature, the speed of sound in water at different temperatures was measured. Our measured values were in relatively good agreement with the published values in [55]. Increasing the temperature from 19℃ to 37℃ caused a small decrease on the phase velocity of compressional and shear waves in both materials, ~3% reduction for PMMA and ~4.7% reduction for Eccosorb MF-117. However, the attenuation was found to increase with frequency. For PMMA, the attenuation increased 35% over this temperature range, while for Eccosorb MF-117, the attenuation increased 30%. It can be concluded that the temperature variation in these acoustic parameters is quite significant, and should be taken into account when using these materials in designing medical ultrasound transducers.

Furthermore, the effects of diffraction in the attenuation measurement were studied in this thesis. In all samples, the ratio of diffraction correction $\left|D_{Ls} / D_{Lw}\right|$ with and without sample inserted was very close to unity. As a result, the effects of diffraction in the attenuation measurement were insignificant and could be ignored.

Last but not least, the errors in measuring velocity and attenuation were also discussed. In the time-of-flight method, errors in sample thickness measurement were the main source of error when calculating the compressional wave velocity. However, in the reverberation method, the uncertainty was more dependent on the measurement of time. In practice, the uncertainty in the incident angle measurement was the main factor that leads to error in measuring velocity. In addition, the errors of compressional and shear wave velocity measurement were also affected by the speed of sound in water. The error in attenuation measurement was more affected by the error in the measurement of transmission coefficients. Furthermore, temperature should be controlled when doing measurements because of its effects on acoustic properties of materials,

especially attenuation. From results that have been achieved, we can use this acoustic characterization system to investigate samples in the future.

When characterizing acoustic material samples using this technique, the sample thickness should be thick enough to ensure that the first and second pulses of the received signal do not overlap. However, the sample thickness should be also not too thick; otherwise, the signal will be attenuated when propagating through the sample, which results in a very small amplitude of the received pulses at the receiver. As a result, it is difficult to distinguish the received pulses and noises. In addition, the surface dimensions of the sample should be large enough to ensure that when rotating the sample beyond the first critical angle, the acoustic waves can impinge onto the sample surface. From the obtained results of Eccosorb MF-117, the measuring capability of the experimental setup is around 50° for the incident angle. For the sample having the first critical angle of the water-sample interface larger than 50°, the shear wave and corresponding attenuation can be measured by changing the immersion liquid in order to decrease the critical angle [54].

6.2 Future works

Based on the results presented in this thesis, following recommendations are made for further works:

- Changing the immersion liquid to reduce the critical angle when it is larger than 50° for measuring the phase velocity and attenuation of shear wave in the sample.
- Fabricating a composite material, e.g. Tungsten-Epoxy composite, and characterizing the acoustic properties of the fabricated material.
- Implementing the theoretical models for composite materials, i.e. the Voigt, Reuss, ATA and Devaney models, to predict the velocity of compressional and shear waves in the fabricated material, and to compare with the measurement results.

Appendix

A1 MATLAB code for calculating the phase velocity of compressional wave

```
%% Plot the phase velocity of the compressional wave of Eccosorb MF-
117 at 19 degree
% Without sample
wfm=readwfm('Received pulse without Eccosorb MF-117 at 19
degree.wfm');
vi=wfm.v;
vic=vi(495:735);
Nw=length(vic);
Nf=2002;
vpw=zeros(Nf,1);
vpw(1:Nw)=vic;
[vhm khm]=max(vpw);
Hw=circshift(vpw,-khm);
Fi=fft(Hw);
phiw=angle(Fi);
% With sample
wfm1=readwfm('Received pulse with Eccosorb MF-117 at normal incidence
angle_19 degree.wfm');
vis=wfm1.v;
visc=vis(495:590);
N0=length(visc);
Nf=2002;
vp=zeros(Nf,1);
vp(1:N0)=visc;
[vm km]=max(vp);
Hs=circshift(vp,-km);
Fs=fft(Hs);
phis=angle(Fs);
phi=phis-phiw;
f=(0:wfm.Np-1)/wfm.Np/wfm.dt;
b=2*pi*f*(km-khm)*(wfm.dt);
c_w=1479.231; % the speed of sound in water at 19 degree
c=(phi'+b).*c_w;
d=5.1595*0.001; % sample thickness
e=2*pi*f*d;
h=c./e;
```

```
h=1+h;
c_l=c_w./h; % phase velocity of the compressional wave
plot(f./10.^6,c_l,'b');
xlabel('Frequency [MHz]');
ylabel('Phase velocity [m/s]');
xlim ([2 6]);
%% THE END
```

A2 MATLAB code for calculating the attenuation coefficient of compressional wave

```
%% Plot the attenuation of the compressional wave of Eccosorb MF-117
at 19 degree
% Without sample
wfm=readwfm('Received pulse without Eccosorb MF-117 at 19
degree.wfm');
vi=wfm.v(640:735);
Nfft=4096;
Fi=fft(vi, Nfft);
A_w=abs(Fi);
% With sample
wfm1=readwfm('Received pulse with Eccosorb MF-117 at normal incidence
angle_19 degree.wfm');
vi1=wfm1.v(495:590);
Nfft=4096;
Fi1=fft(vi1, Nfft);
A_s=abs(Fi1);

fs=1/wfm.dt;
f=(0:Nfft-1)/Nfft*fs;
TL=0.4342;
f=f/10.^6;
d=0.51595; % sample thickness in centimeter
a=(TL.*A_w)./A_s;
b=log(a);
c=b./d;
e=8.686.*c;
alpha_l=e; ; % attenuation of the compressional wave
plot(f,alpha_l,'b')
xlabel('Frequency [MHz]');
ylabel('Attenuation coefficient [dB/cm]');
xlim ([2.0 6.0]);
%% THE END
```

A3 MATLAB code for calculating the phase velocity of shear wave

```
%% Plot the phase velocity of the shear wave of Eccosorb MF-117 at 19
degree
% Without sample
wfm=readwfm('Received pulse without Eccosorb MF-117 at 19
degree.wfm');
vi=wfm.v;
vic=vi(635:740);
Nw=length(vic);
Nf=2002;
vpw=zeros(Nf,1);
vpw(1:Nw)=vic;
[vhm khm]=max(vpw);
Hw=circshift(vpw,-khm);
Fi=fft(Hw);
phiw=angle(Fi);
% With sample
wfm1=readwfm('Received pulse with Eccosorb MF-117 at critical
incidence angle of 45_19 degree.wfm');
vis=wfm1.v;
visc=vis(635:770);
N0=length(visc);

Nf=2002;
vp=zeros(Nf,1);

vp(1:N0)=visc;
[vm km]=max(vp);
Hs=circshift(vp,-km);
Fs=fft(Hs);
phis=angle(Fs);
phi=phis-phiw;
f=(0:wfm.Np-1)/wfm.Np/wfm.dt;
b=2*pi*f*(km-khm)*(wfm.dt);
c_w=1479.231; % the speed of sound in water at 19 degree

c=(phi'+b).*c_w;
d=5.1595*0.001; % sample thickness in centimeter
e=2*pi*f*d;
h=c./e;
theta=pi/4;
m=(h+cos(theta)).^2;
n=((sin(theta)).^2)+m;
ms=sqrt(n);
c_s=c_w./ms; % phase velocity of the shear wave
plot(f./10.^6,c_s,'b--');
xlabel('Frequency [MHz]');
ylabel('Phase velocity [m/s]');
xlim ([2 6]);
%% THE END
```

A4 MATLAB code for calculating the attenuation coefficient of shear wave

```
%% Plot the attenuation of the shear wave of Eccosorb MF-117 at 19
degree
% No sample
wfm=readwfm('Received pulse without Eccosorb MF-117 at 19
degree.wfm');
vi=wfm.v(635:740);
Nfft=4096;
Fi=fft(vi, Nfft);
A_w=abs(Fi);
% With sample
wfm1=readwfm('Received pulse with Eccosorb MF-117 at critical
incidence angle of 45_19 degree.wfm');
vi1=wfm1.v(660:780);
Nfft=4096;
Fi1=fft(vi1, Nfft);
A_s=abs(Fi1);

fs=1/wfm.dt;
f=(0:Nfft-1)/Nfft*fs;
TS=0.69;
f=f/10.^6;
Vi=1479.231; % the speed of sound in water at 19 degree
Vs=1361; % phase velocity of the shear wave
thetai=pi/4;
d=0.516; % sample thickness in centimeter
thetas=asin((Vs/Vi).*sin(thetai));
a3=(log(TS.*(A_w./A_s))).*(cos(thetas)./d);
alpha_s=8.686*a3; % attenuation of the shear wave
plot(f,alpha_s,'b--')
xlabel('Frequency [MHz]');
ylabel('Attenuation  coefficient [dB/cm]');
xlim ([2 6]);
%% THE END
```

A5 MATLAB code for calculating the total transmission coefficient of compressional and shear waves

```
%% Plot the total transmission coefficient of the compressional wave
% Tl
g=[0:pi/10800000:0.63375];% theta i
a=998.405; % the density of water at 19 degree
b=4180; % the density of Eccosorb
Vs=1361; % the velocity of the compressional wave at 5MHz
```

```
Vl=2498; % the velocity of the shear wave at 5MHz
Vi=1479.231; % the speed of sound in water at 19 degree
s=sin(g);
c=asin((Vs/Vi)*s);
d=asin((Vl/Vi)*s);
Zl=(b*Vl)./(cos(d));
Zs=(b*Vs)./(cos(c));
Z=(a*Vi)./(cos(g));
Tl1=(a/b)*((2.*Zl.*(cos(2.*c))).//((Zl.*((cos(2.*c)).^2))+(Zs.*((sin(2.
*c)).^2))+Z));
Tl2=(Vi.*(cos(d))./(Vl.*(cos(g)).*(cos(2.*c)));
Tl3=1-((Z+Zs.*((sin(2.*c)).^2)-
Zl.*((cos(2.*c)).^2))./(Z+Zs.*((sin(2.*c)).^2)+Zl.*((cos(2.*c)).^2)));
Tl=Tl1.*Tl2.*Tl3; % total transmission coefficient of the
compressional wave
gg=(180.*g)./pi;

%% Plot the total transmission coefficient of the shear wave
% Ts
gs=[0:pi/10800000:pi/2];
s=sin(gs);
c=asin((Vs/Vi)*s);
d=asin((Vl/Vi)*s);
Zl=(b*Vl)./(cos(d));
Zs=(b*Vs)./(cos(c));
Z=(a*Vi)./(cos(gs));
Ts1=(-
a/b)*((2.*Zs.*(sin(2.*c))).//((Zl.*((cos(2.*c)).^2))+(Zs.*((sin(2.*c)).
^2))+Z));
Ts2=tan(gs)./(2.*((sin(c)).^2));
Ts3=1-((Z+Zl.*((cos(2.*c)).^2)-
Zs.*((sin(2.*c)).^2))./(Z+Zl.*((cos(2.*c)).^2)+Zs.*((sin(2.*c)).^2)));
Ts=abs(Ts1.*Ts2.*Ts3); % the total transmission coefficient of the
shear wave
ggs=(180.*gs)./pi;
plot(ggs,Ts,'b--') % plot the total transmission coefficient of the
shear wave
hold on
plot(gg,Tl,'b'); % plot the total transmission coefficient of the
compressional wave
xlabel('Incident angle (degree)');
ylabel('Total transmission coefficient');
%% THE END
```

Publications

International conference papers

[1] **Hoa T. K. Tran**, Tung Manh, and Lars Hoff, “Measurements of acoustic properties using ultrasonic through transmission technique,” in Proc. of IMAPS Nordic 2016 Conference, Tønsberg, June 5-7, 2016.

[2] **Hoa T. K. Tran**, Tung Manh, Tonni Franke Johansen, and Lars Hoff, “Temperature effects on ultrasonic phase velocity and attenuation in Eccosorb and PMMA,” **submitted to** IEEE-International Ultrasonics Symposium, Tours, September 18-21, 2016.

.

Publications Enclosed in This Thesis

Paper 1

Title:	"Measurements of acoustic properties using ultrasonic through transmission technique"
Author:	**Hoa T. K. Tran**, Tung Manh, and Lars Hoff
Proceeding:	IMAPS Nordic 2016 Conference
Place:	Tønsberg, Norway
Date:	June 5-7, 2016

Measurements of Acoustic Material Properties Using Ultrasonic Through Transmission Technique

Hoa T. K. Tran[1], Tung Manh[1] and Lars Hoff[1,*]

[1]Department of Micro and Nano Systems Technology, University College of Southeast Norway, Norway

*Contacting author: Lars.Hoff@hbv.no

Abstract

A method to measure phase velocity and attenuation of compressional and shear waves has been developed using a broadband through-transmission technique. Two pairs of transducers were used, one pair with center frequency 5 MHz (Olympus C309-SU), and the other pair with center frequency 10 MHz (Olympus V327-SU). The method was tested on the homogeneous material Polymethylmethacrylate (PMMA) and the composite material Eccosorb MF-117. Our results were compared with published values for the PMMA material, showing a good agreement with literature, hence, verifying the accuracy of our method. In addition, the temperature in the sample was varied from 19℃ to 37℃, to investigate how this influences the parameters. A small variation of around 3% was found for the phase velocity, while the temperature influence on the attenuation was considerably larger, increasing 30% when temperature was changed from 19℃ to 37℃. These acoustic properties and their temperature effects are essential for transducer designs, especially for clinical applications.

Key words: Ultrasound; Phase velocity; Attenuation; Through-transmission technique

Introduction

Acoustic properties of materials such as phase velocity and attenuation are important material properties in many ultrasonic applications, i.e. non-destructive evaluation and ultrasound tissue characterization [1,2]. Design of ultrasound transducers for e.g. clinical applications requires reliable characterization of these properties. Therefore, characterization of the acoustic properties of materials especially transducer materials is necessary to give data for the design and modeling of transducers. For many materials, their acoustic properties vary with both temperature and frequency. However, due to the lack of previous reported data on the temperature dependence of the velocity and attenuation of acoustic waves in composite materials, especially Eccosorb MF-117, the characterization of temperature effects on acoustic properties of materials should be taken. Among the techniques reported in literature, acoustic through-transmission has been considered as the most widely used method for characterizing acoustic material properties. Using this technique with mode conversion, allows measuring acoustic properties of both compressional waves and shear waves in solids, including porous or composite materials [3].

In this paper, the through-transmission technique was employed to characterize samples of one homogenous material, PMMA, as reference because PMMA has well-known acoustic properties. From that, the accuracy of our implemented system was confirmed. Thereafter, a composite material, Eccosorb MF-117 was chosen to characterize because this material has many potential applications such as absorbers and terminations in waveguides, and is used on sensors in ultrasound transducers [4]. The phase velocity and attenuation of both compressional and shear waves in these samples were measured by using two pairs of transducers with different center frequencies of 5 MHz and 10 MHz, and compared with literature. In addition, temperature effects on phase velocity and attenuation of the compressional wave in the PMMA and Eccosorb MF-117 samples were also studied.

Theoretical background

Figure 1 shows the basic principle of the through-transmission technique for characterizing acoustic properties of materials. A through-transmission system consists of a transmitting transducer and a receiving transducer, placed at opposite sides of a sample immersed in a water tank. Acoustic pulses are recorded with and without a sample inserted into the acoustic transmission path. The phase velocity and attenuation of the acoustic waves are determined by comparing the spectra of the received signals with and without samples inserted [5], calculated by Fourier transform of the received pulses. For measuring the compressional wave, an acoustic wave with a normal incidence angle ($\theta_i=0$) is used. The first pulse received at the receiver, without sample inserted, is first acquired. The Fast Fourier Transform (FFT) algorithm is then

used to calculate the magnitude (A_w) and the phase of spectra (ϕ_w) of the acquired signal. After that, the sample is inserted between the two transducers and the second received signal is measured. Its magnitude (A_s) and phase of spectra (ϕ_s) are also computed. The phase velocity (c_l) and the attenuation coefficient (α_l) are calculated from [3,6]:

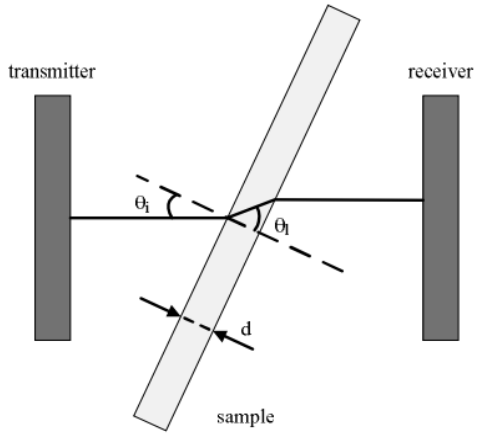

Figure 1: Principle of the through-transmission technique.

$$c_l = \frac{c_w}{1+\frac{(\phi_s-\phi_w+2\pi f\tau)c_w}{2\pi fd}}, \qquad \alpha_l = \alpha_w + \ln\left(\frac{T_{TP}A_w}{A_s}\right)/d, \tag{1}$$

where c_w is the speed of sound in water, d is the sample thickness, τ is the trigger delay of the two time windows used to acquire the signal, T_{TP} is the total transmission coefficient for the compressional wave, and α_w is the attenuation of water. Typically, α_w is much smaller than α_l and can be neglected.

With an incident angle greater than the critical angle of the compressional wave, only the shear wave can propagate through the sample. In this case, the phase velocity (c_s) and the attenuation coefficient (α_s) of the shear wave can be calculated by [3,6]:

$$c_s = \frac{c_w}{\sqrt{\sin^2\theta_i + \left[\frac{(\phi_s-\phi_w+2\pi f\tau)c_w}{2\pi fd}+\cos\theta_i\right]^2}}, \qquad \alpha_s = \alpha_w\cos(\theta_l-\theta_i)+\ln\left(\frac{T_{TS}A_w}{A_s}\right)\frac{\cos\theta_l}{d}, \tag{2}$$

where θ_i is the angle of incidence, θ_l is the refractive angle of the shear wave calculated from Snell's law, and T_{TS} is the total transmission of the shear wave.

Experimental setup

Figure 2 shows the experimental setup of the through transmission technique for characterizing the phase velocity and attenuation of materials. Two pairs of transducers with different center frequencies, 5 MHz (Olympus C309-SU) and another 10 MHz (Olympus V327-SU) were used. The sample was placed between the two transducers which were coaxial aligned and immersed in a cylindrical water tank, and could be rotated using a manual 360° rotation stage. A pulse-receiver (Panametrics 5800, Olympus Inc., Waltham, MA) was used to excite the transmitter with short electrical pulses. The received pulses, after transmission through the sample, were recorded and sampled by a digital oscilloscope (LeCroy 9310AM, Teledyne LeCroy, Chestnut Ridge, NY) at a sampling rate of 100 MS/s. The pulses received by the oscilloscope were transferred to a computer using the GPIB interface, using software written in LabVIEW (National Instruments Inc., Austin, TX) and stored to disk. Processing was done offline using our developed codes in MATLAB software (The MathWorks, Natick, MA).

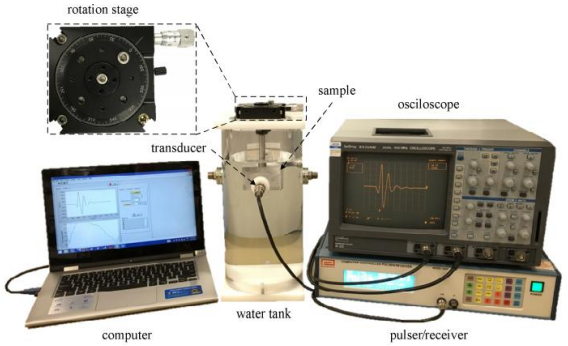

Figure 2: Experiment setup for characterizing acoustic material properties.

Results and discussions

Prior to measuring the acoustic properties of the samples, their densities were measured. The density of the PMMA and Eccosorb MF-117 samples were found to 1.18±0.06 g/cm^3 and 4.18±0.20 g/cm^3, respectively. Based on the -6 dB bandwidth of the power spectrum of the received signal without sample inserted, the useful frequency ranges were chosen from 2.5 MHz to 6 MHz for the 5 MHz transducer pair and from 5.5 MHz to 10.5 MHz for the 10 MHz transducer pair.

Figures 3 and 4 shows the phase velocity and attenuation of compressional and shear waves in the PMMA samples, measured at 20±0.5°C with the 5 MHz transducer pair and 10 MHz transducer pair, respectively. In both cases, the phase velocity of both compressional and shear waves have a small negative dispersion within the investigated frequency range. For the 5 MHz transducer pair, the changes in phase velocities of the compressional and shear waves are 0.2% and 0.4%, respectively (Figure 3), or an average dispersion of approximately 2

m/s/MHz for both compressional and shear wave velocities. The phase velocity found for the compressional wave at 5 MHz is 2741 m/s, which is close to the value reported in [7], i.e. 2750 m/s. In contrast to the phase velocity, the attenuation coefficients increase linearly with frequency, i.e. 0.8 dB/cm/MHz for the compressional wave and 2.0 dB/cm/MHz for the shear wave. Moreover, the attenuation of the shear wave is higher than that of the compressional wave over the investigated frequency range. At 5 MHz, the attenuation of compressional wave is 5.16 dB/cm (59.43 Np/m), which corresponds well to published values, i.e. 60.84 Np/m [7] and 61 Np/m [8].

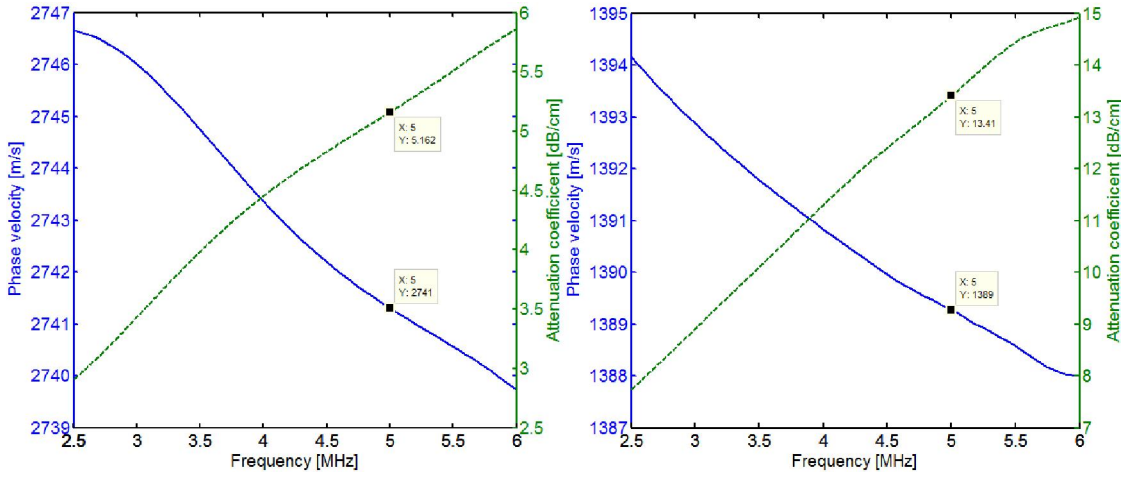

(a) (b)

Figure 3: Phase velocity and attenuation of the (a) compressional and (b) shear waves in PMMA samples measured at 20±0.5°C with the 5 MHz transducer pair.

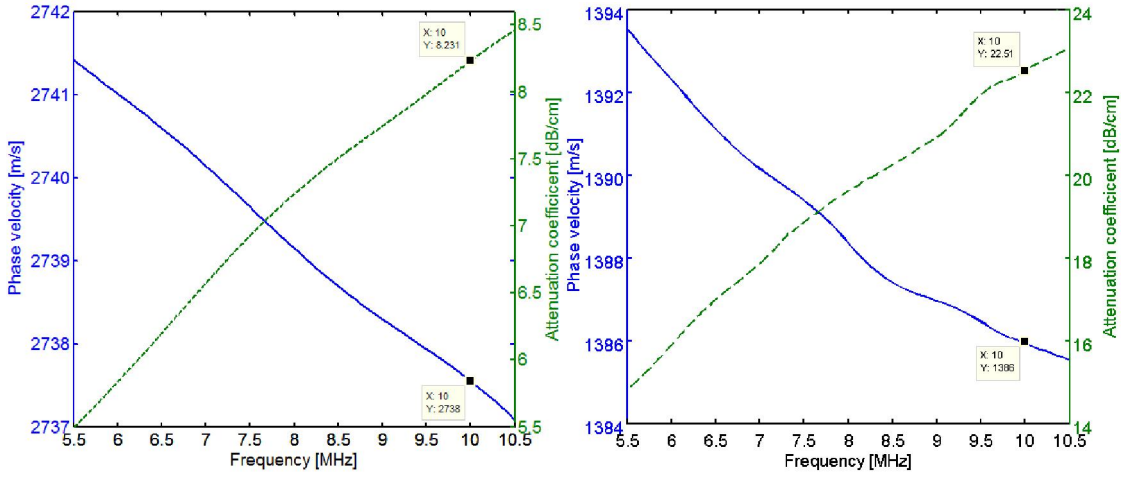

(a) (b)

Figure 4: Phase velocity and attenuation of the (a) compressional and (b) shear waves in PMMA samples measured at 20±0.5°C with the 10 MHz transducer pair.

For the 10 MHz transducer pair, the trend is similar (Figure 4). Their dispersion values are 0.8 m/s/MHz and 1.7 m/s/MHz for the compressional wave and shear wave, respectively. However, the attenuation is significantly increased for both compressional and shear waves, compared with those measured with the 5 MHz transducer pair. According to the power-law relation, the higher the frequency, the higher attenuation obtained [9]. Nevertheless, the increase in attenuation of the compressional and shear waves is slightly lower, i.e. 0.6 dB/cm/MHz and 1.8 dB/cm/MHz, respectively.

Figure 5 shows the phase velocity and attenuation of the compressional and shear waves for the Eccosorb MF-117 measured at 19±0.5°C with the 5 MHz transducer pair. The phase velocities show the same small negative dispersion as PMMA samples, although the dispersion is slightly higher. The changes in phase velocity of the compressional and shear waves are 5 m/s/MHz and 4m/s/MHz, respectively. The attenuation of the compressional and shear waves in the Eccosorb MF-117 samples also increases linearly with frequency. An increase of 91% (2.2 dB/cm/MHz) for the attenuation of compressional wave, and an increase of 101% (5.7 dB/cm/MHz) for the attenuation of shear wave were observed over the frequency range investigated.

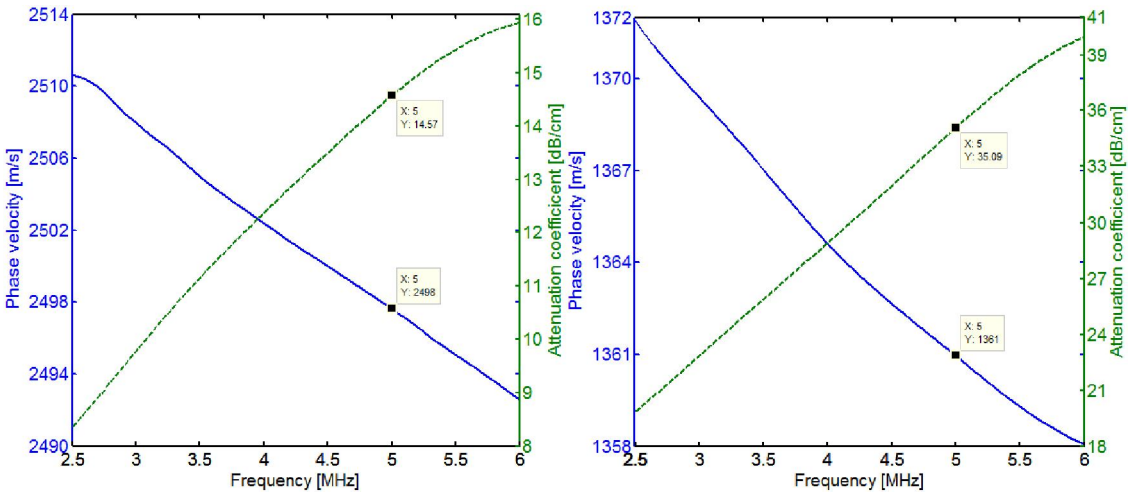

(a) (b)

Figure 5: Phase velocity and attenuation of the (a) compressional and (b) shear waves in Eccosorb MF-117 sample measured at 19±0.5°C with the 5 MHz transducer pair.

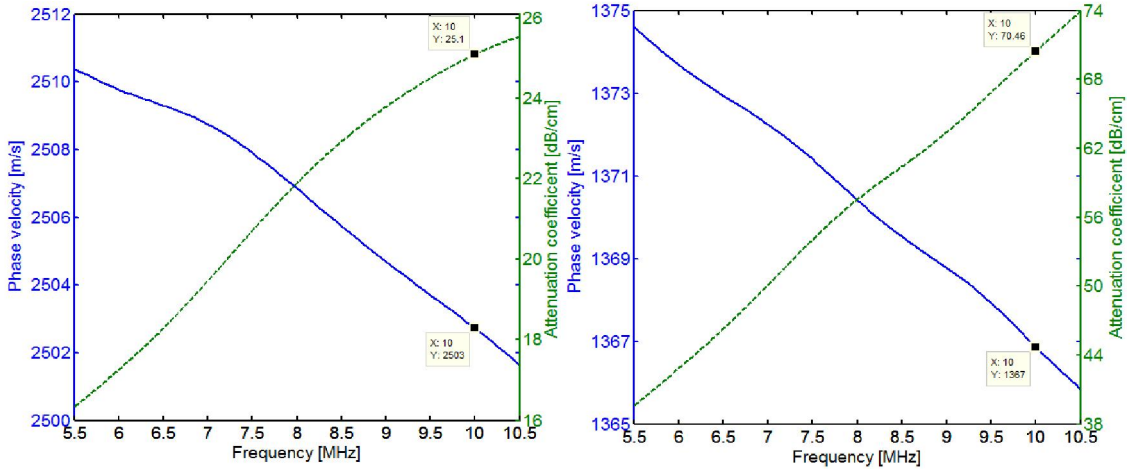

(a) (b)

Figure 6: Phase velocity and attenuation of the (a) compressional and (b) shear waves in Eccosorb MF-117 samples measured at 19±0.5°C with the 10 MHz transducer pair.

For the 10 MHz transducer pair, the phase velocity and attenuation of ultrasonic waves in the Eccosorb samples are shown in Figure 6. The negative dispersions of the phase velocity of the compressional and shear waves are 1.8 m/s/MHz and 2 m/s/MHz, respectively. The attenuation also increases linearly with frequency, i.e. a 36% increase in compressional wave attenuation and an 87% increase in shear wave attenuation. Also here, the attenuation of the shear wave was much larger than that of the compressional wave.

Figure 7 shows the effects of temperature on the phase velocity and attenuation of compressional wave in the PMMA and Eccosorb MF-117 samples. For the measurements, the temperature was controlled by heating the water in the tank containing the sample, and passive cooling down to avoid the creation of air-bubbles. For the PMMA samples, a 3% decrease in phase velocity and a 35% increase in attenuation were observed when increasing the temperature from 20°C to 37°C, at both 5 MHz (5 MHz transducer pair) and 10 MHz (10 MHz transducer pair). The difference in the phase velocity between 5 MHz and 10 MHz is less than 0.3%. In addition, the attenuation increases almost linearly with frequency and temperature over the range studied. Our measured values were found to agree well with published values for 20°C and 37°C. The Eccosorb MF-117 samples show a similar trend. The phase velocity decreases 4.7%, and the attenuation increases 30% with the increasing temperature from 19°C to 37°C, at both 5 MHz and 10 MHz. There is only a small difference in phase velocity between 5 MHz and 10 MHz, less than 0.4%. Eccosorb MF-117 contains particles with diameters ranging from 1 μm to 5 μm, which are much smaller than the wavelength of the acoustic waves studied here, (491 μm at 5 MHz, and 246 μm at 10 MHz), thus may not have significant effects on the phase velocity. In addition, the attenuation also

increases nearly linearly with the increasing temperature.

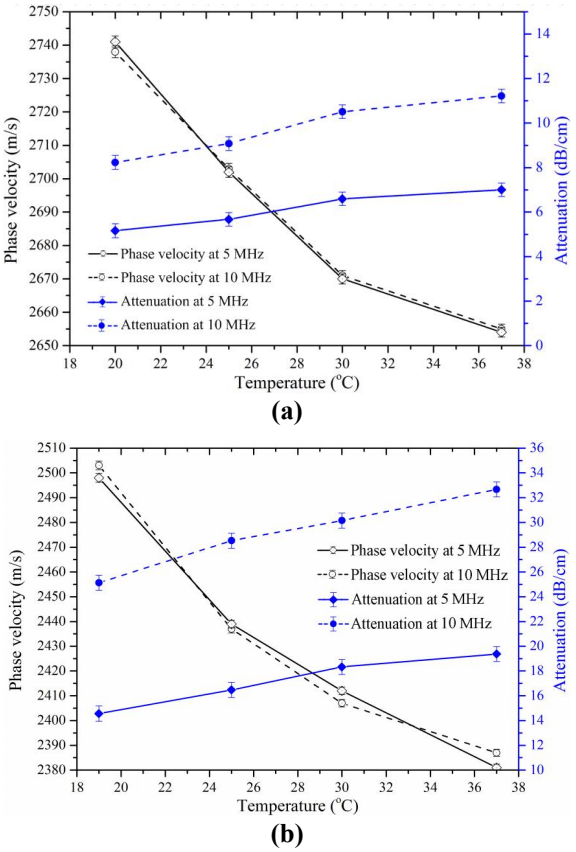

Figure 7: Phase velocity and attenuation of the compressional wave in (a) PMMA, and (b) Eccosorb MF-117 samples versus temperature. The error bar is the uncertainty of measurements.

Conclusion

An experimental setup for the broadband through-transmission technique was implemented for characterizing the phase velocity and attenuation of the compressional wave and shear wave in solids. The parameters can be measured over the frequency range from 2.5 to 10.5 MHz, using two pairs of transducers. For known materials, i.e. PMMA, the measurement results showed a good agreement with values from literature, hence, verifying the accuracy of our measurements. Our verified system was then used to characterize Eccosorb MF-117 which has many potential applications. The velocity dispersion was found to be small, below 1.2%, for both the compressional and shear waves in both characterized materials. However, the attenuation was much higher in the composite Eccosorb MF-117 samples than in the PMMA samples. The study of temperature effects showed that the temperature slightly affects the phase velocity in both PMMA and Eccosorb MF-117, whereas it significantly influences the attenuation. In both materials, increasing the temperature from 19°C to 37°C caused a small decrease on the phase velocity, i.e. 3% reduction for PMMA and 4.7% reduction for Eccosorb MF-117. In contrast to the phase velocity, larger increases in the attenuation were observed, 35% increase for PMMA and 35% increase for Eccosorb MF-117. The results were not corrected for diffraction, but this effect was estimated to be negligible [10]. These measured acoustic properties of PMMA and Eccosorb MF-117 materials are important for ultrasound transducer designs, and their temperature effects should be taken into account, especially for clinical applications.

References

[1] R. L. Weaver, and Y. H. Pao, "Dispersion relations for linear wave propagation in homogeneous and inhomogeneous media", Journal of Mathematical Physics, Vol. 22, pp. 1909-1918, 1981.

[2] R. A. Kline, "Measurement of attenuation and dispersion using an ultrasonic spectroscopy technique", The Journal of the Acoustical Society of America, Vol. 76, 498-504, 1984.

[3] H. Wang, W. Jiang, and W. Cao, "Characterization of lead zirconate titanate piezoceramic using high frequency ultrasonic spectroscopy", Journal of Applied Physics, Vol. 85, pp. 8083-8091, 1999.

[4] Eccosorb® MF, http://www.eccosorb.com/Collateral/Documents/English-US/MF.pdf.

[5] J. Wu, "Determination of velocity and attenuation of shear waves using ultrasonic spectroscopy", The Journal of the Acoustical Society of America, Vol. 99, pp. 2871-2875, 1996.

[6] E. E. Franco, M. A. B. Andrade, R. T. Higuti, J. C. Adamowski, and F. Buiochi, "Acoustic transmission with mode conversion phenomenon," in Proceedings of the 18th International Congress of Mechanical Engineering-COBEM, Ouro Preto, November 6-11, pp. 113-120, 2005.

[7] J. E. Carlson, J. Van Deventer, A. Scolan, and C. Carlander, "Frequency and temperature dependence of acoustic properties of polymers used in pulse-echo systems", in 2003 IEEE Symposium on Ultrasonics, October 5-8, 2003.

[8] M. Treiber, J.-Y. Kim, L. J. Jacobs, and J. Qu, "Correction for partial reflection in ultrasonic attenuation measurements using contact transducers," The Journal of the Acoustical Society of America, Vol. 125, pp. 2946, 2009.

[9] P. He, "Experimental verification of models for determining dispersion from attenuation", IEEE Transactions on Ultrasonics Ferroelectrics, and Frequency Control, Vol. 46, pp. 706–714, 1999.

[10] P. H. Rogers, and A. L. Van Buren, "An exact expression for the Lommel diffraction correction integral", The Journal of the Acoustical Society of America, Vol. 55, 724-728, 1974.

Paper 2

Title:	"Temperature effects on ultrasonic phase velocity and attenuation in Eccosorb and PMMA"
Author:	**Hoa T. K. Tran**, Tung Manh, Tonni Franke Johansen, and Lars Hoff
Submitted to:	IEEE-International Ultrasonics Symposium
Place:	Tours, France
Date:	September 18-21, 2016.

Temperature Effects on Ultrasonic Phase Velocity and Attenuation in Eccosorb and PMMA

Hoa T. K. Tran[1], Tung Manh[1], Tonni Franke Johansen[2], and Lars Hoff[1,*]

[1]Department of Micro and Nano Systems Technology, University College of Southeast Norway, Horten, Norway.
[2]Sintef, Information and Communication Technology, Trondheim, Norway
*Contacting author email: Lars.Hoff@hbv.no

Background, Motivation, Hypothesis and Objectives

Ultrasonic velocity and attenuation are important material properties when designing a transducer. For many materials, these properties vary with temperature and frequency. This paper presents an experimental study on how the temperature influences the phase velocity and attenuation for compressional wave and shear wave, measured in the PMMA and Eccosorb MF117 materials using a broadband through-transmission technique.

Statement of Contribution/Methods

A through-transmission system was implemented with a sample immersed in a water tank between transmitting and receiving transducers, where the sample could be rotated to vary the incident angle of the acoustic wave [1]. Two pairs of transducers were used, one pair with center frequency 5 MHz and another pair with 10 MHz. Phase velocity and attenuation as function of frequency were calculated from the phase and magnitude of the received spectra, for compressional and shear waves. The temperature was controlled by heating the water in the tank containing the sample, and letting it cool down slowly to avoid the creation of air-bubbles. Measurements were done in the temperature range from 19℃ to 37℃.

Results, Discussion and Conclusion

Figure 1 shows the phase velocity and attenuation of the compressional and shear waves in Eccosorb MF117 versus the temperature. At both 5 MHz and 10 MHz, we found a ~5% decrease in phase velocity and a ~30% increase in attenuation when increasing the temperature from 19℃ to 37℃, for both compressional wave and shear wave. The differences in phase velocity between 5 MHz and 10 MHz were less than 0.3%. The particles contained in Eccosorb MF117 have diameters ranging from 1 µm to 5 µm, which is much smaller than the wavelengths studied here, being larger than 250 µm; thus having minor effects on the phase velocity. The attenuation was found to increase almost linearly with both frequency and temperature, and similar to PMMA. The attenuation of the shear wave is around ~2.5 times higher than that of the compressional wave. For PMMA, the phase velocity decreased ~3%, and the attenuation increased ~35% over the temperature range from 19℃ to 37℃, at both 5 MHz and 10 MHz. The acoustic properties of PMMA were found to agree well with published values for 20℃ and 37℃. We conclude that variations in acoustic parameters with temperature should be taken into account when using these materials in transducer design.

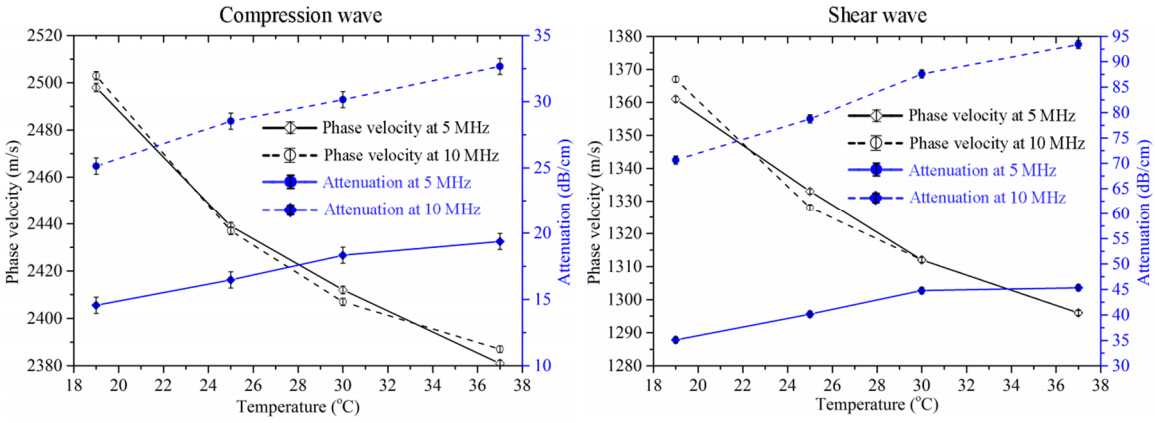

Fig. 1. Phase velocity and attenuation of compression wave and shear wave in Eccosorb MF117.

References

[1] J. Wu, "Determination of velocity and attenuation of shear waves using ultrasonic spectroscopy," *J. Acoust. Soc. Am.*, vol. 99, pp. 2871–2875, 1996.

Bibliography

[1] R. L. Weaver, and Y. H. Pao, “Dispersion relations for linear wave propagation in homogeneous and inhomogeneous media,” Journal of Mathematical Physics, vol. 22, pp. 1909-1918, 1981.

[2] R. A. Kline, “Measurement of attenuation and dispersion using an ultrasonic spectroscopy technique”, The Journal of the Acoustical Society of America, vol. 76, pp. 498-504, 1984.

[3] D. I. Bolef, and J. D. Klerk, “Some continuous-wave techniques for the measurement of velocity and attenuation of ultrasonic waves between 1 and 1000 Mc,” Transactions on Ultrasonics Engineering, vol. 10, pp. 19-26, 1963.

[4] H. J. McSkimmin, “Ultrasonic methods for measuring the mechanical properties of solids and liquids,” W.P. Mason. Physical Acoustics, vol. 1, Part A. Academic Press, New York 27-417, 1964.

[5] P. H. F. Nicholson, G. Lowet, C. M. Langton, J. Dequeker, and G. Van der Perre, “A comparison of time-domain and frequency-domain approaches to ultrasonic velocity measurement in trabecular bone,” Physics in Medicine and Biology, vol. 41, pp. 2421-2435, 1996.

[6] D. J. McClements, and E. Dickinson, “Advances in food colloids”, Chapman and Hall, Springer US, pp. 187-188, 1996.

[7] A. R. Selfridge, “Approximate material properties in isotropic materials,” IEEE Transactions on Sonics and Ultrasonics, vol. 32, pp. 381–394, 1985.

[8] T. L. Szabo, “Diagnostic ultrasound imaging: inside out,” 2nd Edition, Academic Press, 2013.

[9] J. Wu, “Determination of velocity and attenuation of shear waves using ultrasonic spectroscopy,” The Journal of the Acoustical Society of America, vol. 99, pp. 2871-2875, 1996.

[10] R. A. Webster, “Passive materials for high frequency piezocomposite ultrasonic transducers,” Ph.D thesis, University of Birmingham, 2009.

[11] Y. Levy, Y. Agnon, and H. Azhari, “Measurement of speed of sound dispersion in soft tissues using a double frequency continuous wave method,” Ultrasound in Medicine and Biology, vol. 32, pp. 1065-1071, 2006.

[12] M. Agrawal, A. Prasad, J. R. Bellare, and A. A. Seshia, “Characterization of mechanical properties of materials using ultrasound broadband spectroscopy,” Ultrasonics, vol. 64, pp. 186–195, 2016.

[13] H. Wang, W. Jiang, and W. Cao, “Characterization of lead zirconate titanate piezoceramic using high frequency ultrasonic spectroscopy,” Journal of Applied Physics, vol. 85, pp. 8083-8091, 1999.

[14] C. Landais, “Ultrasonic methods for the characterization of complex materials and material systems: polymers, structured polymers, soft tissue and bone” M.S. thesis, University of Nebraska-Lincoln, 2011.

[15] A. S. Birks., R. E. Green, Jr., and P. McIntire, “Nondestructive testing handbook,” Columbus 2nd Edition, American Society for Nondestructive Testing, 1991.

[16] P. He, and J. Zheng, “Acoustic dispersion and attenuation measurement using both transmitted and reflected pluses,” Ultrasonics, vol.39, pp. 27-32, 2001.

[17] P. J. White, G. T. Clement, and K. Hynynen “Longitudinal and shear wave mode ultrasound propagation in human skull bone,” Ultrasound in Medicine and Biology, vol.32, pp. 1085-1096, 2006.

[18] T. Sukomski, "Ultrasonic nondestructive methods in inspection of steel," Ph.D thesis, AGH-University of Science and Technology, 2012.

[19] L. E. Kinsler, A. R. Frey, A. B. Coppens, and J. V. Sanders, "Fundamentals of acoustic ," 4th Edition, John Wiley & Sons, 2000.

[20] R. S. C. Cobbold, "Foundations of biomedical ultrasound," Oxford University Press, New York, 2008.

[21] D. Royer, and E. Dieulesaint, "Elastic waves in solid I," Springer, New York, 2000.

[22] T. N. Nguyen, M. Letiecq, F. Levassort, and L. Pourcelot, "Experimental verification of the theory of elastic properties using scattering approximations in (0-3) connectivity composite materials," IEEE Transactions on Ultrasonics Ferroelectrics and Frequency Control, vol. 43, pp. 640-645, 1996.

[23] S.A. Shtrikman, and Z. Hashin, "Variational approach to the theory of the elastic behavior of multiphase materials," Journal of the Mechanics and Physics of Solids, vol. 11, pp. 127-140, 1963.

[24] A. J. Devaney and H. Levine, "Effective elastic parameters of random composites," Apply Physical Letter, vol. 37, pp. 377-379, 1980.

[25] R. E. Brennan IV, "Ultrasonic nondestructive evaluation of armor ceramics," ProQuest, 2007.

[26] S. K. Bhargava, "Principles and practice of ultrasonography," 1st Edition, Jaypee Brothers Medical Publishers (P) Ltd, New Delhi, 2002.

[27] Measurement and uncertainty, http://physics.wustl.edu/introphys/Fall/Archives/FL13/MeasUncertLab_FAll13.pdf

[28] R. L. O'Leary, "Investigation into passive materials utilized within the construction of piezoelectric composite transducers," Ph.D thesis, University of Strathclyde, 2003.

[29] J. G. Proakis and D. G. Manolakis, "Digital signal processing - Principles, Algorithms, and Applications," 3rd Edition, Prentice-Hall of India Private Limited, New Delhi, 1997.

[30] I. Fujii and K. Kawashima, “Digital measurement of ultrasonic velocity,” Review of Progress in Quantitative Nondestructive Evaluation, vol. 14, pp. 203–209, 1995.

[31] E. E. Franco, M. A. B. Andrade, R. T. Higuti, J. C. Adamowski, and F. Buiochi, “Acoustic transmission with mode conversion phenomenon,” in Proceedings of the 18th International Congress of Mechanical Engineering-COBEM, pp. 113-120, 2005.

[32] J. L. Rose, “Ultrasonic guided waves in solid media,”. New York NY: Cambridge University Press, 2014.

[33] S. Hashmi, G. F. Batalha, C. J. Van Tyne, and B. S. Yilbas, “Comprehensive Materials Processing,” Amsterdam: Elsevier, 2014.

[34] P. He, “Experimental verification of models for determining dispersion from attenuation,” IEEE Transactions on Ultrasonics, Ferroelectrics, and Frequency Control, vol. 46, pp. 706–714, 1999.

[35] H. Wang, T. A. Ritter, W. Cao, and K. K. Shung, “High frequency properties of passive materials for ultrasonic transducers,” IEEE Transactions on Ultrasonics, Ferroelectrics, and Frequency Control, vol. 48, pp. 77-84, 2001.

[36] L. M. Brekhovskikh and O. A. Godin “Acoustics of layered media 1,” 2nd Edition, Springer, 1998.

[37] W. Xu and J. J. Kaufman, “Diffraction correction methods for insertion ultrasound attenuation estimation,” IEEE Transactions on Biomedical Engineering, vol. 40, pp. 563-570, 1993.

[38] R. Bass, “Diffraction effects in the ultrasonic field of a piston sources,” The Journal of the Acoustical Society of America, vol. 30, pp. 602-605. 1958.

[39] P. H. Rogers and A. L. Van Burren, “An exact expression for the Lommel diffraction correction integral,” The Journal of the Acoustical Society of America, vol. 55, pp. 724-728, 1974.

[40] https://www.cdiweb.com/datasheets/heidenhain/heidenhain_metro_0.5.pdf.

[41] http://www.denverinstrument.com/denverusa/balances/summit.php

[42] http://www.farnell.com/datasheets/1598887.pdf

[43] V. A. Del Grosso and C. W. Mader, "Speed of sound in pure water," The Journal of the Acoustical Society of America, vol. 52, pp. 1442-1446, 1972.

[44] N. Bilaniuk, and G. S. K. Wong, "Speed of sound in pure water as a function of temperature," The Journal of the Acoustical Society of America, vol. 93, pp. 1609-1612, 1993.

[45] G. W. C. Kay and T. H. Laby "Tables of Physical and Chemical Constants and Some Mathematical Functions," 15th Edition, Longman, London,1995.

[46] http://www.kayelaby.npl.co.uk/general_physics/2_4/2_4_1.html

[47] http://www.diracdelta.co.uk/science/source/a/l/aluminium/source.html#.VqIsVVLCagw

[48] D. O. Thompson and D. E. Chimenti, "Review of Progress in Quantitative Nondestructive Evaluation," vol. 12A, Plenum Press, New York, 1993.

[49] J. D. N. Cheeke, "Fundamentals and applications of ultrasonic waves," Boca Raton: CRC Press, 2002.

[50] W. Sachse, "Measurement of phase and group velocities of dispersive waves in solids," in Proceedings of the ARPA/AFML Review of Progress in Quantitative NDE, September 1976-June 1977, pp. 24, 1978.

[51] D. O. Thompson and D. E. Chimenti, "Review of Progress in Quantitative Nondestructive Evaluation," vol. 2A, Plenum Press, New York, 1983.

[52] K. Raum, U. Cobet, L. Smitmans, and J. Brandt, "Quantitative scanning acoustic microscopy investigation of cortical bone using a multilayer analysis method," in IEEE Proceedings of Ultrasonics Symposium, vol. 1, pp. 593–596, 1999.

[53] D. R. Christman, "Dynamic properties of poly (Methylmethacrylate)(PMMA)-(Plexiglas)," DTIC Document, 1972.

[54] H. G. Aksoy, "Broadband ultrasonic spectroscopy for the characterization of viscoelastic materials," Ultrasonics, vol. 67, pp. 168–177, 2016.

[55] J. E. Carlson, J. Van Deventer, A. Scolan, and C. Carlander, “Frequency and temperature dependence of acoustic properties of polymers used in pulse-echo systems,” IEEE Symposium in Ultrasonics, vol. 1, pp. 885–888, 2013.

[56] M. Treiber, J.-Y. Kim, L. J. Jacobs, and J. Qu, “Correction for partial reflection in ultrasonic attenuation measurements using contact transducers,” The Journal of the Acoustical Society of America, vol. 125, pp. 2946, 2009.